

NCHRP Web Document 16

(Project 1-29)

Contractor's Final Report

IMPROVED SURFACE DRAINAGE OF PAVEMENTS

FINAL REPORT

Prepared for
National Cooperative Highway Research Program
Transportation Research Board
National Research Council

by

David A. Anderson, R. Scott Huebner, Joseph R. Reed, John C. Warner,
and John J. Henry
The Pennsylvania Transportation Institute
The Pennsylvania State University

The Pennsylvania Transportation Institute
The Pennsylvania State University
Research Building B
University Park, PA 16802

PTI 9825

June 1998

LIBRARY
TRANSPORTATION RESEARCH BOARD

ACKNOWLEDGMENT

This work was sponsored by the American Association of State Highway and Transportation Officials (AASHTO), in cooperation with the Federal Highway Administration, and was conducted in the National Cooperative Highway Research Program (NCHRP), which is administered by the Transportation Research Board (TRB) of the National Research Council.

DISCLAIMER

The opinion and conclusions expressed or implied in the report are those of the research agency. They are not necessarily those of the TRB, the National Research Council, AASHTO, or the U.S. Government.

This report has not been edited by TRB.

TABLE OF CONTENTS

	Page
LIST OF FIGURES	vii
LIST OF TABLES	x
ACKNOWLEDGMENTS	xi
ABSTRACT	xii
SUMMARY	xiii
CHAPTER 1 INTRODUCTION	1
Research Approach	2
Water Film Thickness	3
Methods for Reducing Water Film Thickness	6
Research Program	7
Research Products	7
CHAPTER 2 LITERATURE REVIEW AND CURRENT PRACTICE AND TECHNIQUES FOR IMPROVED SURFACE DRAINAGE	11
Summary of Models Needed to Develop Guidelines	12
Methods for Controlling Water Film Thickness	13
Controlling Water Film Thickness Through Pavement Geometry	14
Controlling Water Film Thickness Through Use of Appurtenances	21
Controlling Water Film Thickness with Internally Draining Asphalt Surfaces (OGAC)	25
Controlling Water Film Thickness with Grooving	32
Controlling Water Film Thickness with Surface Texture	36
Proposed Design Guidelines for Improving Pavement Drainage—Implementation of Findings	37
Pavement Geometry	37
Pavement Properties	38
Drainage Appurtenances	39
PAVDRN Software	40
Design Example Using Slotted Drains	41
CHAPTER 3 SELECTION AND DEVELOPMENT OF MODELS FOR PAVDRN	45
Water Film Thickness Model	45
Empirical Model	46
One-Dimensional Analytical Models	47
Two-Dimensional Analytical Models	50
Model of Choice	50
Subsurface Flow Model	52
Manning's n	55
Determination of Manning's n	56
Relationships for Manning's n used in PAVDRN	57
Hydroplaning Speed Model	59
Rainfall Intensity	66

TABLE OF CONTENTS (CONTINUED)

	Page
CHAPTER 4 EXPERIMENTAL STUDIES	69
Test Facilities	70
Indoor Artificial Rain Facility	70
Production and Placement of Porous Mixes	75
Outdoor Test Facilities	80
Penn State Pavement Durability Research Facility	81
Wallops Flight Facility	88
Measurement Techniques	88
Measurement of Water Film Thickness	88
Measurement of Surface Texture	96
Measurement of Manning's n	98
Measurement of Permeability	98
Test Results	102
Flow on Porous Asphalt Sections	102
Texture Measurements	105
Full-Scale Skid Testing	107
CHAPTER 5 SUMMARY, FINDINGS, AND RECOMMENDATIONS	117
Summary	117
Findings	121
Recommendations and Conclusions	127
Additional Studies	128
REFERENCES	131
APPENDIX A Program Overview	A-1
APPENDIX B Review of Models	B-1
APPENDIX C Determination of Manning's n	C-1
APPENDIX D Model Evaluation	D-1

LIST OF FIGURES

	Page
Figure 1. Definition of water film thickness, mean texture depth, and total flow	4
Figure 2. Definition of flow path and design plane	5
Figure 3. Research tasks	8
Figure 4. Different lateral drainage configurations with and without lateral drains	18
Figure 5. Typical slotted drain	22
Figure 6. Typical grooving patterns for portland cement concrete pavement (30)	33
Figure 7. Predicted water film thickness, WFT, for grooved portland cement concrete pavement, rainfall intensity 75 mm/h (30)	35
Figure 8. Water film thickness versus distance along flow path for several pavement surfaces as calculated using PAVDRN	53
Figure 9. Manning's n versus length of flow path for various rainfall rates, portland cement concrete, $500 < N_R < 1000$	60
Figure 10. Manning's n versus length of flow path for various rainfall rates, portland cement concrete, $N_R < 500$	61
Figure 11. Manning's n versus length of flow path for various rainfall rates, dense-graded asphalt concrete	62
Figure 12. Manning's n versus length of flow path for various rainfall rates, porous asphalt concrete	63
Figure 13. Hydroplaning speed versus water film thickness	65
Figure 14. Rainfall intensity versus sight distance for various vehicle speeds	68
Figure 15. Cross-section of pavement used in laboratory rainfall simulator	71
Figure 16. Overall view of test channel used with laboratory rainfall simulator	72
Figure 17. Laboratory rainfall simulator	73
Figure 18. Cross-section of flow for porous asphalt sections in laboratory	76

LIST OF FIGURES (CONTINUED)

	Page
Figure 19. Gradations of laboratory and field porous asphalt mixtures	77
Figure 20. Photograph of vibratory compactor	79
Figure 21. Schematic of test sections at the Penn State Pavement Durability Research Facility . . .	82
Figure 22. Introduction of water onto test section at the Penn State Pavement Durability Research Facility	86
Figure 23. Skid test in progress at the Penn State Pavement Durability Research Facility	87
Figure 24. Test in progress at the Wallops Flight Facility	89
Figure 25. Grooved concrete surface at the Wallops Flight Facility	90
Figure 26. Measurement of water film thickness with point gauge on a porous asphalt surface in laboratory	92
Figure 27. Schematic of color-indicating water film thickness gauge	93
Figure 28. Correlation of water film thickness measurements obtained with the color-indicating gauge and point gauge	95
Figure 29. Steps in determining texture depths using profiling method (42)	97
Figure 30. Schematic of drainage lag permeameter	100
Figure 31. Definition of base and surface flow in porous asphalt sections	103
Figure 32. Plot of total flow versus flow path to determine flow depth	104
Figure 33. Skid resistance measurements at the Penn State Pavement Durability Research Facility, mixture 1	109
Figure 34. Skid resistance measurements at the Penn State Pavement Durability Research Facility, mixture 2	110
Figure 35. Skid resistance measurements at the Penn State Pavement Durability Research Facility, mixture 3	111
Figure 36. Skid resistance measurements at the Penn State Pavement Durability Research Facility, mixture 4	112
Figure 37. Test results for plain concrete sections at the Wallops Flight Facility	115

LIST OF FIGURES (CONTINUED)

	Page
Figure 38. Test results for grooved concrete sections at the Wallops Flight Facility	116
Figure 39. Flow diagram representing PAVDRN design process in “Proposed Design Guidelines for Improving Pavement Surface Drainage” (2)	118
Figure 40. Factors considered in PAVDRN program	122

LIST OF TABLES

	Page
Table 1. Maximum recommended grades (I)	16
Table 2. Typical cross-slopes for different pavement surfaces (I)	19
Table 3. Maximum allowable superelevation (I)	20
Table 4. Gradations used for internally draining asphalt mixes	28
Table 5. PAVDRN summary output table	41
Table 6. Tangent section properties	41
Table 7. PAVDRN output for tangent section	42
Table 8. Mixture designs for porous asphalt laboratory mixes	78
Table 9. Air voids in laboratory porous asphalt mixes	80
Table 10. Porous asphalt mix designs at the Penn State Pavement Durability Research Facility . .	84
Table 11. Texture depth measurements on laboratory porous asphalt sections	106
Table 12. Sand patch data obtained at the Penn State Pavement Durability Research Facility . .	107
Table 13. Skid resistance test data obtained at the Wallops Flight Facility	114

ACKNOWLEDGMENTS

The work conducted during this study could not have been accomplished without the help of many individuals and organizations. The support of HRI, Inc., especially Jeff Reeder, in producing and placing the porous asphalt sections at the Penn State Test Track is gratefully acknowledged. Mr. Tom Yager of the Wallops Flight Facility was especially helpful in arranging for the work at the facility; the assistance provided by the facility in support of the skid testing is also recognized. The work of several graduate students was of great value in completing this study: Mr. Randy T., who helped with the laboratory studies and in the analysis of the data to determine Manning's n and Mr. R. Robert Morrison and Mr. Steven L. Golembiewski, Jr., who helped with the development of PAVDRN. The excellent support provided by the engineers, technicians, and graduate students at Penn State who helped with the field and laboratory testing at Penn State was also essential to the completion of the study, and their work is recognized. Finally, the guidance provided by Frank McCullagh and the NCHRP 1-29 panel is gratefully recognized.

ABSTRACT

The purpose of this project was to identify techniques for improving the drainage of multi-lane highway pavements and to develop guidelines for implementing the most promising of these techniques. The drainage of highway pavement surfaces is important in the mitigation of splash and spray and hydroplaning. This study focused on improving surface drainage to reduce the tendency for hydroplaning. The main factor affecting the propensity for hydroplaning is the thickness of the water film on the pavement surface. Three general techniques were identified for reducing the water film thickness: controlling the pavement geometry, the use of textured surfaces to include porous asphalt surfaces and grooved surfaces, and the more effective use of drainage appurtenances.

The prediction of the water film thickness is based on the use of the kinematic wave equation as a model to predict the depth of flow on pavement surfaces. Data supporting the model were obtained from the literature and from studies conducted to measure Manning's n for a brushed concrete surface and for porous asphalt surfaces. Expressions for Manning's n as a function of Reynold's number were developed for portland cement concrete, concrete, asphalt concrete, and porous asphalt surfaces. Full-scale skid testing was also conducted on grooved and brushed concrete surfaces and on porous asphalt surfaces; texture measurements were obtained for all of the tested surfaces (laboratory and field). The results have been integrated into an interactive computer program, PAVDRN. This interactive program allows the pavement design engineer to select values for the critical design parameters. The program then predicts the water film thickness along the line of maximum flow and determines the hydroplaning potential along the flow path. If the predicted hydroplaning speed is less than the design speed, the designer is prompted to choose from alternative designs that reduce the thickness of the water film.

SUMMARY

The primary objective of this research project was to identify improved methods for draining rainwater from the surface of pavements and to develop guidelines for their implementation. Improved methods are needed for draining the surface of multi-lane pavements because of the important role that drainage plays in the mitigation of hydroplaning and splash and spray. A model for predicting the depth of flow, or water film thickness (WFT), resulting from rainfall on multi-lane pavements was developed and incorporated into a computer-based design procedure. The water film thickness is needed as a quantitative measure of the effect of applying different drainage methods and because the propensity for hydroplaning is directly related to the water film thickness. In the process of completing this study, a number of specific tasks were addressed. These included:

- A literature review to establish the state of practice regarding analytical models for predicting rainfall water depths and to establish current design practice for removing rainfall runoff from multilane pavements;
- Improved models that describe the water film thickness resulting from sheet flow on impervious and pervious multi-lane pavement surfaces;
- Laboratory rainfall runoff data for determining the roughness coefficient (Manning's n) for pavement surfaces for which data was not available in the literature;
- Skid resistance measurements to supplement hydroplaning data in the literature and to better quantify the onset of hydroplaning as a function of the depth of the water film (WFT) flowing over the pavement surface.

Five methods for improving drainage and reducing water film thickness were identified from the review of the literature:

- Optimization of pavement geometric design parameters, such as cross-slope;
- Reduction of the distance that the water must flow (flow path) by installing drainage appurtenances;
- Use of internally draining (porous asphalt) wearing course mixtures;
- Use of grooving on portland cement concrete pavements;
- Maximization of surface texture on portland cement concrete and asphalt pavements.

Most transportation agencies use the American Association of State Highway and Transportation Officials' (AASHTO) Policy on Geometric Design of Highways and Streets as criteria for geometric design. The geometric design criteria in this policy limit the degree to which geometric factors, such as cross-slope, may be altered to maximize surface drainage. Thus, other methods for enhancing drainage are required to attain the water film thicknesses that are needed to guard against hydroplaning.

The use of slotted drains, especially between adjacent lanes on pavements with three or more lanes, is one of the methods recommended in this study for enhancing drainage. Another method is the use of internally draining surface layers (porous asphalt), which are widely and successfully used in several European countries. These mixtures are not a panacea for correcting inadequate drainage and must be used with due consideration in wet-freezing climates where black ice formation and delamination caused by freezing water can occur. Recently developed microsurfacing techniques offer the advantage of the large surface texture generated by porous asphalt without the disadvantages of delamination and black ice formation in wet-freezing climates.

Grooving of portland cement concrete pavements can enhance surface drainage by providing a reservoir for water and by draining water from the pavement surface. Grooving must be parallel to the flow of water to be fully effective, but this is usually not practical given that the water flow path is usually skewed to the direction of traffic. Increasing the texture of the pavement surface can also enhance drainage and decrease the tendency for hydroplaning. Based on tests conducted in this study, once the grooves are filled with water, the water film thickness that causes hydroplaning is indexed to the top of the grooves rendering the grooves ineffective in terms of reducing the WFT.

Surface texture can be controlled through the consideration of mixture design (maximum aggregate size and surface macrotexture) and by selecting porous asphalt for the pavement surface. Based on hydroplaning studies conducted in this study, the primary advantage offered by porous asphalts to reduce hydroplaning is the large macrotexture these asphalts offer.

A number of models were necessary in order to develop the proposed design guidelines. A model was needed for predicting the depth of sheet flow (WFT) on pavement surfaces as a function of pavement geometry, rainfall intensity, and the surface characteristics of the pavement. A one-dimensional kinetic wave equation was selected for this purpose, and additional development of the model was accomplished during the study. A model for predicting hydroplaning speed as a function of water film thickness was also needed because the tendency for hydroplaning is directly dependent on the water film thickness. Equations from the literature were selected for this purpose.

A number of field and laboratory experiments were conducted to support the development of the models and selection of the design criteria. In the laboratory, permeability measurements were obtained for porous asphalt mixtures, drainage studies were conducted to establish Manning's n (hydraulic roughness coefficient) for porous asphalt and portland cement concrete, and macrotexture measurements were obtained for the mixes that were studied. In the field, full-scale skid testing of flooded porous asphalt and portland cement concrete surfaces (broomed and grooved surfaces) was conducted to obtain data to establish the hydroplaning tendency of these surfaces. Water film thickness measurements were obtained in the laboratory and in the field with a newly developed water film thickness gage.

The proposed design methods and criteria that were developed as part of this project were incorporated into a user-friendly computer program (PAVDRN) and a set of proposed design guidelines, "Proposed Design Guidelines for Improving Pavement Surface Drainage." PAVDRN is an interactive computer program that can be used by pavement design engineers to optimize the design of new or rehabilitated pavements to enhance pavement drainage.

Many of the recommendations in this study are based on the literature review and the predictions offered by the PAVDRN program. Once flooded, the grooved portland cement concrete pavement showed no improvement in hydroplaning tendency over a similar section of broomed

pavement without grooves. Hydroplaning was also observed on the porous asphalt sections. The relatively low speed at which hydroplaning was observed on these surfaces was unexpected and needs to be verified in subsequent studies. Field trials with porous asphalt and asphalt microspheres should be conducted to demonstrate their effectiveness in reducing hydroplaning and to demonstrate their durability. Lastly, more development work is needed to determine the best use of slotted drains. This research should include schemes for locating and installing the drains between travel lanes and a review of their structural and hydraulic design. Lastly, PAVDRN and the "Proposed Design Guidelines for Improving Pavement Surface Drainage" should be used on a trial basis in the field and improved and revised as needed. The test methods needed to implement the proposed guidelines and PAVDRN are currently available, although additional work is needed to expand the database of pavement surface properties.

CHAPTER 1

INTRODUCTION AND RESEARCH APPROACH

INTRODUCTION

The primary objective of this research project was to identify improved methods for draining rainwater from the surface of multi-lane pavements and to develop guidelines for their implementation. Improved methods for draining water from the surface of multi-lane pavements are needed because of the important role that drainage plays in the mitigation of hydroplaning and splash and spray. The tendency for hydroplaning and splash and spray depends on the thickness of the film of water on the pavement. Therefore, in order to quantitatively evaluate the effectiveness of the different methods, a model for predicting the depth of flow, or water film thickness, resulting from rainfall on multi-lane pavements was developed and incorporated into computer-based design guidelines. In the process of completing this study, a number of specific tasks were addressed. These included:

- A literature review to establish the state of practice regarding analytical models for predicting rainfall water depths and to establish current design practices for removing rainfall runoff from multilane pavements.
- A review of current design methods and analytical procedures for estimating sheet flow across highway pavements.

- The development of improved models that describe the water film thickness resulting from sheet flow on impervious and pervious pavement surfaces.
- Laboratory rainfall runoff data for determining the roughness coefficient (Manning's n) for pavement surfaces for which data was not available in the literature.
- Skid resistance measurements to supplement current hydroplaning data in the literature and to better quantify the onset of hydroplaning as a function of the depth of the water film flowing over the pavement surface.
- Design procedures and criteria that can be used by user agencies in the selection of the most cost-effective means for controlling surface drainage and incorporate the procedures and criteria into a computer program.

RESEARCH APPROACH

The need for improved drainage is prompted by the hydroplaning and excessive splash and spray that can result when thick films of water develop on the pavement surface. The tendency for hydroplaning and splash and spray are minimized if the thickness of the water film on the pavement surface is minimized. Therefore, the main focus of this study concentrated on methods for predicting and controlling the flow and flow path length of rain water flowing across the pavement surface.

Water Film Thickness

Figure 1 provides a definition of the water film thickness as it flows across the pavement surface. The thickness of the water film that contributes to hydroplaning is the mean texture depth (MTD) plus the thickness of the water film above the tops of the surface asperities. The MTD depends on the macrotexture of the pavement surface. The macrotexture is the texture or roughness of the pavement surface that is caused primarily by the coarse aggregate. Techniques for measuring the macrotexture are described later in this report. The water below the MTD is trapped in the surface and does not contribute to the drainage of the pavement. Drainage or flow occurs in the total flow layer, y , which is the water film thickness (WFT) plus the mean texture depth. Increasing the macrotexture or depth is important because it allows a reservoir for water (depth below the MTD) and enhances drainage (depth above the MTD).

The flow path for a particle of water falling on a pavement surface is simply defined as the line determined by the slope along the pavement surface. Thus, the maximum flow path for a pavement section is the longest flow path for the section—the maximum distance that a rainfall droplet can flow between the point of contact with the water film and its point of exit from the pavement, as presented in figure 2. For a given quantity of rainfall per unit area of pavement, reducing the flow path will result in a more shallow depth of flow and a concomitant reduction in the propensity for hydroplaning or excessive splash and spray.

Figure 1. Definition of water film thickness, mean texture depth, and total flow.

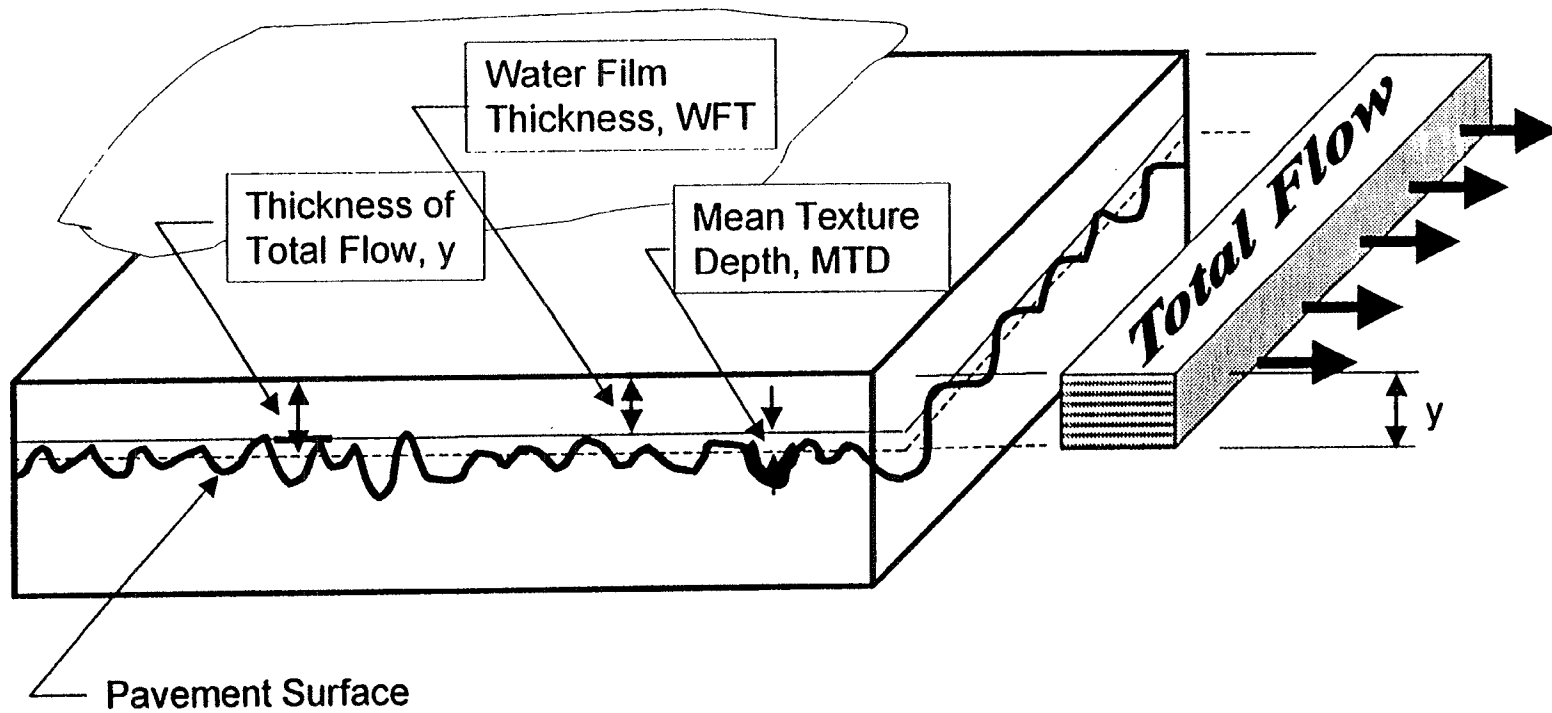
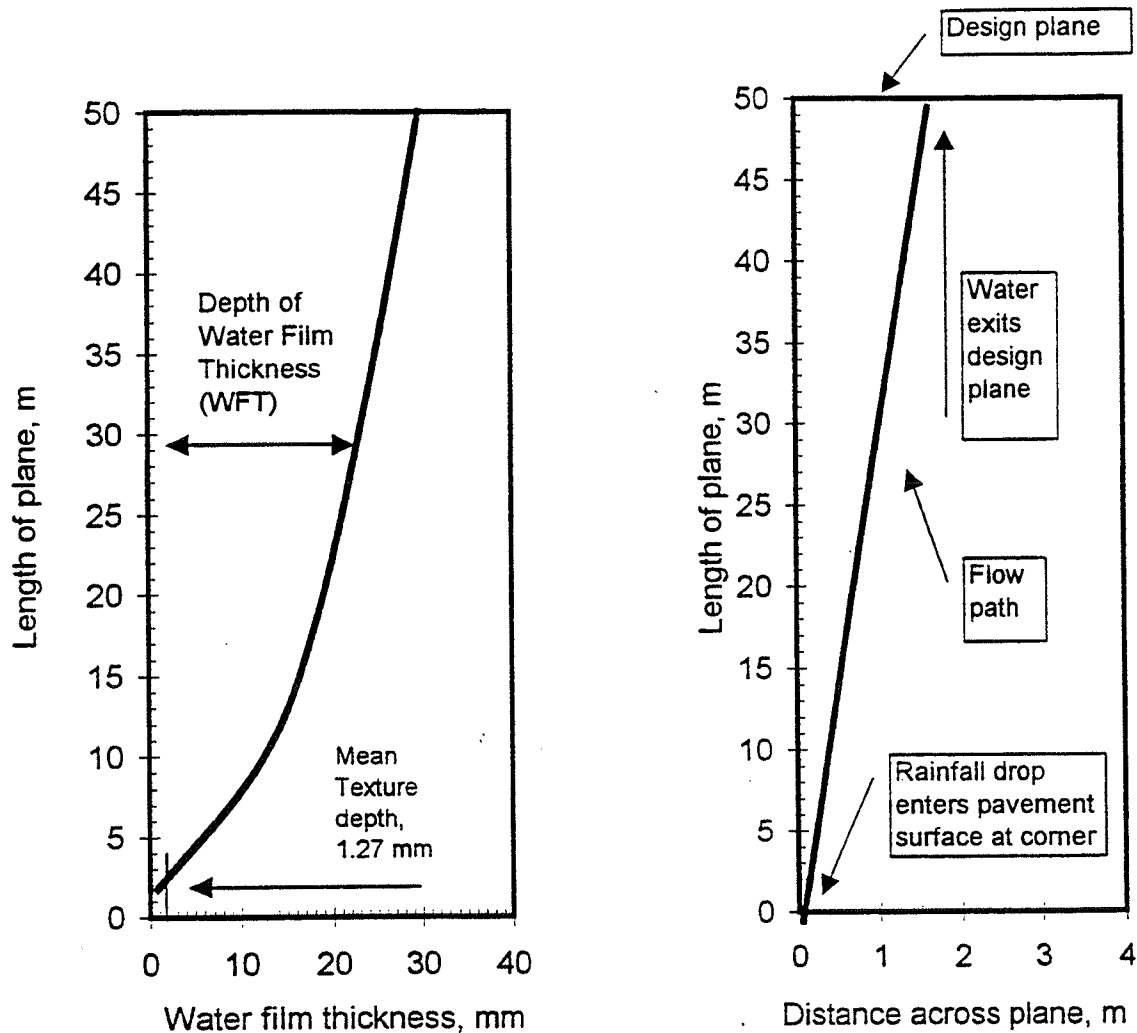


Figure 1. Definition of water film thickness, mean texture depth, and total flow.



Note: The figures above show a plan view of a design plane (right) and a profile of the water film thickness (WFT) as water flows along flow path (left). Water falling on the pavement first fills the macrotexture (lower left, here 1.27 mm deep) at which point it reaches tops of the asperities of the coarse aggregate particles. At this point, the depth of the water film increases (from zero) until the water exits either an edge of the pavement plane (case here) or a drainage appurtenance.

A plane is defined as a section of pavement that has the same geometric characteristics. In the drainage model used in this study, the drainage across the pavement is modeled by linking adjacent design planes.

Figure 2. Definition of flow path and design plane.

In order to develop quantitative guidelines for increasing pavement surface drainage, it was necessary to develop models that can predict the thickness of the water film flowing over the pavement surface. This type of flow is called sheet flow. The aforementioned models, which are an essential part of the guidelines, depend on values of Manning's n (hydraulic roughness coefficient) for the pavement surface. This fact necessitated the measurements of Manning's n for some selected surfaces for which data was not available in the literature.

Methods for Reducing Water Film Thickness

There are five techniques that can be used to reduce water film thickness: alteration of surface geometry, installation of drainage appurtenances, use of permeable or porous asphalt paving mixtures, grooving (portland cement concrete), and enhancement of surface texture through mixture selection and design. Surface geometry factors, such as cross-slope and superelevation, have traditionally been employed to remove water from the pavement surface. However, pavement geometry must be designed in accordance with American Association of Highway and Transportation Officials (AASHTO) design guidelines (1), limiting the degree to which surface geometry can be used to minimize water film thickness. Therefore, other approaches, in addition to the modification of surface geometry, are needed.

Appurtenances, such as grate inlets and slotted drains, are a means for removing surface water from the pavement. Permeable asphalt concrete pavements, such as open-graded friction courses (OGAFC) used in the United States and porous asphalt as used in many parts of Europe, are another means for reducing the flow of surface water across the pavement.

These surfaces also provide a means for draining water from beneath the tire, thereby reducing hydroplaning potential. Finally, texture modification, as typified by the recent developments in the texturing of concrete pavements, and the grooving of asphalt and portland cement concrete (PCC) pavements also provide a means for reducing water film thickness.

Research Program

The research program that was followed during this study was designed to provide the additional data needed to implement the methods that were identified for reducing water film thickness, to provide models that predict the depth of sheet flow when these techniques are used, and to provide guidelines so that the design engineer can facilitate their implementation. An overview of the research program is illustrated in figure 3. The primary focus of the research was placed on identifying the most promising techniques for predicting and controlling water film thickness as a means for minimizing the potential for hydroplaning. Limited attention was given during the research project to the mitigation of splash and spray.

Research Products

The two major products of this research were (1) a set of guidelines (2) that can be used by highway design engineers to consider alternate methods for improved surface drainage and (2) an interactive computer program (PAVDRN) for predicting the depth of sheet flow on pavement surfaces. In order to develop the guidelines, it was necessary to develop a hydraulic model for predicting the depth of the water flow on the pavement surface. This model is the

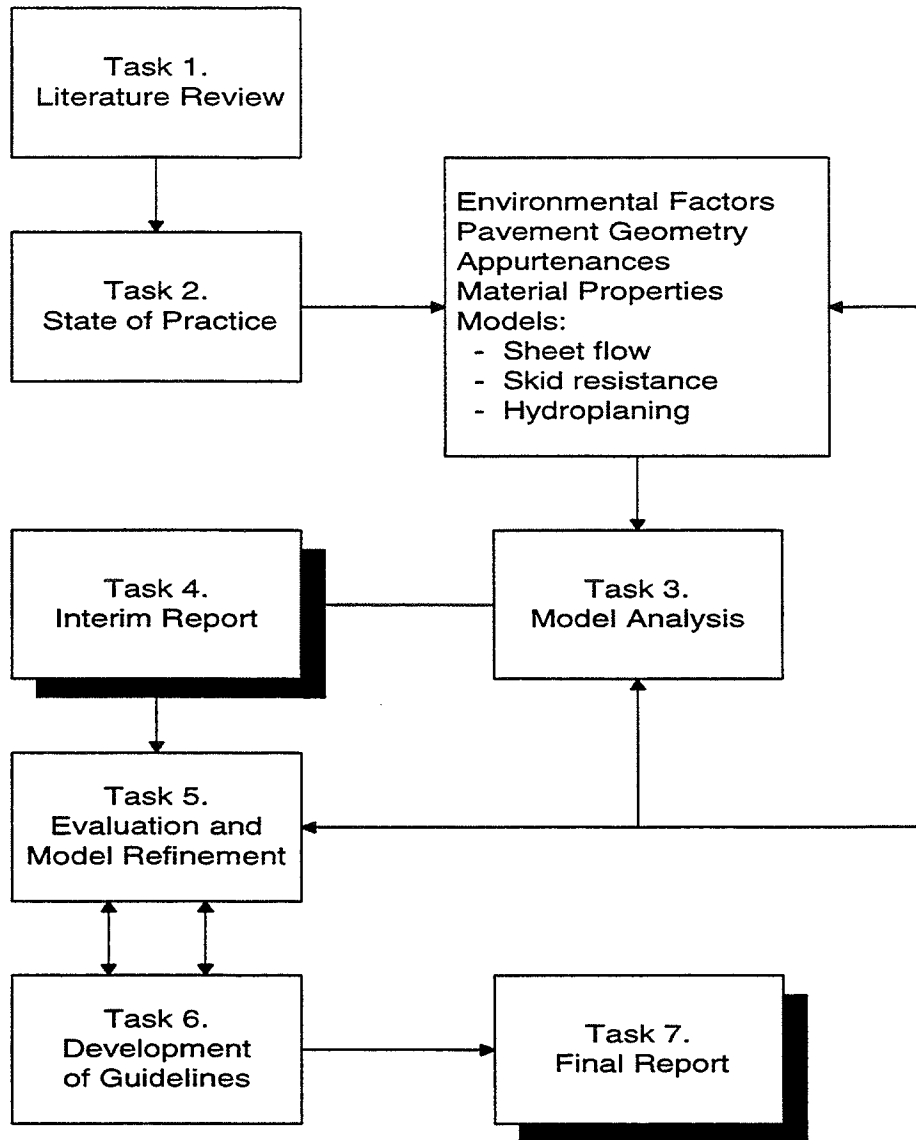


Figure 3. Research tasks.

basis of an interactive computer program that can be used by a design engineer in the process of designing a highway pavement section. The model, which predicts the depth of sheet flow resulting from rainfall, is based on pavement geometry, pavement surface type and texture, the presence of appurtenances, and rainfall rate. By selecting maximum allowable water film thicknesses that can be allowed without the onset of hydroplaning, the design engineer can use the proposed design guidelines to select and specify the pavement geometry, surface characteristics and mixture type, and appurtenance design required to satisfy the hydroplaning criteria. The design guidelines and associated computer program allow the design engineer to select pavement geometries that minimize sheet flow; to select and locate drainage appurtenances; and to select various mixture types and surface textures that will also minimize water film thickness and the potential for hydroplaning.

In order to develop the computer model and the design guidelines, it was necessary to conduct permeability studies on various open-graded or porous asphalt mixtures, to establish Manning's n for selected PCC and asphalt concrete surfaces, and to conduct full-scale skid testing on open-graded pavement surfaces.

Findings from the literature review and based on assessment of the current state-of-the-art based are summarized in Chapter 2 along with an overview of the proposal methods for controlling surface drainage. The rationale for choosing the models that were used in developing the guidelines is provided in Chapter 3. The results of testing performed during this study are presented in Chapter 4, and a set of recommendations and conclusions are given in Chapter 5. An overview of the interactive computer or program, PAVDRN, which was

developed as part of this study, is given in Appendix A. Other supporting documentation is given in Appendices B through D. The “Proposal Design Guidelines for Improving Pavement Surface Drainage” and the PAVDRN program are available from NCHRP via the internet and present detailed descriptions of several of the experiments to determine Manning’s n.

CHAPTER 2

LITERATURE REVIEW AND CURRENT PRACTICE AND TECHNIQUES FOR IMPROVED SURFACE DRAINAGE

Water films develop on the pavement surface during natural rainfall and tend to increase in thickness along the water drainage or flow path. At the onset of rainfall, the water first occupies the macrotexture on the pavement surface and is contained within the macrotexture of the pavement surface or is drained from the surface through grooves or internal drainage (porous asphalt surfaces). With increasing rainfall, a film of water forms above the macrotexture. The flow of water on the pavement surface under these conditions is referred to as sheet flow; the depth of the sheet flow tends to increase in the direction of the drainage path. The depth of the sheet flow is of critical importance because the depth of this flow controls the skid resistance of the pavement and the tendency for hydroplaning. The vehicle speed at which hydroplaning occurs is inversely proportional to the depth of the sheet flow.

The pavement design engineer must be able to identify any points on the pavement where sheet flow is sufficient to cause hydroplaning and must provide alternative or complementary strategies for reducing the depth of the water film thickness. The models identified during this study provide the tools needed to calculate the depth of sheet flow as a function of four general pavement characteristics: pavement geometry, location and capacity of drainage appurtenances, surface texture of the pavement surface, and any internal drainage

offered by open-graded asphalt concrete (OGAC) surfaces or grooved portland cement concrete pavements. The term open-graded asphalt concrete is used in this study to indicate either open-graded asphalt friction courses (OGAFC) or porous asphalt. Both types of mixes provide internal drainage; OGAFC is typical of U.S. practice, porous asphalt is typical of European practice. By varying any one or any combination of these characteristics, the pavement design engineer can predict the effect of the characteristics on the water film thickness and, in turn, the propensity for hydroplaning. As part of this study, an interactive computer program, PAVDRN, was developed to predict water film thickness and the potential for hydroplaning. The program is described in Appendix A.

SUMMARY OF MODELS NEEDED TO DEVELOP GUIDELINES

The one-dimensional, steady-state, kinematic wave equation was selected for calculating water film thickness in the computer-based design program, PAVDRN. The selection of a one-dimensional flow equation was based on computational stability and efficiency. The major advantage of the one-dimensional, kinematic wave model is that it is easy to apply and is computationally stable. A full description of this model is given in Chapter 3, where the development and rationale for choosing the various models used within PAVDRN are discussed.

A number of other models were needed to develop PAVDRN. These include models for:

- Predicting the flow through porous pavement surface layers: For this purpose, the water film thickness model for impervious surfaces was modified to account for internal flow.
- Relating sight distance and vehicle speed to rainfall intensity i : a model from the AASHTO design guide (1) was selected for this purpose.
- Predicting hydroplaning speed (HPS): A model first proposed by Gallaway (3) was used for this purpose. The HPS is a function of water film thickness and pavement macrotexture (MTD).
- Determining the hydraulic roughness coefficient, Manning's n : This is an empirical parameter (see equation 18) that depends on the type of surface and the Reynold's number, N_R . The Reynold's number is a dimensionless parameter that is used to identify flow as laminar or turbulent (see equation 20). Relationships were developed on the basis of data in the literature and new data collected as part of this study for three cases; portland cement concrete pavements, dense-graded asphalt surfaces, and open-graded asphalt concrete surfaces.

A full description of the rationale used in selecting these models and in their development is given in Chapter 3 and in Appendices B through D.

METHODS FOR CONTROLLING WATER FILM THICKNESS

A literature survey and a questionnaire were used to establish the current state-of-the-art methods for pavement surface drainage. Implementable techniques for improving surface

drainage that resulted from the literature survey and from a questionnaire sent to 72 highway agencies can be grouped into four broad categories:

- Optimization of geometric design parameters such as cross-slope;
- Reduction of the distance that the water must flow (flow path) by installing drainage appurtenances;
- Use of internally draining (asphalt concrete) wearing course mixtures;
- Use of grooving (per hard cement concrete); and
- Maximization of surface texture.

Controlling Water Film Thickness Through Pavement Geometry

Highway geometric design criteria have evolved over many years and are designed to ensure the safe and efficient movement of vehicles. State agencies and many other transportation agencies use the guidelines issued by the American Association of Highway and Transportation Officials (AASHTO) (*1*) for geometric design. The drainage capacity of a highway surface is determined primarily by its surface geometry, especially cross-slope. Geometric design criteria that enhance drainage are often in conflict with the design criteria for safety and driver comfort. Thus, although changes in the criteria contained in current geometric design guidelines may be desirable from the standpoint of improved drainage, there is little possibility that such changes will be effected solely for the sake of enhanced drainage. Geometric design criteria are presented in detail in the AASHTO design guidelines (*1*) but are

reviewed briefly here to illustrate geometric criteria that control surface drainage, but that must be satisfied during the pavement design process.

The longitudinal slope of the pavement is referred to as its "grade." Criteria for both minimum and maximum grades are necessary for proper geometric design. Minimum allowable grades are necessary for drainage concerns, while maximum allowable grades must be specified for safety reasons and to control traffic flow. The longitudinal slope of the pavement and its surrounding gutters and ditches is usually the same within each section of highway. Therefore, this discussion covers all three areas of the pavement system.

Maximum grades have been established based on vehicle operating characteristics, particularly, the operating performance of larger vehicles such as tractor semitrailers. Steep grades can be difficult to descend and vehicles often reduce speed when ascending excessively steep grades. In general accordance with the AASHTO policy (1), maximum grades are determined by the functional class and design speed of the roadway and the surrounding topography. Typical maximum longitudinal grades are shown in table 1. The development of many of the models that were reported in the literature also was performed using regression in English units. The original form of the models is retained throughout this report to maintain the integrity of the original analyses. Where English units occur, conversions between English and System International (SI) units are given in the text.

Minimum grades are required to ensure adequate drainage. This is important for curbed roadways since water cannot drain laterally from a roadway when curbs are present.

Table 1. Maximum recommended grades (1).

Design Section	Design Speed, mi/h (km/h)				
	30 (48)	40 (64)	50 (80)	60 (96)	70 (112)
Rural Sections,					
Maximum Grade, %					
Level	--	5	4	3	3
Rolling	--	6	5	4	4
Mountains	--	8	7	6	5
Urban Sections,					
Maximum Grade, %					
Level	8	7	6	5	-
Rolling	9	8	7	6	-
Mountains	11	10	9	8	-

The minimum grade recommended is 0.5 percent, but, if this cannot be obtained, 0.3 percent can be used as long as no curbs are present, and the roadway is crowned properly (1).

Vertical curves connect segments of constant grade. Since these curves often represent a change between a positive and negative grade, a level section exists at the transitions between positive and negative grades. AASHTO policy (1) is to design vertical curves using a "K-value." The K-value is defined as the horizontal distance in feet (meters) required to effect a 1-percent change in the gradient of the grade. To limit drainage problems, according to AASHTO (1), K-values used in design should be less than or equal to 167 ft (51 m) for both crest and sag vertical curves. Basically, a K-value of 167 ft (51 m) states that a 0.3-percent grade is the minimum grade allowed with 50 ft (15 m) of the level pavement on a vertical

curve. If K-values greater than 167 ft (51 m) are used, special attention should be given to the selection of pavement geometry to ensure adequate drainage. This is critical in sag vertical curves since water tends to collect at the bottom of these curves.

Pavement cross-slopes (transverse) are a compromise between drainage (steep slopes) and driver comfort and safety (flat slopes). Cross-slopes may be formed in a number of ways, as shown in figure 4. In this figure, section 2 removes the water from the roadway faster than section 1, but more inlets are needed to collect the water at the edge of the pavement. These sections are recommended if freeze-thaw is common. Drainage can be directed in two ways, sloping toward the median or sloping toward the shoulder. If a highway slopes toward the median, more inlets will be needed, but less water will be in the outer travel lane, while more water will be in the inner, high-speed lane. Figure 4 shows a variety of drainage configurations including drains located within the traveled way. These are discussed in more detail in Chapter 2. This shows that cross-slopes are a compromise between many factors, and each has to be given serious consideration.

As with longitudinal pavement slopes, a maximum and minimum superelevation is suggested by AASHTO (1). Research by Gallaway et al. (4) has shown that superelevations of two percent have little effect on driver comfort or vehicle stability. The maximum transverse slope recommended by AASHTO is two percent per successive lane. The maximum slope permissible, as recommended by AASHTO (1), is four percent. Typical cross-slopes for various pavement types are presented in table 2.

Figure 4. Different lateral drainage configurations with and without lateral drains.

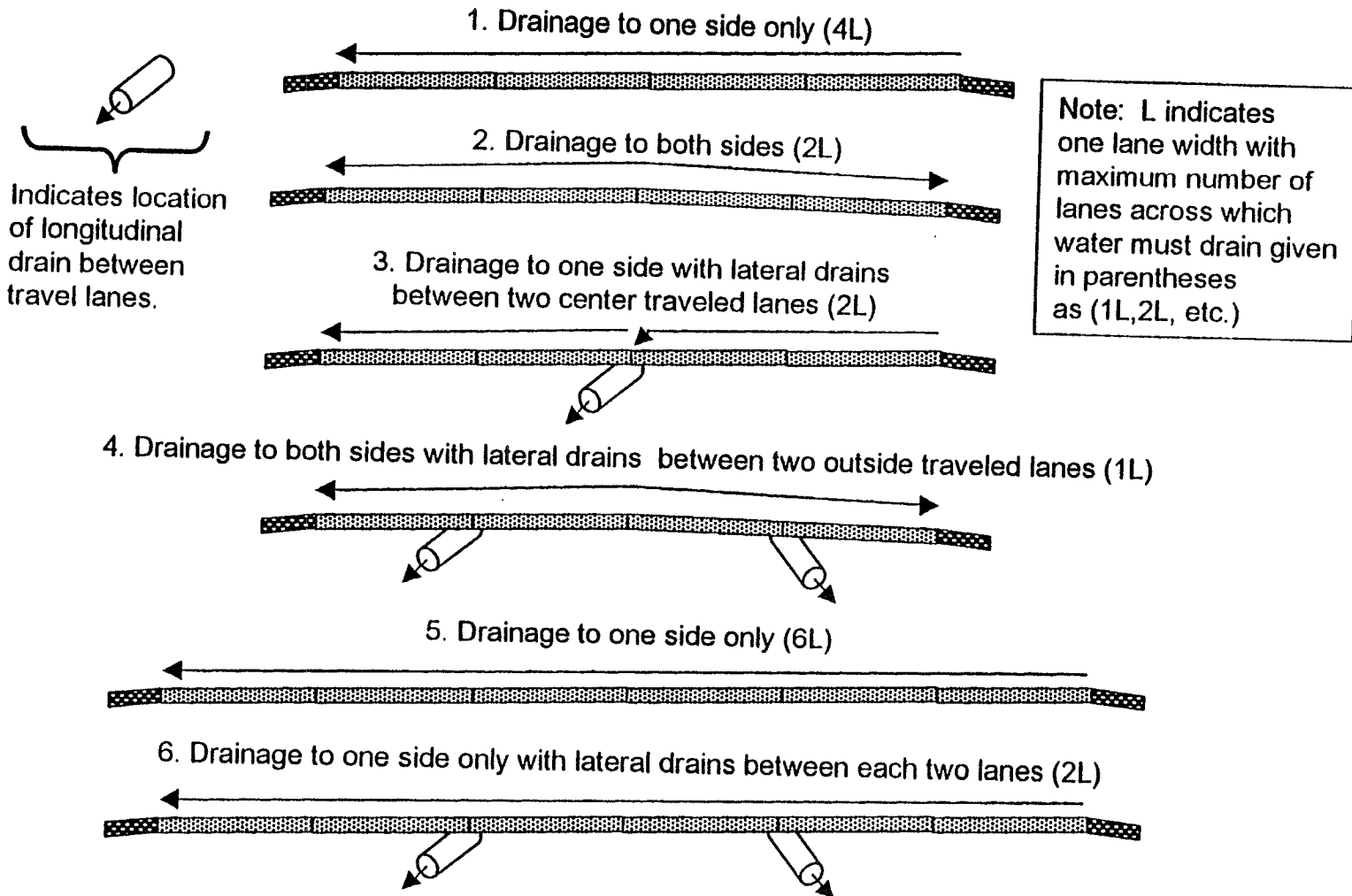


Table 2. Typical cross-slopes for different pavement surfaces (1).

Pavement Type	Cross-slope (%)
High	1.5-2
Intermediate	1.5-3
Low	2-6

On longitudinal curved sections of highways, the pavement is typically superelevated. A limit is placed on the rate of superelevation for driver comfort and safety. If the superelevation is too high and speeds are too low, drivers will need to steer up the slope. Also, vehicles can slide toward the inside of the curve if ice is present on pavements with high superelevations.

For reasons given above, the absolute maximum superelevation is 12 percent. Other maximum cross-slopes exist and are applied depending on the situation (1). If ice and snow are common, a maximum superelevation of eight percent is used. When heavy traffic volumes and low speeds prevail, a maximum slope of six percent is used. In urban areas, when speeds are low, curves can be designed without superelevation. A summary of maximum allowable values for superelevation rates is presented in table 3.

Table 3. Maximum allowable superelevation (1).

Situation	Slope (%)
Absolute Maximum	12
Ice and Snow Uncommon	10
Ice and Snow Common	8
Urban, Low Speed	6

In order to obtain full superelevation on the curve from a tangent section of roadway, the "1/3 rule" is commonly applied. This rule states that 2/3 of the superelevation should be obtained before the beginning of the horizontal curve. This transition distance is called the length of "runoff." This runoff length can be obtained from most highway design manuals and is a function of design speed, highway curvature, and lane width. Transition is an important element in drainage design: When moving from a normally crowned pavement to a superelevated pavement, the pavement surface is usually rotated about the center line of the highway. This causes a section of the pavement to be level. Consequently, when considering pavement surface drainage, special attention should be paid to these transition areas.

After the water has drained from the traveled lanes, the shoulders or parking lanes must either convey the water to an inlet or drain the water to ditches. Shoulders are typically used on rural roadways, while parking lanes and gutters are used in urban areas. Consideration of curbs, gutters, and other drainage appurtenances is beyond the scope of this project; they are examined elsewhere (5,6).

Based on this research project, the authors recommend that *AASHTO review its current policy on the geometric design of highways and streets to consider establishing minimum cross-slope recommendations for highway pavements (I)*. The results of this study show that as the longitudinal slope or grade increases, the cross-slope of a pavement section should also be increased in order to remove water more rapidly from the pavement. This effectively shortens the distance a droplet of water must travel to reach the nearest appurtenance of a pavement edge (maximum flow path length; see figure 5), a critical design parameter for pavement drainage.

In summary, the use of geometry to reduce water film thickness on pavements is constrained by the need to ensure driver comfort and vehicle stability. This effectively limits the maximum cross-slopes that can be used to remove water from the pavement, and thus other methods are required to enhance drainage and reduce the depth of water on the pavement. Most importantly, even though pavement geometry is an important factor in determining water film thicknesses, it alone may not correct drainage situations that lead to the potential for hydroplaning. Consequently, other means of drainage and water film thickness control are needed as described in the following.

Controlling Water Film Thickness Through Use of Appurtenances

Drainage appurtenances are a very effective means for removing water and shortening the distance that water must flow in order to be removed from the pavement surface. Shortened flow paths imply reduced water film thickness. Traditionally, flow from the

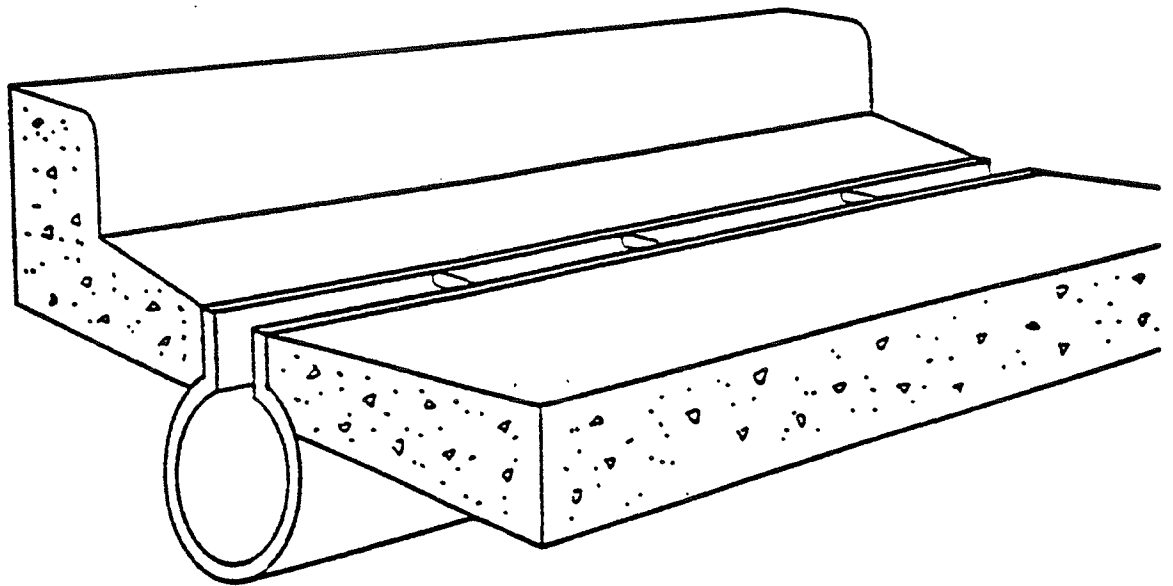


Figure 5. Typical slotted drain.

pavement has been directed to the shoulder area and collected there. Drains installed between traveled lanes in the roadway surface itself have received little attention from design engineers or manufacturers of drainage appurtenances. Slotted drains in particular offer considerable potential as a means for shortening the length of the water flow path by simply reducing the distance that the water must flow before it is removed from the surface as illustrated in figure 4.

Comprehensive analyses of the interception capacity and spacing recommendations for drainage appurtenances have been performed in many studies (7,8). These studies have traditionally evaluated appurtenances located along the outer edge of the travel lanes. This section discusses the use of appurtenances located within the traveled section of the roadway between adjacent travel lanes.

A questionnaire was sent to transportation agencies in August of 1993 as part of this project to identify current drainage practice. The responses indicate a general agreement among the agencies as to the preferred choice of methods for removing water from the pavement surface. The traditional procedure is to allow the water on multilane, high-speed highways to flow over the pavement surface to the shoulder(s). There, the water is channeled to a drainage swale or to a curb or gutter inlet. Depending on the geometry of the roadway section, appurtenances for collecting surface water can be placed on the outer edge of the travel lane or in the median section. Responses from the questionnaire indicate that the selection and spacing of curb opening inlets is usually determined in accordance with standard highway design guidelines such as the *AASHTO Policy on Geometric Design of Highways and*

Streets, Highway Drainage Guidelines published by AASHTO, *Drainage of Highway Pavements: HEC-12*, or individual agency standards (1,6,8).

Responses from the questionnaire indicated that only seven agencies use slotted drains along the outer edge of the travel lane. One agency reported spacing slotted drains at intervals of 800 mm (2 ft 8 in). Two agencies were considering using longitudinal slotted drains to drain curbed medians. Four states reported using longitudinal slotted drains between traffic lanes, and several state DOT's were considering their use. Slotted drains are pipe sections with an opening cut along the longitudinal axis and with transverse bars spaced in the opening to form slots, as shown in figure 5. Many configurations exist. They are produced by a number of manufacturers, and all manufacturers provide detailed descriptions of their drains as well as design criteria for their use.

Although longitudinal slotted drains appear to be very attractive in terms of enhancing pavement drainage, slotted and other drains located within the traveled way do pose several potential problems that should be addressed. A possible disadvantage of such a system is the potential for plugging. In the event of plugging, severe ponding could develop on the pavement surface, creating a safety hazard. Retrofitting existing pavements to accommodate slotted drains within or between the traveled lanes would be costly except, during major rehabilitation if the pavement cross-slope must be modified to accommodate the drains.

Drainage structures within trafficked areas are subject to settlement resulting from traffic loads, causing unevenness in the roadway surface. Design procedures for supporting slotted drains when they are installed within the traveled (loaded) portion of the pavement need to be established. For this reason, the installation of slotted drains at the edge of existing pavements may be the most cost-effective use of slotted drains.

In summary, slotted drains are used only on a limited basis by highway agencies to drain the roadway surface. Their use by design agencies is encouraged. Placing longitudinal drains between traveled lanes is especially effective in reducing the flow path length (see figure 5), particularly for multi-lane pavements. Special consideration may be needed to provide structural support for drains within the traveled way; on the basis of this study, more widespread use of slotted drains is warranted, and studies held to implement the wider use of slotted drains should be initiated. The design of slotted as well as other drains and their capacity was beyond the scope of this study.

Controlling Water Film Thickness with Internally Draining Asphalt Surfaces (OGAC)

Another technique for reducing water film thicknesses on a roadway surface is the use of internally draining or open-graded asphalt concrete. The purpose of this discussion is not to research these asphalt surfaces per se, but to point out their potential use in minimizing water film thickness and hydroplaning potential. Therefore, a brief summary of the use of internally

draining asphalt concrete is given in this section. These surface mixtures can reduce the water film thickness; by (1) allowing internal drainage, which effectively reduces the amount of water that must be drained across the surface of the pavement and (2) by increasing the mean texture depth. Most research reports and engineers emphasize the internal drainage aspects of these mixtures, but the enhanced surface texture that they afford may be of equal or more importance than the internal drainage that they provide.

The first use of porous or permeable surface layers in the United States occurred in the State of Oregon in the early 1930's (9). This pavement consisted of a surface treatment that was placed on an impermeable base layer. The permeable surface layer increased the frictional resistance of the surface, but the pavement was short-lived during periods of heavy traffic load. From this early work, open-graded asphalt friction courses (OGAFC) developed. These mixes typically contain 10 to 13 percent air voids (9) and are hot-laid with a paving machine to a depth of approximately 19 mm. The maximum aggregate size ranges from 13 to 19 mm. Asphalt content is selected as the maximum amount of asphalt that the hot mix can retain without appreciable drainage when the mixture is still hot. This is determined by placing mixes with differing asphalt contents on a plate in an oven and measuring the amount of asphalt that drains from the mix. These mixes offer increased skid resistance and allow internal drainage of surface water from the pavement surface (10).

Open-graded mixtures with larger air-void contents, referred to as porous asphalt, drainage asphalt, or permeable asphalt, have evolved from the early use of open-graded

asphalt friction course OGAFc (9-17). These mixtures have been used extensively in Europe; they are placed in a thicker lift than OGAFc (usually greater than 25 mm thick) with binders that are modified with fiber or polymer (18,19). These mixtures contain approximately 20 percent air voids, which is significantly higher than the OGAFc surface mixes used in the United States. Porous asphalt surfaces offer high values of skid resistance and contribute to the removal of water from the pavement surface. A summary of the mixture characteristics for different porous pavements as used in the United States and Europe is provided in table 4 (10-17,20).

The effectiveness of porous asphalt can be enhanced if drains are installed internally within the pavement layers. Continuous fabric drains that can be placed either transverse to or longitudinally with the direction of traffic have been used successfully for a number of years. The drains can be laid flat (drains have a rectangular cross-section) and may be placed with a new porous asphalt layer when the pavement is overlaid or during new construction. Details of this system and its use are given elsewhere (21).

The use of porous asphalt pavements is a controversial subject with many state highway agencies. Although porous asphalt pavements are generally accepted as useful with respect to reducing hydroplaning, their performance has been unsatisfactory in many states, to the extent that several states have eliminated their use entirely. In contrast, they are used extensively on the motorways in Europe, especially in France and the Netherlands. By the year 2002, all of the motorways in the Netherlands must be surfaced with porous asphalt mixtures (22).

Table 4. Gradations used for internally draining asphalt mixes.

Size	Percent Passing				
	Oregon (9)	Typical Europe (22)	Swiss (13)	Belgium (14)	France (17,18)
25.0 mm	99-100	-	-	-	-
19.0	85-96	100	-	-	-
14.0	-	-	-	100	100
12.5	60-71	-	-	-	-
11.2	-	90-95	-	-	-
10.0	-	-	100	-	55
9.5	-	-	-	-	-
8.0	-	28-40	-	-	-
6.3	17-31	-	-	-	23
5.0	-	18-23	-	-	-
4.75	-	-	-	-	-
2.75	-	-	-	-	-
2.36	-	-	-	-	-
2.0	7-19	10-12	-	17	14
710 μ	-	6-8	-	-	-
250	-	4-6	-	-	-
90	-	2-4	-	5	-
74	1-6	-	-	-	-
Air Voids (%)	5.7-10	17-22	14-20	16-28	24
Thickness (mm)	1.5-2.0	40-50	28-50	40	42
Permeability, (l/s)	-	0.06-0.12	0.057	0.0078- 0.023	0.02

The following are cited as advantages of porous asphalt pavements:

1. Hydroplaning. Porous asphalt pavements reduce the thickness of the water film on the surface of the pavement, thus greatly reducing tendency for splash and spray from vehicles and the hydroplaning potential of the pavement.
2. Skid Resistance. The skid resistance for porous asphalt pavement is generally considered to be equal to that of traditional pavements. Testing performed by van der Zwan et al. (12) showed that at higher vehicle speeds, where aggregate macrotexture has a greater effect on skid resistance, porous pavement actually gives a higher skid resistance than conventional pavements.
3. Splash and Spray. Surface water can quickly infiltrate into porous asphalt, greatly reducing the amount of free surface water, which causes splash and spray from the vehicle tires. This reduction in splash and spray provides greater visibility, resulting in safer roadway conditions than on portland cement concrete or conventional dense-graded asphalt pavements (23-25).
4. Headlight Reflection. With the surface water infiltrating into the pavement, the reflections of vehicle headlights are greatly reduced and the visibility of roadway markings is increased.

Porous asphalt surfaces offer a significant increase in surface texture over conventional dense-graded surfaces. The increased texture, in conjunction with internal drainage, can result in a significant reduction in the hydroplaning potential. However, there are a number of disadvantages associated with these surfaces:

1. Skid Resistance. At lower speeds, the skid resistance of porous asphalt is lower than for conventional asphalt surfaces, because there is less aggregate surface at the

tire-pavement interface for porous asphalt mixes. The microtexture of these surfaces is generated primarily by the coarse-sized aggregate particles. This is not considered a serious disadvantage because on high speed motorways, skid resistance is critical at high speeds, not low speeds.

2. **Plugging.** There is a tendency for the voids in porous asphalt surfaces to become plugged and filled with antiskid material and other roadway debris such as sediment runoff and material spilled on the road surface. During their first year of use, approximately one third of the permeability of porous pavements is lost as a result of plugging (26). The French have concluded that a level of approximately 20 percent voids is needed for porous pavements to perform effectively. Therefore, current design practice in France requires initial void contents of 27 to 30 percent (17).
3. **Deicing Performance.** Road salts tend to infiltrate into the surface voids reducing the effectiveness of the salt or requiring larger application rates than for conventional surfaces. It takes three times the amount of salt on porous pavements as on traditional pavement types to produce the same deicing effects (18). Anti-skid materials also tend to plug the voids in porous pavements.
4. **Black Ice.** Porous asphalt surfaces have a tendency to develop black ice more quickly than conventional dense-graded pavements. Black ice can occur suddenly at the onset of a light rainfall when the internal pavement temperature is near or above freezing, and the air temperature is at or below freezing. Because porous asphalt conducts heat less readily than dense-graded mixtures the water on the pavement surface freezes more rapidly. The formation of black ice is a serious safety concern and has caused French authorities to discontinue the use of porous asphalt surfacings in the Alps where the conditions for the formation of black ice are common.

5. Raveling. Raveling and loss of adhesion between porous asphalt surface layers and the underlying layers are the most frequently cited performance problems in the United States. However, the raveling problem may be alleviated by carefully selecting proper modifiers or the amount and type of asphalt binder in the mix (17-19).
6. Delamination. There have been instances when the open or porous mixtures delaminated from the underlying pavement. This behavior, which occurred in Maryland in the winter of 1994, is apparently caused by the freezing action of water when the porous layer is saturated (27). The cause of the delamination is hypothesized as follows: If the freezing of the water in the layer proceeds simultaneously from the top and the bottom simultaneously, there is no outlet for the expanding water as it freezes. The expanding water then creates sufficient force to delaminate the surface layer. Extensive delamination caused Maryland to abandon open-graded mixtures.

There appears to be a general consensus among pavement engineers that porous asphalt surfaces can greatly reduce the potential for hydroplaning. Porous asphalt surfaces also reduce tire noise and minimize splash and spray, thereby increasing driver visibility (11,18,25,26,28). Reducing splash and spray makes the roadway safer to travel on during periods of rainfall. Tappeiner (20) cites a European report that states that there were 20 percent fewer fatalities and injuries by motorists while traveling on porous asphalt pavements during wet weather conditions. A similar reduction was also reported in the United States (9). These claims for improved safety must be considered within the context of the French experience where problems with black ice formation have been observed.

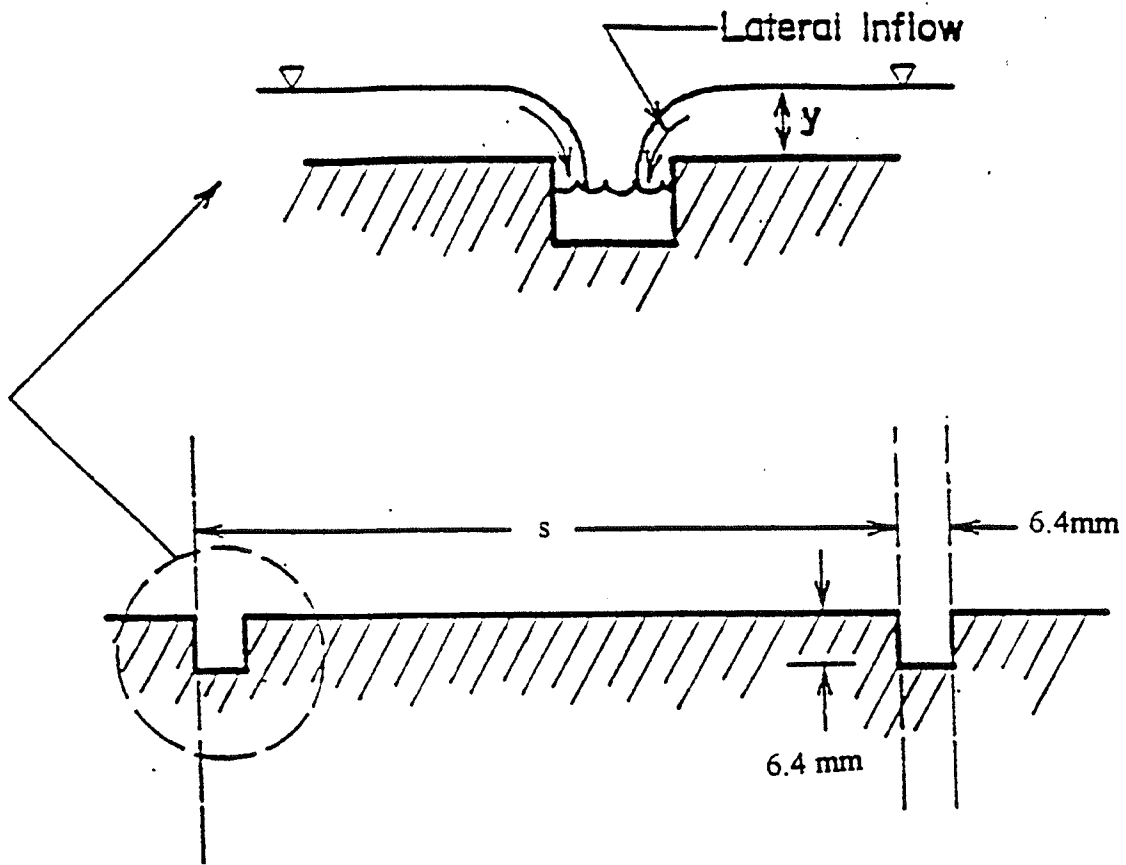
In reviewing the advantages and disadvantages of porous asphalt surfaces, it can be seen that this type of pavement has many positive attributes if careful attention is given to mix proportions, materials selection, and construction details. Porous asphalt surfaces, especially

newer mixture designs with special binders, warrant greater use in the United States although their disadvantages must also be carefully considered.

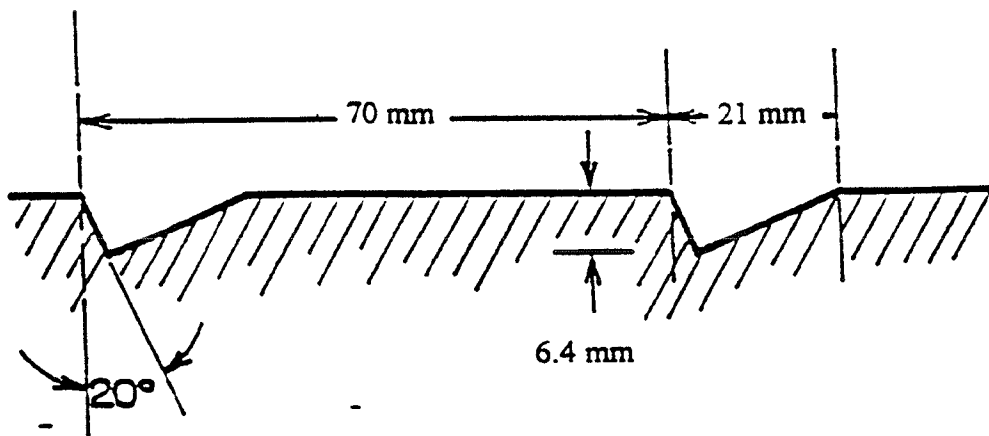
Controlling Water Film Thickness with Grooving

The fourth method for reducing water film thicknesses is the use of grooving on portland cement concrete surfaces. Grooving is generally ineffective on asphalt concrete surfaces because the grooves close quickly under the action of traffic. The grooves in portland cement concrete act as subsurface channels that drain water from the pavement surface. The use of grooving for airport pavement has considerable attention by researchers (29). Typical grooving patterns used for airport runways are shown in figure 6 (30). A typical airport runway may consist of two 30-m (100-ft) wide lanes, each sloping laterally from a center crown at 1.5 percent. Hence, grooves are perpendicular to the wheel path and in the direction of the water flow. To be fully effective, the grooves should be parallel to the direction of flow; for highways with both a longitudinal and across slope, the grooves must be skewed to the direction of traffic if the grooves are to be parallel to the water flow. This is often not practical and reduces the effectiveness of the grooves as drainage channels.

Reed et al. (30) used dye tests to confirm that all the rain falling on the upstream end of the flow path was carried in the grooves in such a way that the slab surface, although wet, had zero water film thickness. The width of the area contributing lateral inflow to the grooves was equal to the groove spacing for spacings of 127 mm (5 in) or less. It was also possible to predict the location where the grooves began to overflow, overflowing water contributes to the water film thickness. The down-slope point at which the grooves were full, and runoff began to spill out onto the pavement surface was called the breakout point. This point serves as the origin for sheet flow and the point where water film starts to develop.



(a) Rectangular groove pattern
 $s = \infty, 127 \text{ mm}, 64 \text{ mm}, 32 \text{ mm}.$



(b) Reflex-percussive groove pattern.

Figure 6. Typical grooving patterns for portland cement concrete pavement (30).

The breakout point was computed by considering the equilibrium flow rate and the capacity of the grooves, both of which were a function of rainfall rate and down-slope distance. The equation for the breakout point is (31):

$$L = (1.50) / (s i n_g) \quad (1)$$

where

- L = Breakout distance measured from top edge of pavement (ft) (1 ft = 3.05 m)
- s = Groove spacing (in) (1 in = 25.4 mm)
- i = Rainfall rate (in/h) (1 in/h = 25.4 mm/h)
- n_g = Manning roughness coefficient for grooves

The coefficient 1.50 is a function of groove geometry, and as given in equation 1 is for 6-mm-by-6-mm (0.25in-by-0.25-in) rectangular grooves with a pavement surface slope equal to 1.5 percent.

The results of data generated by Reed et al. (30) for grooved portland cement concrete pavements are summarized in figure 7. The figure was developed for a rainfall intensity of 75 mm/h (3 in/h). The breakout points are shown on the graph as the intersection of the curves with the abscissa. The smaller the groove spacing, the greater is the distance to the breakout point L. The Manning roughness coefficient for the grooves, n_g , was taken as 0.01 (31).

Grooving can reduce the water film thickness on pavements by acting as drainage channels and thereby carrying water from the pavement surface. However, unless grooves are parallel to the slope of the pavement, their ability to conduct flow is reduced and their effectiveness minimized. In summary, grooving portland cement concrete pavements can reduce water film thickness and thus increase the speed at which hydroplaning will occur. This has been demonstrated for grooves whose principal orientation is in the direction of the flow path of the water (30). The PAVDRN model, documented in Appendix A, uses

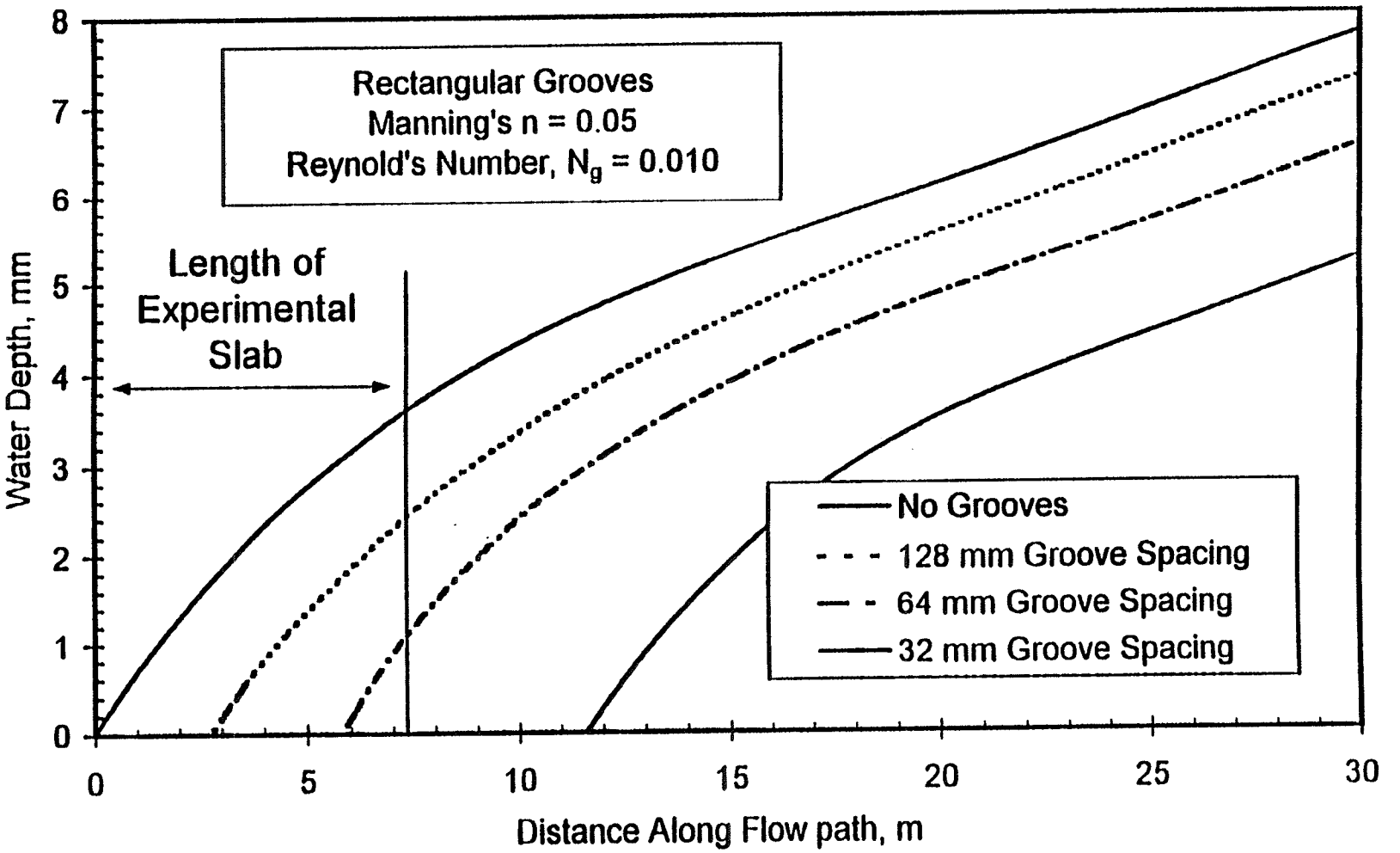


Figure 7. Predicted water film thickness, WFT, for grooved portland cement concrete pavement, rainfall intensity 75 mm/h (30).

information about groove spacing, width, and depth to effectively increase the mean texture depth of the pavement and thus increase the speed at which hydroplaning occurs.

Controlling Water Film Thickness with Surface Texture

Another method for controlling water film thickness is by maximizing the texture of the pavement surface. The water film thickness is the total thickness of the film of water on the pavement minus the water trapped in the macrotexture of the pavement surface. Water film thickness is reduced in direct proportion to the increase in macrotexture (total macrotexture volume, not MTD). The importance of macrotexture for asphalt surfaces is discussed in a previous section on the use of porous asphalt to control water film thickness. Since porous asphalt surfaces are typically prepared from relatively coarse aggregates or gradations with a minimal quantity of sand-sized material, they generally yield large levels of macrotexture. The macrotexture of other asphalt surfaces is also controlled by the gradation of the aggregate, ranging from very low levels of macrotexture for sand asphalt to relatively large levels of macrotexture for coarse-graded mixture and surface treatments. The importance of macrotexture is recognized in French practice where microsurfacing techniques are now widely used and have replaced porous asphalt in areas where the performance of porous asphalt has been suspect (see also the section on porous asphalt as a method for controlling water film thickness). Microsurfaces are thin lifts of hot-mix asphalt concrete graded to maximize surface texture.

Macrotexture is also important for portland cement concrete surfaces. New portland cement concrete pavement surfaces in the United States are typically constructed with tined surfaces to enhance macrotexture. Macrotexture produced by tining or brooming is to be distinguished from grooving. The texture of portland cement concrete pavement can be enhanced by etching away the mortar exposing the coarse aggregate (new construction) or by grinding (to restore texture in old pavements) although these techniques are not used often in practice and often result in high levels of tire noise.

The importance of texture is recognized in the "Proposed Design Guidelines for Improving Pavement Surface Drainage" (2) where the pavement texture is one of the design options. The importance of macrotexture may not always be demonstrated with the standard ASTM E 274, "Standard Test for Skid Resistance of Paved Surfaces Using a Full-Scale Tire," locked wheel tests because the test is not conducted on a flooded pavement. Instead, the water introduced in front of the tire of the moving skid tester. For example, in full-scale tests conducted at the Turner-Fairbanks Highway Research Center, no correlation was shown between macrotexture and hydroplaning speed (32).

PROPOSED DESIGN GUIDELINES FOR IMPROVING PAVEMENT DRAINAGE-IMPLEMENTATION OF FINDINGS

The design guidelines were developed as a "stand-alone" document for use by design engineers in the design of new roadway systems or the rehabilitation of existing pavements (2). The guidelines can be used by highway design engineers to evaluate the effect of different pavement parameters on the water film thickness and the potential for hydroplaning. The guidelines are complemented by an interactive computer program, PAVDRN, which allows the pavement engineer to predict water film thickness and the propensity for hydroplaning (Appendix A). The treatment of the different design parameters is reviewed briefly in this section. The reader is referred to the "Proposed Design Guidelines for Improving Pavement Surface Drainage" (2) for details.

Pavement Geometry

Five different types of design sections are considered in the guidelines and in the PAVDRN computer program. They include (1) tangent sections, (2) superelevated horizontal curves, (3) transition sections, (4) vertical crest curves, and (5) vertical sag curves. Each of these sections can be analyzed using the PAVDRN model. In the analysis, the pavement is divided into successive sections or planes according to one of the five types of design section

(see Appendix A, especially figure A-2). The flow from one type of section to another can be linked in the analysis. Geometric information is required for each section in the analysis.

For tangent sections, the guidelines recommend that, as grade increases, pavement cross-slope should also be increased up to maximum recommended values. The guidelines also recommend other control methods such as slotted drains between traveled lanes. For superelevated sections the guidelines suggest the use of a maximum recommended superelevation to minimize water film thickness on horizontal curves and the use of other methods, such as increased mean texture depth or grooving, if superelevation does not reduce the potential for hydroplaning to desired levels.

In transition sections, the effects of changes in the pavement geometry on the flow path length are fairly complex. The location of the maximum flow path length changes depending upon the difference between the cross-slope at the curve end of the transition and the cross-slope at the tangent end. Runout length also affects the location of the flow path and its length. The runout length is the distance, measured from the start of the plane and in the direction of the traveled way, to the point where the flowpath exits the plane. In general, the guidelines recommend that the runout length be shortened as cross-slopes increase. However, in transition sections concern for safety and driver comfort must be balanced. Other measures to control water film thickness might need to be applied if the shortest recommended runout length is used, and the potential for hydroplaning still exists.

Pavement Properties

There are two pavement-related factors that can be controlled by the designer to control the water film thickness: (1) pavement type and (2) mean texture depth. Four pavement types are considered in the guidelines and the PAVDRN software. The four pavement types are: (1) portland cement concrete (PCC), (2) grooved PCC (GPCC), (3) dense-graded asphalt concrete

(DGAC), and (4) OGAC, which includes both porous asphalt and open-graded asphalt friction course (OGAFC).

The design information required to specify the design section varies with the pavement type. In PAVDRN, the mean texture depth (MTD) is a function of several parameters that are determined by the designer. For PCC surfaces, the water-to-cement ratio and the surface finish (e.g. degree of tining) affect the MTD. Maximum aggregate size, gradation, and air void content affect the texture of asphalt concrete mixes. OGAFC and porous asphalt surfaces have larger macrotexture than dense-graded surfaces. Porous mixtures and high air-void content mixtures both contribute to the mean texture depth and, in turn, to a reduction in the water film thickness.

Grooving PCC pavements reduces water film thickness if the grooves are oriented so that they conduct flow off the pavement. Otherwise, the effect of grooving is localized and can lead to increased water film thickness on other parts of the pavement. The guidelines provide specific recommendations with respect to groove size and spacing based upon an analysis using PAVDRN and survey responses from highway engineers.

Drainage Appurtenances

The designer's ability to reduce water film thickness on a highway pavement using geometry and pavement properties is limited. Drainage appurtenances are typically necessary to control water film thickness, especially on large, multilane facilities where the flow path length spans more than two travel lanes. The most promising technology for multilane highways is the use of slotted drains placed between the travel lanes. At least four state transportation departments reported using slotted drains in this manner. Slotted drains can also be placed transversely or across the traffic lane to capture flow. Drains used in either manner reduce the water film thickness on a pavement by removing or reducing flow over the pavement.

PAVDRN SOFTWARE

PAVDRN is intended for use by highway design engineers to determine the likelihood of hydroplaning on various highway pavement sections. It does this by computing the longest flow path length over the design pavement section and determining the water film thickness (depth of water above the asperities of the pavement surface) at points along the path. The water film thickness is used to estimate the speed at which hydroplaning will occur (if at all) along the longest flow path, the critical path in the section. The predicted hydroplaning speed along this path is then compared to the design speed of the facility, a parameter selected by the designer.

PAVDRN runs under WindowsTM 3.1 and above. The user interface was programmed in Visual Basic. The computational algorithms were programmed in FORTRAN 77. The user interface uses point-and-click technology with pull-down menus and context-sensitive help. The user's guide is available on-line and is installed as part of the help files with the PAVDRN program.

Since it is a one-dimensional model, PAVDRN first analyzes the section geometry to determine the maximum or longest flow path length over the pavement section. The program determines water depth, time to equilibrium, and velocity at points along the longest flow path length; equations for determining these values are presented in Chapter 3. The mean texture depth is subtracted from the depth to determine the water film thickness. The water film thickness, computed in this manner, is used to determine the speed at which hydroplaning will occur. Results are printed in a summary report format. They are also available as a text file that can be imported to a third-party graphics program and plotted. A sample of the summary output table is provided in table 5 based on the analysis of a tangent section with zero grade and standard 1.5-percent cross-slope.

Table 5. PAVDRN summary output table.

X (ft,m)	Y (ft,m)	Distance (ft,m)	WFT (in,mm)	Flow/width (cfs/ft,cms/m)	Manning's n	Reynold's No.	Hydr. Speed (mi/h)
150.0	.0	.00	-.50E+00	.00E+00	.000	0.	999999
150.0	1.0	1.00	.64E+00	.14E-04	.110	11.	109
150.0	2.0	2.00	.88E+00	.28E-04	.076	21.	100
150.0	3.0	3.00	.10E+01	.42E-04	.061	32.	96*
150.0	4.0	4.00	.12E+01	.56E-04	.052	42.	93*
150.0	5.0	5.00	.13E+01	.69E-04	.046	53.	91*

*Indicates hydroplaning speed is less than design speed.

Note: PAVDRN has the option of producing output in SI or English units. The data shown in the table above are in U.S. units.

Design Example Using Slotted Drains

This analysis considers a tangent section consisting of three lanes of travel in the same direction. The geometric input for the analysis of the tangent section in this example is listed in table 6.

Table 6. Tangent section properties.

Property	Value
No. of Planes	3
Length of Each Plane	300 m
Longitudinal Slope	0.02 m/m
Width of Each Plane	4 m
Pavement Type	PCC
Mean Texture Depth	0.50 mm
Cross-Slope of Plane 1	0.015 m/m
Cross-Slope of Plane 2	0.025 m/m
Cross-Slope of Plane 3	0.035 m/m

Additionally, a rainfall intensity of 80 mm/h is assumed, and a kinematic viscosity of the water of $1.306 \times 10^{-6} \text{ m}^2/\text{s}$ (water temperature = 10 °C) was chosen. These values of intensity and water temperature are conservative but might be observed in some locations in the United States. A summary of the output of the model is shown in table 7.

Table 7. PAVDRN output for tangent section.

End of Plane	Drainage Length (m)	Water Film		Hydroplaning Speed (km/h)
		Thickness (mm)	Flow/Width ($\text{m}^3/\text{s}/\text{m}$)	
1	6.66	1.3	0.00013	90
2	11.79	1.5	0.00023	88
3	16.39	1.6	0.00032	86

The results in table 7 present the final value of the water film thickness at the end of the longest drainage path length across each section of the pavement. In this example, since each lane has a different cross-slope a plane consists of one lane of travel. At the end of the first plane, the model has predicted that the flow length of water across the innermost lane will be 6.66 mm, and the hydroplaning speed at that point is 90 km/h. The lane is only 4 m wide, but the flow length will be along a distance that is the resultant of the cross-slope and the longitudinal slope. Therefore, the drainage path length will be greater than the 4-m width.

For a design speed of 90 km/h, the computed hydroplaning speed just meets the criteria to prevent hydroplaning. However, as the drainage length increases across the second and third lanes of travel, the water film thickness increases to a point where the hydroplaning speed for the third, outermost lane of travel is significantly below the design speed of 90 km/h. One solution for increasing the hydroplaning speed could be to install a longitudinal slotted drain between the second and third lanes of travel in the direction of travel (see figure 5). This drain

would intercept the flow from the second lane, reduce the water film thickness at the end of the second lane, and additionally reduce the water film thickness across the entire third lane of travel. This would reduce the hydroplaning potential of the entire roadway system to be in accordance with a design speed of 90 km/h.

From the analysis, the flow at the end of the second plane needs to be reduced to a value that will eliminate the hydroplaning potential for the system. A slotted vane grate is selected and placed between the second and third lanes. Using a design chart provided by the manufacturer to obtain a grate inlet coefficient, $K = 39$, the grate will capture $(0.000516 \text{ m}^3/\text{s})$ per meter of length of the slotted drain inlet) as determined by equation 2:

$$Q = K D^{5/3} \tag{2}$$

where

- Q = Flow rate (cfs/ft) (1cfs = 0.028 m³/s, 1 ft = 305 mm)
- D = Depth of flow (ft)

At this location in the pavement, the flow is only $0.00023 \text{ m}^3/\text{s}/\text{m}$, and therefore the total flow will be captured.

THIS PAGE INTENTIONALLY LEFT BLANK

CHAPTER 3

SELECTION AND DEVELOPMENT OF MODELS FOR PAVDRN

In order to develop guidelines for improving the drainage of water from pavement surfaces, it was necessary to select a model for predicting the depth of sheet flow on pavement surfaces. Since the maximum allowable water film thickness is the minimum flow depth at which hydroplaning is initiated, it was also necessary to select a model that can be used to predict the onset of hydroplaning as a function of water film thickness. A literature search was conducted to identify and evaluate water film thickness and hydroplaning models in the existing literature. From the literature search, a one-dimensional, steady-state form of the kinematic wave equation was selected for the prediction of the depth of sheet flow. Additional development of the model was also undertaken as part of this project.

The models and predictive equations that are contained in PAVDRN are described in this section. A more comprehensive discussion of surface flow models and the development of values for Manning's n can be found in Appendices B and C and the references cited therein.

WATER FILM THICKNESS MODEL

Before discussing the water film thickness model, the terms water film thickness (WFT), mean texture depth (MTD), and water depth, y , must be clearly be defined (see figure 1). Water depth is defined as the total thickness of the water film on the surface of the

pavement. It is the sum of the MTD and the WFT. The water below the MTD is trapped in the macrotexture and is considered immobile and does not contribute to the flow depth, y . The WFT is the thickness of the water film above the tops of the asperities on the pavement surface. The total depth of flow, y , is the thickness of the WFT plus the MTD.

There are two general types of models that can be used to determine water film thickness: (1) an analytical model and (2) an empirical model. Both types have been developed and used for this purpose.

Empirical Model

A one-dimensional, steady-state model was developed by Gallaway (2) as presented in equations 3 and 4:

$$\text{WFT} = \frac{0.003726 L^{0.519} i^{0.562} \text{MTD}^{0.125}}{S^{0.364}} - \text{MTD} \quad (3)$$

and

$$y = \text{WFT} + \text{MTD} \quad (4)$$

where

WFT = Water film thickness (in) (1 in = 25.4 mm)

L = Plane length of flowpath (ft) (1 ft = 305 mm)

i	=	Rainfall intensity (in/h)	(1 in/h = 25.4 mm/h)
MTD	=	Mean texture depth (in)	(1 in = 25.4 mm)
S	=	Pavement slope (m/m)	(1 in = 25.4 mm)
y	=	Depth of water contributing to flow (in)	(1 in = 25.4 mm)

In equations 3 and 4, the flow path, L , is presumed to be over a simple, planar surface. Gallaway's equation is based on an extensive set of water depth data for a variety of pavement types. The equation, however, does not contain a variable, such as Manning's n , to describe the hydraulic resistance of the pavement surface. The equation was developed by combining data from pavements with different types of surfaces in a single regression analysis. Since Gallaway's equation does not include a term for the hydraulic resistance of the pavement surface, does not differentiate between different surfaces, and is empirical, the equation was not considered for use in this project.

One-Dimensional Analytical Models

Two analytical models were considered during the project. The first is a fully dynamic model based on the principles of conservation of mass and momentum. The model has been used by many investigators to represent the equations of state for shallow wave motion, equations 5 and 6. Equations 5 and 6 represent spatially varied, unsteady flow in one dimension.

$$\frac{\delta h}{\delta t} + h \frac{\delta u}{\delta x} + u \frac{\delta h}{\delta x} = i - f = I \quad (5)$$

where

- y = Depth of flow
- u = Spatially averaged velocities (x - direction)
- i = Rainfall rate over the domain
- f = Infiltration rate
- I = Rainfall rate adjusted for infiltration

$$\frac{\delta u}{\delta t} + u \frac{\delta u}{\delta x} + g \frac{\delta h}{\delta x} = g(S_{ox} - S_{fx}) - \frac{u(i-f)}{h} + \frac{v_r \cos \theta_x}{h} \quad (6)$$

where u, h, i, and f are the same as described in equation 5 and

- g = Acceleration due to gravity (32.2 ft/s² or 9.81 m/s²)
- S_{ox} = Slope of the flow path in the x-direction
- S_{fx} = Slope of the energy grade line in the x-direction
- v_r = Terminal rainfall velocity
- θ_x = Angle of rainfall input with respect to the x-axis

The last term on the right-hand side of equation 6 represents the momentum due to the angle of incidence of rainfall velocity in the x-direction. The term θ_x is often taken to be

negligible; thus $\cos\theta_x$ can be assumed equal to zero, and the right-most term is dropped from the equation.

Under steady-state conditions where the friction slope, S_{fx} , is equal to the slope of the flow plane, S_{ox} , equations 5 and 6 simplify to a form known as the kinematic wave equations as presented in equations 7 through 9:

$$h_{eq} = I t_{eq} \quad (7)$$

$$t_{eq} = \left(\frac{1}{I} \right) \left(\frac{L I}{a} \right)^{1/m} \quad (8)$$

$$u = a h^{m-1} \quad (9)$$

where

h_{eq}	=	Equilibrium water flow depth (ft)	(1 ft = 305 mm)
i	=	Excess rainfall rate (ft ³ /s/ft ²)	(1 ft ³ /s/ft ² = 305 mm ³ /s/mm ²)
t_{eq}	=	Time to equilibrium (s)	
L	=	Plane length (ft)	(1 ft = 305 mm)
a	=	Friction loss coefficient	
m	=	Friction loss exponent	
u	=	Velocity of flow (ft/s)	(1 ft/s = 305 mm/s)

Equations 7 through 9 represent the kinematic wave solution for steady-state, one-dimensional flow.

Two-Dimensional Analytical Models

An analytical two-dimensional flow model written by Zhang and Cundy (33) was evaluated as part of this study. Their model is representative of two-dimensional models and illustrates the difficulties that are typical of two-dimensional models. The primary limitation of their model is the lack of stability and convergence in the solutions. Stability and convergence are relatively easy to obtain with sets of linear equations, but difficult to acquire with the nonlinear sets of equations implicit in the Zhang and Cundy model. The computational stability and convergence for nonlinear sets of equations are usually obtained by assuming linearity and using the linear solution as a conservative first approximation of the nonlinear case. As a consequence, extremely small time steps are used that result in dramatically increasing execution times as the geometric complexity of the flow surfaces augments. For a multilane pavement, this may result in hundreds of thousands of iterations to reach equilibrium conditions. Therefore, no further use was made of two-dimensional models, which are discussed in Appendix B.

Model of Choice

The one-dimensional kinematic model, represented by equations 7 through 9, was chosen as the preferred model for predicting water film thickness. This model is based on theories and includes a variable, Manning's n , that accounts for the hydraulic effect of surface roughness on water depths. The one-dimensional, steady-state form of the model was used in

developing the surface drainage guidelines and the PAVDRN program. The selection of the one-dimensional flow equation was determined by its computational stability and efficiency of solution.

The flow domain, i.e. flow paths and channels, for a one-dimensional model must be defined by the user or must be established by an analysis of the topography of the surface prior to applying equations that determine flow, depth, and/or velocity. For example, PAVDRN analyzes the topography of a section and determines the longest flow path length before applying the kinematic wave equation to determine water film thickness at points along the flow path. The longest flow path is determined from geometric conditions as the path from the point where the water falls on the pavement to the point where it exits the surface of the pavement.

The following equation is used in PAVDRN to calculate the water film thickness:

$$WFT = \left[\frac{n L i}{36.1 S^{0.5}} \right]^{0.6} - MTD \quad (10)$$

where

- n = Manning's roughness coefficient
- L = Drainage path length (in) (1 in = 25.4 mm)
- i = Rainfall rate (in/h) (1 in/h = 25.4 mm/h)

S = Slope of drainage path (mm/mm)

MTD = Mean texture depth (in) (1 in = 25.4 mm)

Values of water film thickness calculated according to equation 10 are presented in figure 8.

Subsurface Flow Model

For porous asphalt surfaces, flow within the porous asphalt layer parallel to the pavement surface must be considered. Two options were explored for the subsurface flow model. The first was based upon the consideration of three-dimensional, fully saturated flow, represented by equation 11. The second, a one-dimensional model, is discussed in the following.

$$\frac{\delta}{\delta x} \frac{(K_{xx} \delta h)}{\delta x} + \frac{\delta}{\delta y} \frac{(K_{yy} \delta h)}{\delta y} + \frac{\delta}{\delta z} \frac{(K_{zz} \delta h)}{\delta z} = W - S_s \frac{\delta h}{\delta t} \quad (11)$$

where

h = Piezometric head or potential

K_{ss} = Hydraulic conductivity of the porous material in the direction of the principal axes

W = Sources and sinks of water

S_s = Storage coefficient or specific storage of the porous material

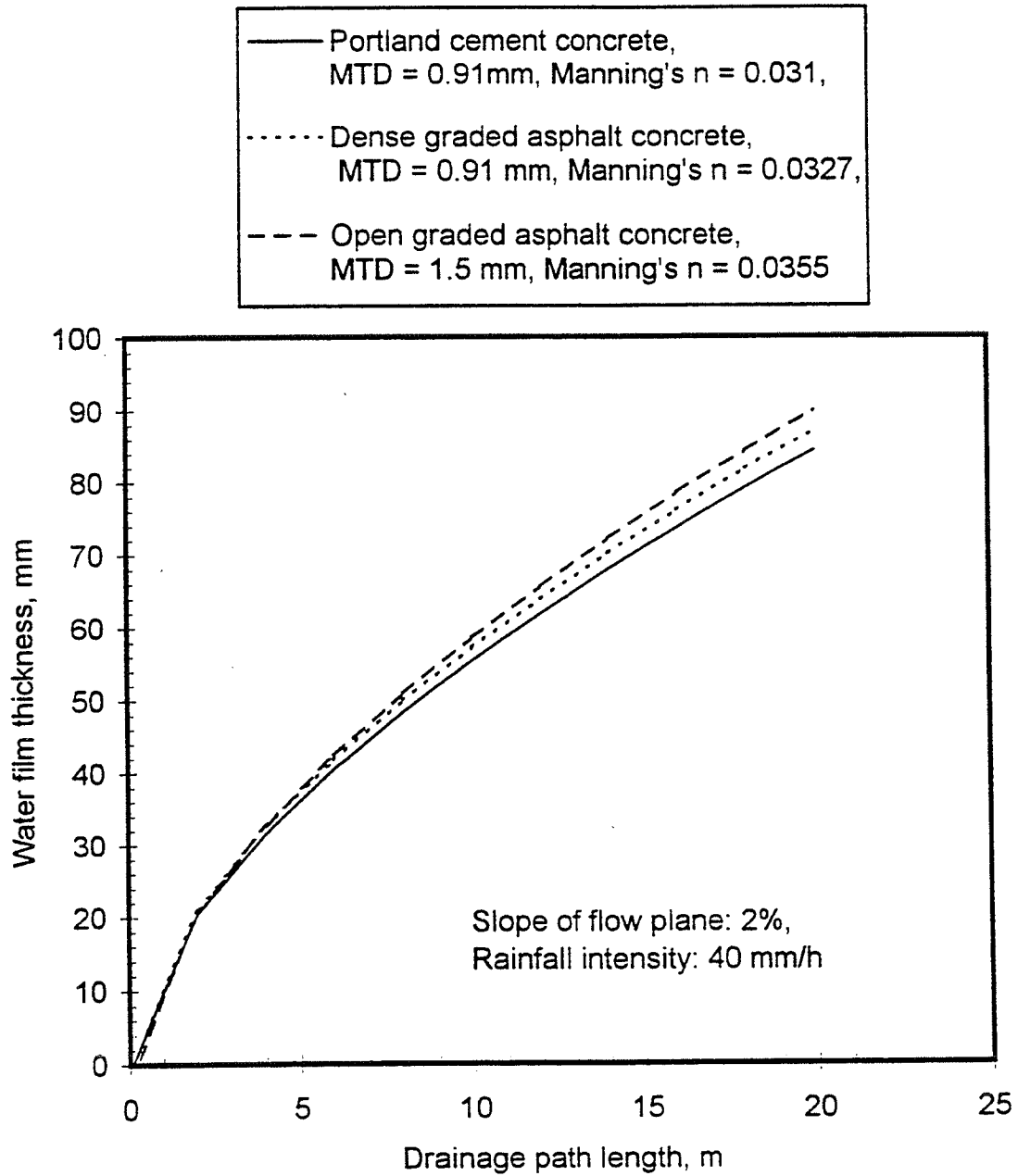


Figure 8. Water film thickness versus distance along flow path for several pavement surfaces as calculated using PAVDRN.

The solution of equation 11 for the quantity of flow can include the full dynamic nature of the effects of hydroplaning in the porous asphalt drainage layer. However, the computational effort required to arrive at a solution for either a two- or three-dimensional model is unjustified when the desired solution is the surface water film thickness. In this case a one-dimensional model is sufficient. In some cases, the multidimensional models do not converge and require operator intervention in selecting different boundary conditions or, in the case of transient analysis, varying time steps and computational grids.

The other option for flow through porous asphalt, a steady-state, one-dimensional model, has several advantages. Like the one-dimensional surface flow model, it is unconditionally stable. As a consequence, little or no operator intervention is necessary to arrive at a solution. Appropriate material properties can be quantified with a reasonable level of effort. Therefore, the one-dimensional surface flow model, which was modified as described in the following, was chosen to compute water film thicknesses on porous pavements.

For determining water film thickness on porous pavement sections it is necessary to modify equation 10 to account for the infiltration rate. The addition of a term to account for infiltration rate results in equation 12. This form of the equation was used in PAVDRN to estimate the water film thickness for porous surfaces:

$$\text{WFT} = \left[\frac{n L I}{36.1 S^{0.5}} \right]^{0.6} - \text{MTD} \quad (12)$$

where

n = Manning's roughness coefficient

I = $(i - f)$ = Excess rainfall rate (in/h) (1 in/h = 25.4 mm/h)

and

i = Rainfall rate (1 in/h = 25.4 mm/h)

f = Infiltration rate or permeability of pavement
(in/h) (1 in/h = 25.4 mm/h)

MANNING'S N

In order to predict the water film thickness that occurs on a pavement surface during sheet flow, as presented in equations 10 and 12, Manning's n must be known. The hydraulic roughness of a surface, Manning's n , can be expressed in terms of an n -value as used above and defined by Manning (34). Manning's n -value is surface-specific, requiring different expressions for different surfaces. During the course of this project, the hydraulic resistance of three different types of pavement surfaces was determined:

- Portland cement concrete
- Porous asphalt
- Dense-graded asphalt concrete

A great deal of experimental data that can be used to determine Manning's n -values is available in the literature (4,35,36), and these data were reanalyzed during this project to verify the work of the previous researchers. However, additional experimental data were needed in order to extend values of Manning's n to rough portland cement concrete surfaces and to porous asphalt surfaces. Manning's n must be determined through laboratory or field experimentation during which the water film thickness is observed as a function of rainfall intensity on different surfaces. The procedure used to establish Manning's n may be summarized as follows and is presented in detail in Appendix C.

Determination of Manning's n

Manning's n is a function of the nature of the surface texture. Therefore, it is necessary to consider portland cement concrete, dense graded asphalt concrete, and porous asphalt each as separate cases with a unique relationship for each surface. Manning's n can be determined experimentally under either artificial or natural rainfall. An artificial rainfall simulator that had been used in previous projects at Penn State was available and used for this study. The facility is well calibrated and produces uniform rainfall rate over an area of approximately 3 m by 10 m (29). Given the unpredictability of natural rainfall, this facility was used to generate the experimental data needed to extend Manning's n to larger Reynold's numbers on portland cement concrete and to determine Manning's n for porous asphalt. Details of the experimentation are given in Appendix C of this report.

Manning's equation (34) may be written as:

$$q = \frac{h^{5/3}}{n} S_{ox}^{1/2} \quad (13)$$

where

- q = Quantity of flow per unit width (m³/s/m)
h = Depth of flow (m)
S_{ox} = Slope of the flow plane in direction of flow (m/m)
n = Manning's roughness coefficient

Manning's equation applies to conditions of turbulent (rough) flow. Flow is considered turbulent because of the impact of raindrops on relatively thin films of water flowing over pavement surfaces (34). Equations 14 and 15 can be derived from equations 13 or 9:

$$a = \frac{1.0}{n} S_{ox}^{1/2} \quad (14)$$

and

$$m = \frac{5}{3} \quad (15)$$

Relationships for Manning's n used in PAVDRN

The regression analyses and assumptions used to derive the relationships for Manning's n that are used in PAVDRN are detailed in Appendix C. The following equations, based on

experimental data and the regression of the data with various forms of equations 13 through 15, were developed and used in PAVDRN to determine Manning's n:

1. Portland cement concrete surfaces:

$$n = \frac{0.319}{N_R^{0.480}} \quad (N_R < 1000) \quad (16)$$

$$n = \frac{0.345}{N_R^{0.502}} \quad (N_R < 500) \quad (17)$$

2. Dense-graded asphalt concrete :

$$n = 0.0823 N_R^{-0.174} \quad (18)$$

3. Porous asphalt concrete:

$$n = \frac{1.490 S^{0.306}}{N_R^{0.424}} \quad (19)$$

where

$$N_R = \frac{q}{v} \quad (20)$$

and

N_R = Reynold's number

q = Quantity of flow per unit width ($m^3/s/m$)

ν = Kinematic viscosity of water

Equations 16 through 19 are presented graphically in figures 9 through 12.

HYDROPLANING SPEED MODEL

The hydroplaning model selected for the study is based upon the work of Gallaway and his colleagues (4) and as further developed by others (37,38). On the basis of the work reported by these authors, for water film thicknesses less than 2.4 mm (0.095 in), the hydroplaning speed is determined by:

$$HPS = 26.04 WFT^{-0.259} \quad (21)$$

where

HPS = Hydroplaning speed (mi/h) (1 mi/h = 1.61 km/h)

WFT = Water film thickness (in) (1 in = 25.4 mm)

For water film thicknesses greater than or equal to 2.4 mm (0.095 in), the hydroplaning speed is:

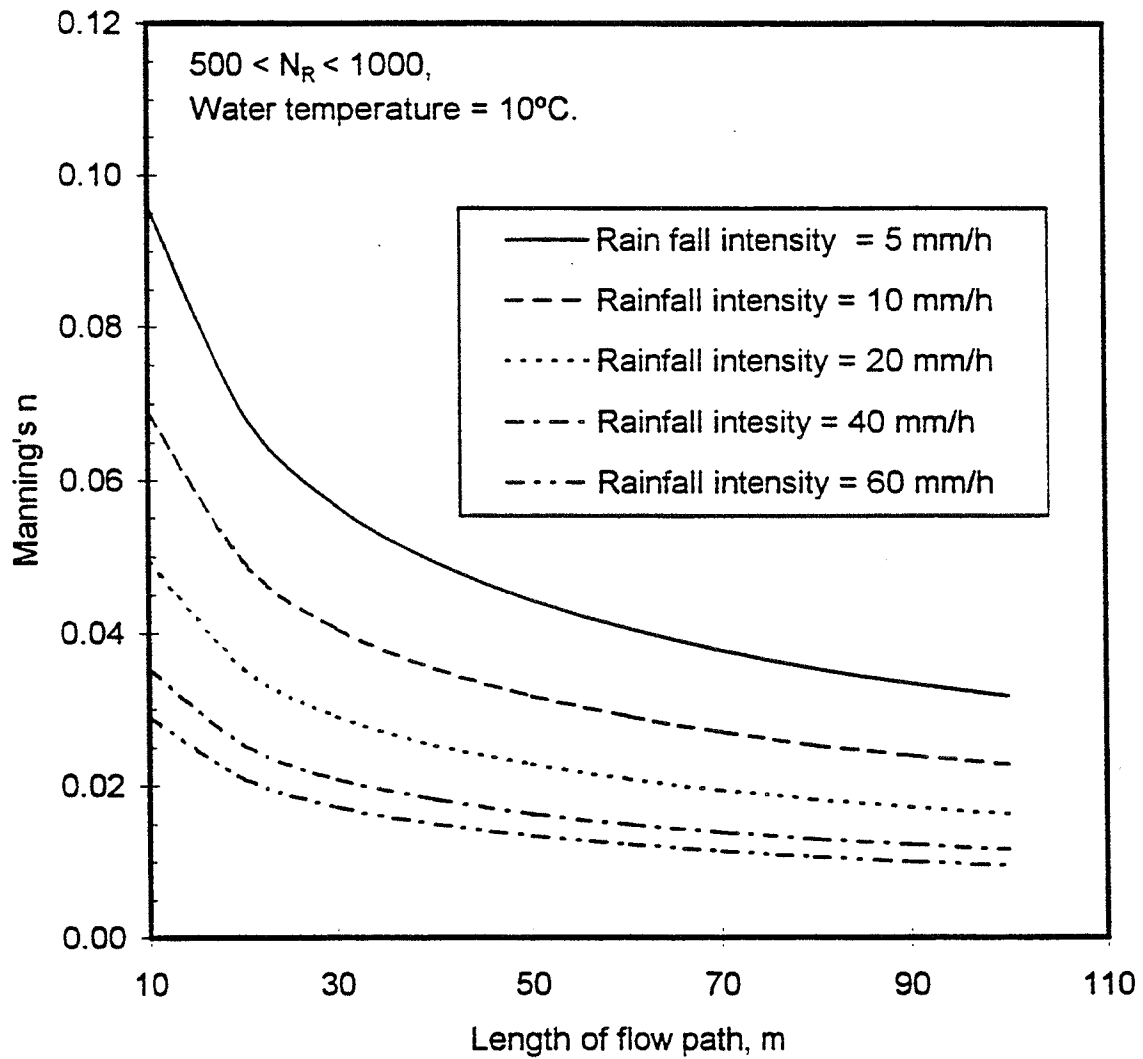


Figure 9. Manning's n versus length of flow path for various rainfall rates, portland cement concrete, $500 < N_R < 1,000$.

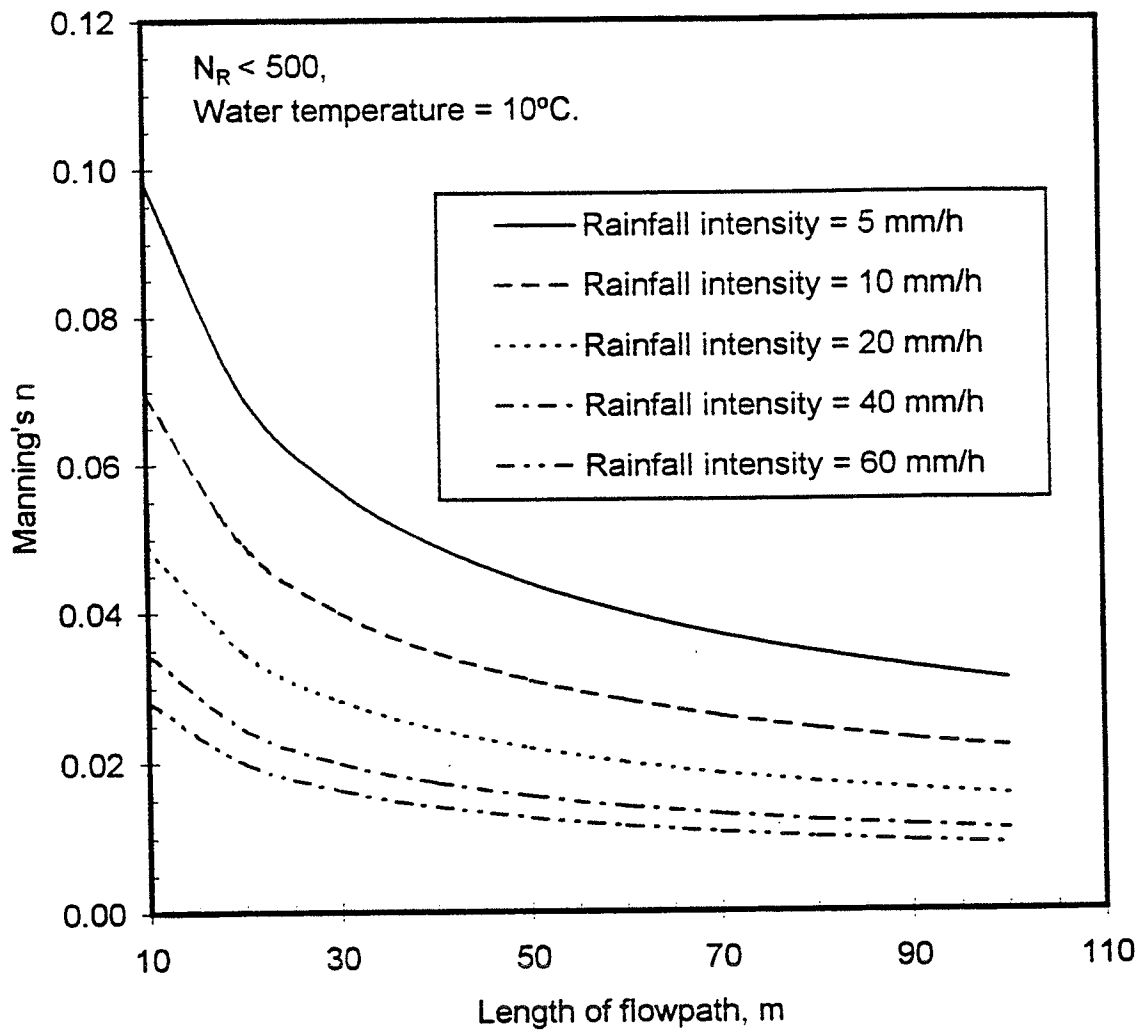


Figure 10. Manning's n versus length of flow path for various rainfall rates, portland cement concrete, $N_R < 500$.

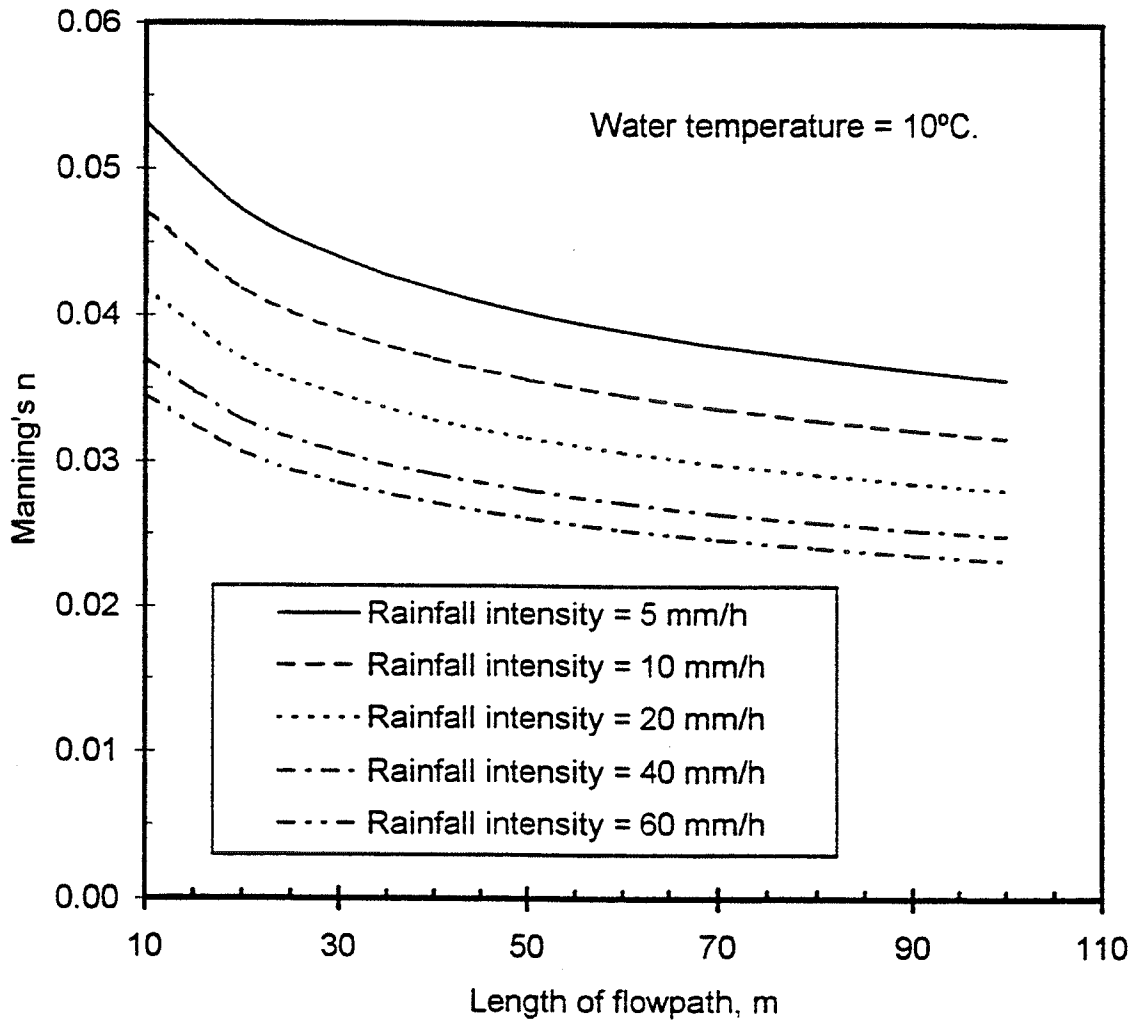


Figure 11. Manning's n versus length of flow path for various rainfall rates, dense-graded asphalt concrete.

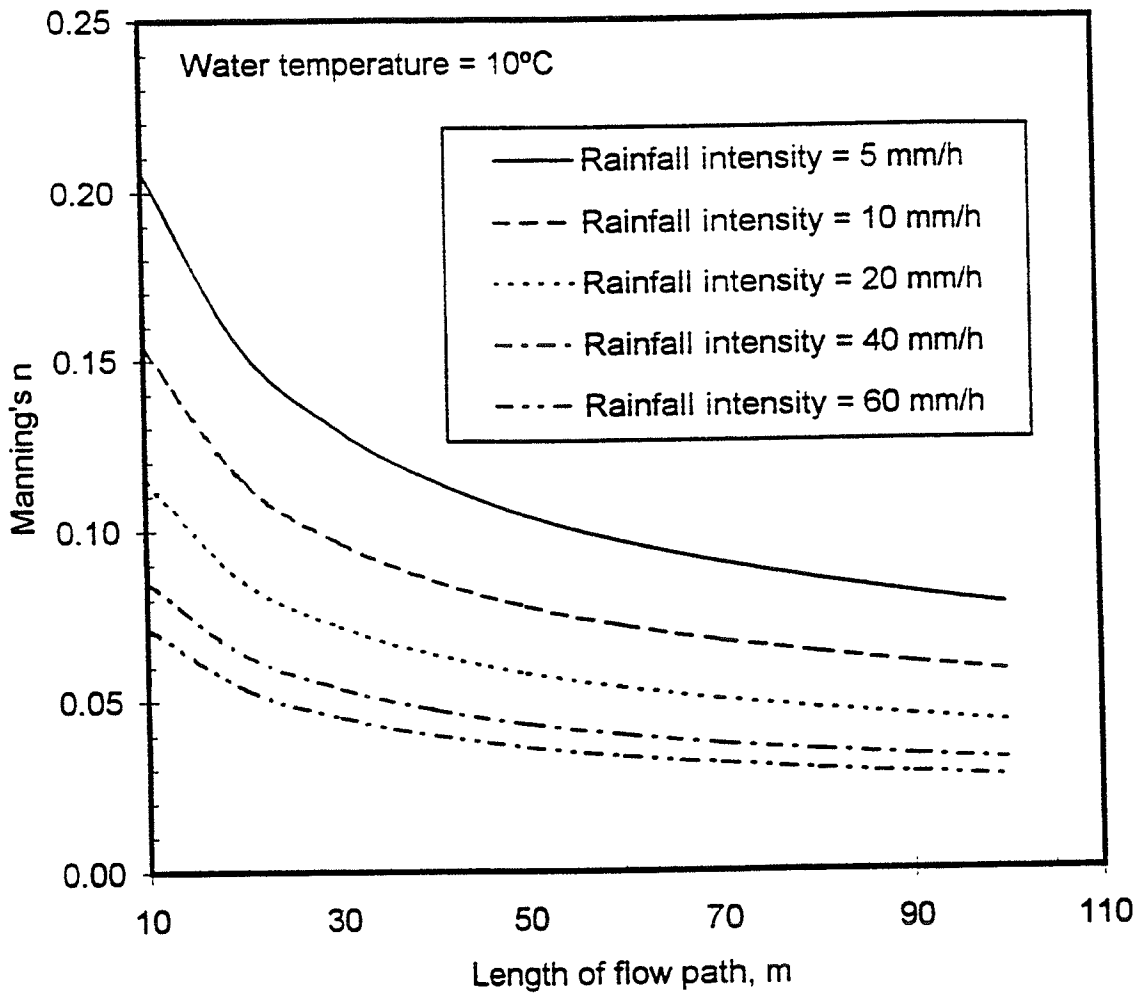


Figure 12. Manning's n versus length of flow path for various rainfall rates, porous asphalt concrete.

$$\text{HPS} = 3.09 A \quad (22)$$

where A is the greater of the values calculated using equations 23 and 24:

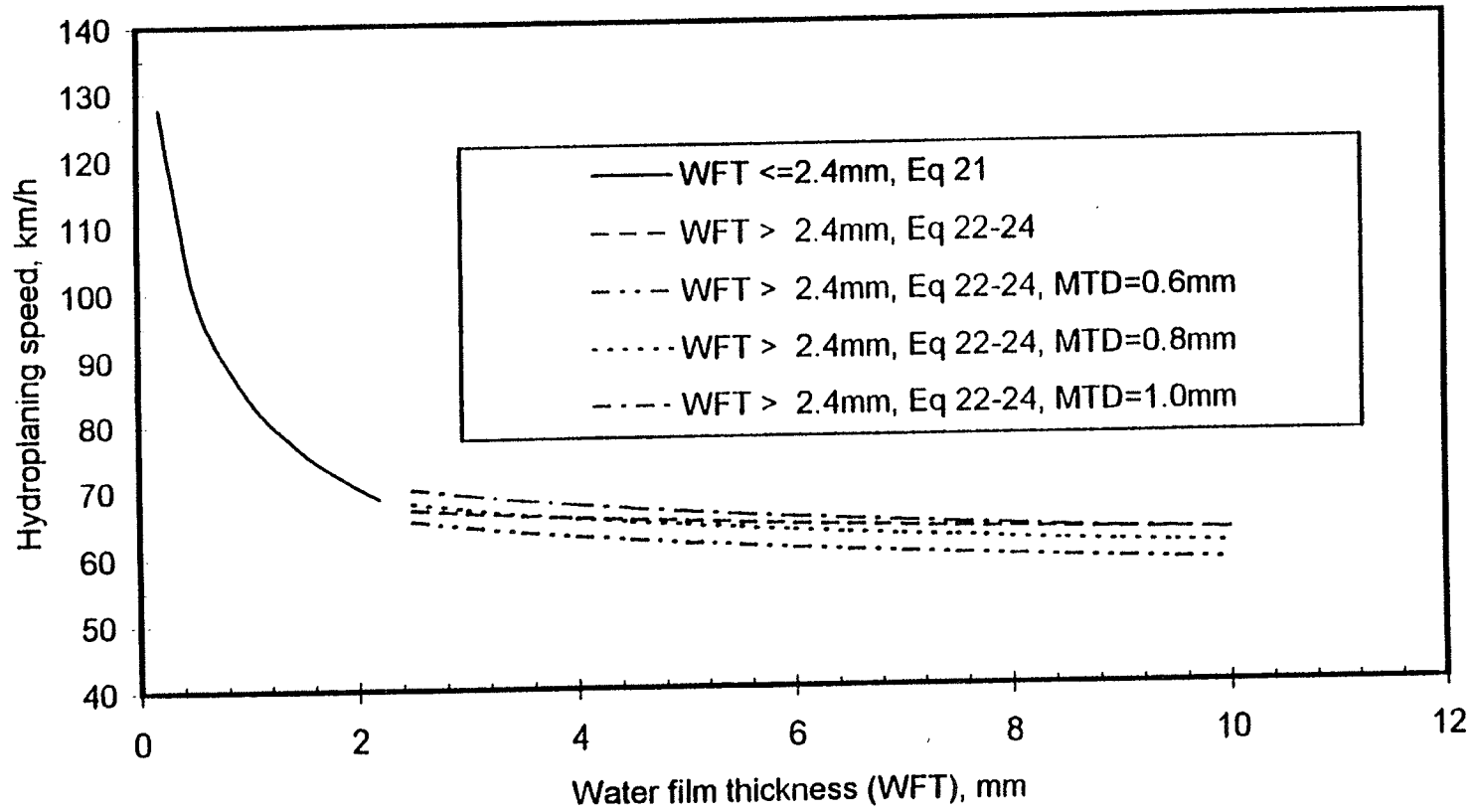
$$\left[\frac{10.409}{\text{WFT}^{0.06}} + 3.507 \right] \quad (23)$$

or

$$\left[\frac{28.952}{\text{WFT}^{0.06}} - 7.817 \right] \text{MTD}^{0.14} \quad (24)$$

The model predicts the onset of hydroplaning on the basis of the water film thickness where water film thickness is the *thickness of the water film above the mean texture depth*, as presented in figure 1. The results of equations 21 through 24 are shown graphically in figure 13. The mean texture depth can be determined from sand patch or micro profile measurements. Suggested levels of macrotexture are presented in the guidelines for design situations where actual measurements are not available. Although the hydroplaning prediction models (equations 2 through 24) are empirical, they represent the state of the art: The development of rational equations was considered too ambitious an undertaking given the complexity of the problem, the resources required, and the extent of the data that would be needed for a rational model.

Figure 13. Hydroplaning speed versus water film thickness.



Unfortunately, experimental test data needed to verify the prediction of water depths on the surface of porous asphalt pavement was not obtained during this study and such data are not available in the literature. In order to obtain reliable experimental data, very high rainfall rates are needed and the experimental section must be well isolated so that the entire flow is contained within the boundaries of the test sections. In simple terms, very high, uniform rainfall rates are needed on a “leak-proof” test section. These conditions could not be satisfied with the available equipment, neither in the laboratory nor in the field. Capturing a natural event was considered but the idea was discarded because of the coordination effort and costs associated with capturing such an event. Therefore, it was not possible to validate equations 21 through 24 for porous asphalt surfaces.

Rainfall Intensity

The AASHTO highway design guides include an equation for relating rainfall intensity, vehicle speed, and maximum allowable sight distance as follows:

$$i = [80,000 / (S_v \cdot V_i)]^{1.47} \quad (25)$$

where

- | | | |
|-------|-----------------------------|----------------------|
| i | = Rainfall intensity (in/h) | (1 in/h = 25.4 mm/h) |
| S_v | = Sight distance (ft) | (1 ft = 0.305 m) |
| V_i | = Vehicle velocity (mi/h) | (1 mi/h = 1.61 km/h) |

This relationship is depicted in figure 14.

Although it appears in equation 25 that intensity is a function of sight distance, sight distance is a function of intensity. As intensity increases, sight distance decreases. Likewise, vehicle velocity decreases with increased intensity and decreasing sight distance.

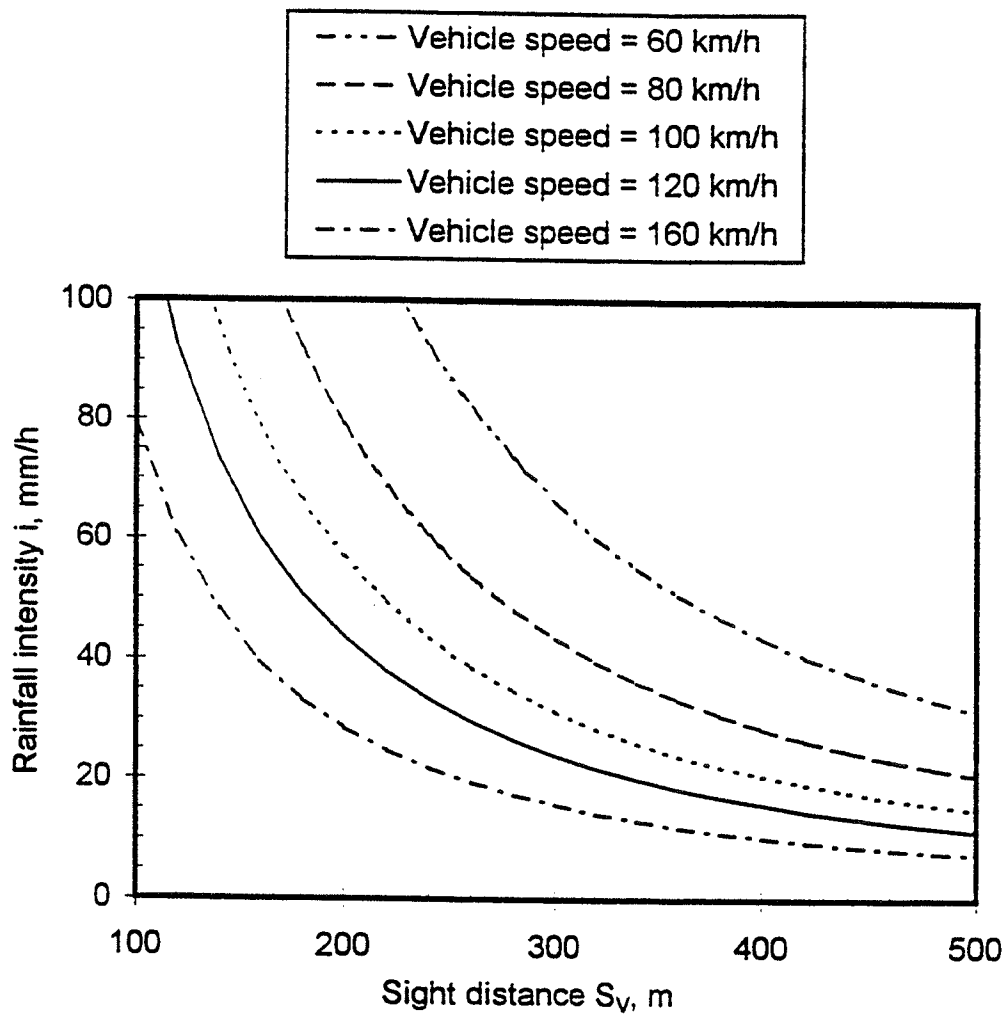


Figure 14. Rainfall intensity versus sight distance for various vehicle speeds.

CHAPTER 4

EXPERIMENTAL STUDIES

A number of experimental field and laboratory studies were necessary in order to provide the data needed to develop the models used in the PAVDRN software. Permeability measurements were obtained in the laboratory for open-graded laboratory and field asphalt mixtures in order to obtain their coefficients of permeability. Mean texture depth measurements were obtained for all of the pavement surfaces tested in the laboratory and field using either the sand patch or a profiling method. Water film thickness measurements were obtained in the laboratory with a color-indicating gauge and a point gauge. The color-indicating gauge was used exclusively in the field for water film thickness measurements.

The indoor artificial rainfall simulator at Penn State was used in the laboratory to determine Manning's n for porous asphalt surfaces and to extend the existing data on portland cement concrete surfaces to longer flow paths as required for PAVDRN.

In the field, full-scale skid testing measurements were needed to extend the hydroplaning model to porous pavement surfaces and to verify the effect of portland cement concrete grooving on hydroplaning speed. These data were obtained by conducting full-scale skid test measurements on porous asphalt surfaces installed at the Penn State Pavement Durability Research Facility. Full-scale skid testing was also performed on grooved PCC surfaces at the Wallops Flight Facility. The full-scale field skid testing required measurements

at different speeds on the surfaces flooded with water at different film thicknesses. The test facilities, test methods, and test results are discussed in this chapter.

TEST FACILITIES

Indoor Artificial Rain Facility

The pavement test surfaces were formed in a rectangular channel that was 0.30 m wide and 7.3 m long. The sides of the channel were formed by two 80-mm by 160-mm steel angles that were mounted 0.30 m apart, as shown in figure 15. To complete the channel, the steel angles and 20-mm thick sheets of plywood were bolted to the top flange of a 7.3-m wide flange W12x53 steel beam as shown in figure 16. A jacking system allowed the longitudinal slope of the beam to be adjusted to provide a range of slopes. The porous asphalt concrete and portland cement concrete were placed in the channel, providing the test surfaces for measuring Manning's n .

Artificial rainfall was generated with a series of nozzles placed above the test surface, as shown in figure 17. Extensive evaluations were performed previously to calibrate the rainfall rate and to select appropriate nozzles, spray angles, nozzle distances from the channel, pressure settings, etc., to ensure that the rainfall rate was uniform over the entire surface (35). Consequently, the procedures and testing equipment developed previously were used for this study (29).

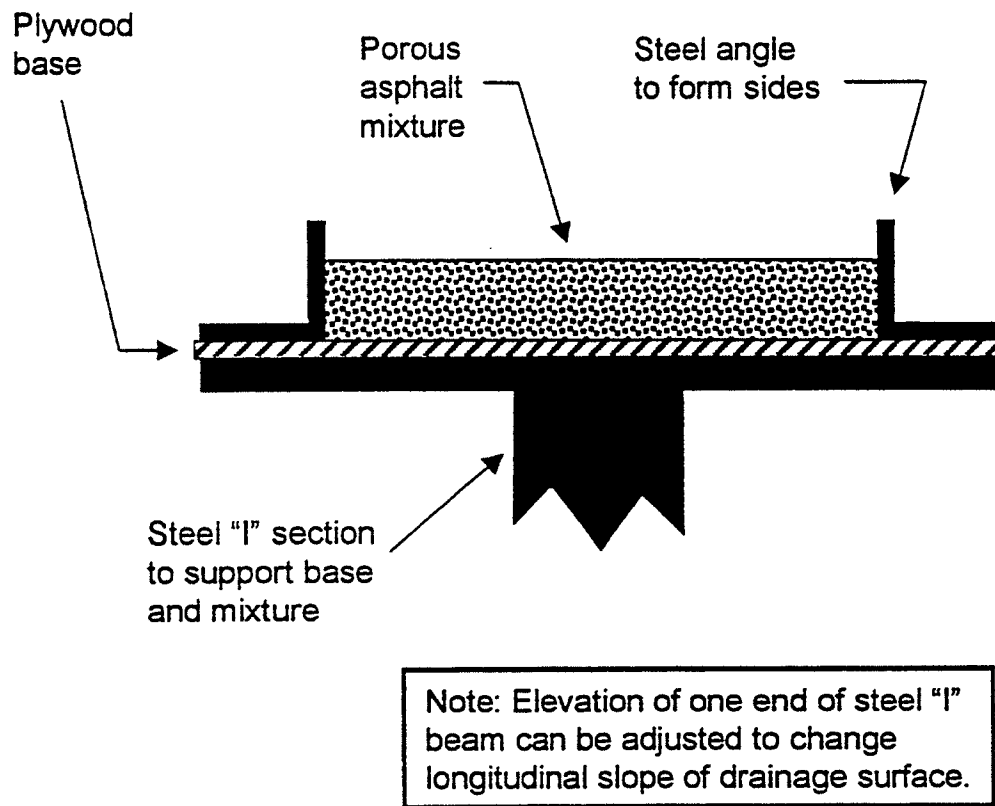


Figure 15. Cross-section of pavement used in laboratory rainfall simulator.

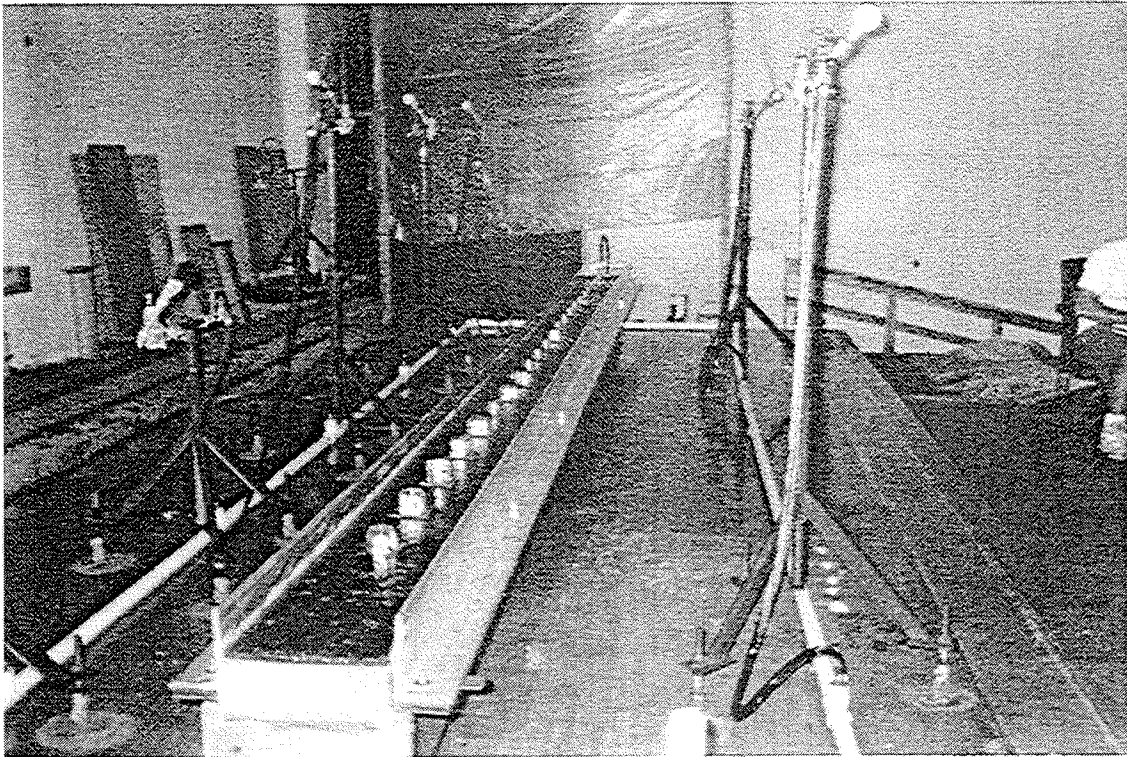


Figure 16. Overall view of test channel used with laboratory rainfall simulator.

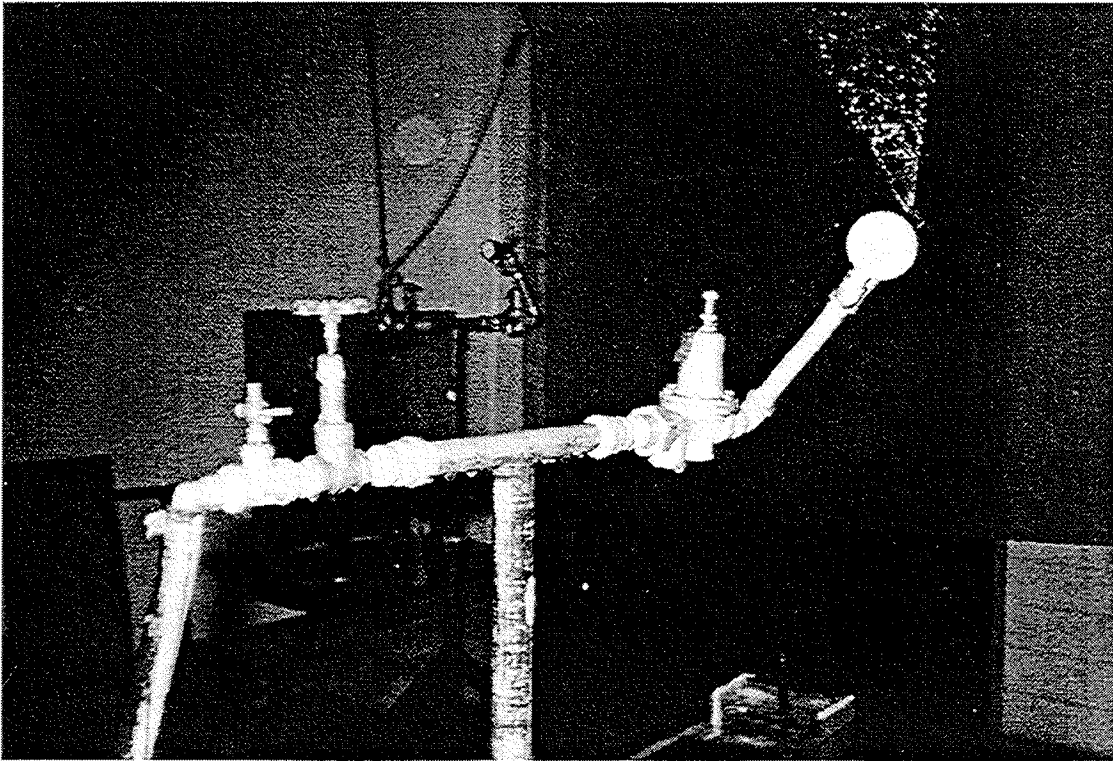


Figure 17. Laboratory rainfall simulator.

The channel was limited in length to 7.3 m. With this length and the maximum rainfall rate, the largest Reynold's number that could be generated was approximately 130. However, in this study it was necessary to measure WFT values in flow regimes with Reynold's numbers greater than 140. Since the maximum rainfall intensity was 75 mm/h, it was necessary to effectively increase the drainage path lengths to achieve higher Reynold's numbers. This was done by introducing a flow at the top of the channel so that the channel represented the last 7.3-m segment of a longer flow path. For example, to create a 14.6-m long flow path, the flow that would be accumulated over the first 7.3-m segment was introduced at the top of the channel, effectively making the channel act as the last 7.3-m segment of a 14.6-m long flow path.

The flow introduced at the top of the channel was commensurate with the rainfall rate on the channel, adjusted for non-turbulent conditions in the first 0.5 m of flow. A small adjustment in the introduced flow rate, as calculated on the basis of the rainfall rate, was necessary because the turbulence caused by pelting raindrops impede flow. Approximately 0.5 m was required to develop fully turbulent flow, causing the actual flow to be greater than under conditions where the flow on the entire 7.3-m channel length was fully turbulent. This phenomenon has been observed by others when analyzing the short, sudden rise in flow at the end of rainfall-runoff hydrographs (39). The adjustment was determined experimentally by measuring the flow at the end of the channel for different rainfall rates. The flow was introduced at the top of the channel in a gentle spray applied directly onto the concrete surface in the channel.

For the porous asphalt mixtures, the flow through the mixture had to be determined and evaluated. A distribution box with a baffle was placed at the top of the channel to provide a base flow through the porous mixes. The bottom of the channel was sealed to a depth of 12 mm below the top of the surface, effectively forming a dam to prevent drawdown effects of the flow through the porous asphalt. If the bottom was left completely open, the water surface profile would draw down dramatically at the end of the channel, which would lessen the length of the channel that could be used for experimentation. This arrangement is shown in figure 18.

Production and Placement of Porous Mixes

Three porous mixes were tested in the laboratory under artificial rainfall. Each mixture was designed to yield a different mean texture depth and air-void content. Attempts to place hot-mixed asphalt in the channel were not successful, and instead, a slow-setting epoxy was used as the binder for these mixtures by replacing the asphalt binder on a volumetric basis. The epoxy had a curing time of six hours, which allowed for an adequate time to place and compact the mixes.

A number of trial mixtures were prepared to obtain a range in air void content and MTD. The composition of the resulting three porous asphalt mixtures placed in the laboratory is shown in table 8, and the gradations are presented in figure 19. The mixes were prepared from a blend of two coarse aggregates (PennDOT gradation 1B and 2B, both limestone, retained on No. 4 sieve) and washed glacial sand (siliceous, passing No. 4 sieve). Nominal

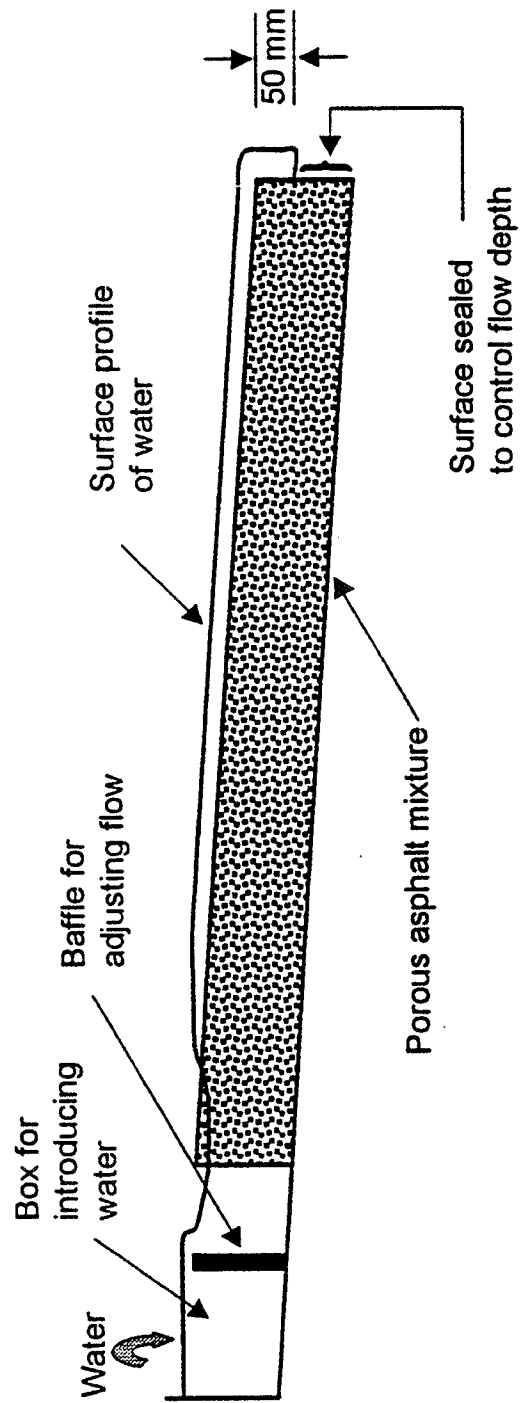


Figure 18. Cross-section of flow for porous asphalt sections in laboratory.

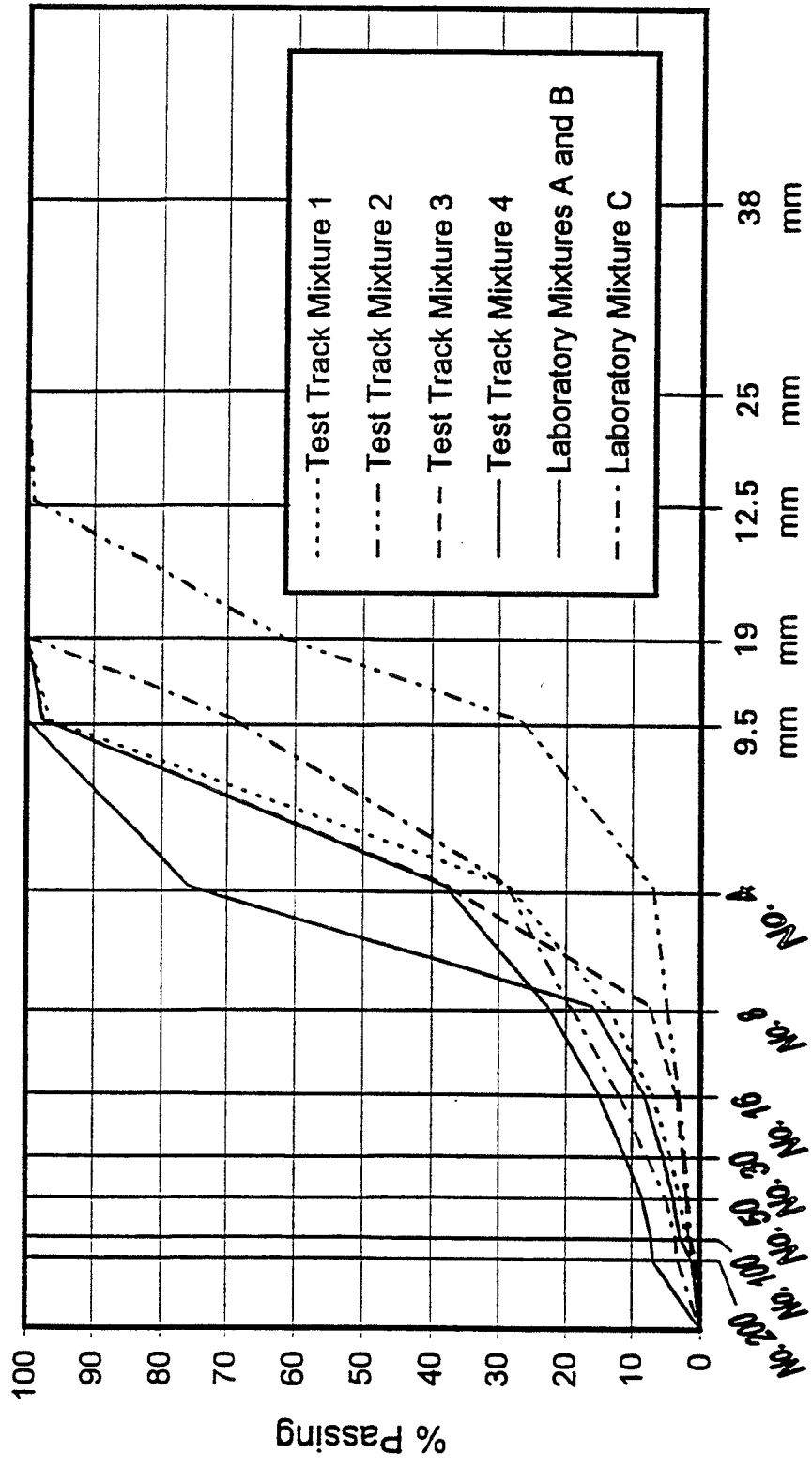


Figure 19. Gradations of laboratory and field porous asphalt mixtures.

Table 8. Mixture designs for porous asphalt laboratory mixes.

Component (% by total weight of aggregate)	Mixture		
	A	B	C
2B Aggregate	--	--	44
1B Aggregate	75	75	34
Washed Sand	19	19	20
Hydrated Lime	6	6	2
Epoxy (%wt. of total mix)	7	7	5.5

maximum size is 9 and 18 mm for 1B and 2B aggregates, respectively. Hydrated lime was added to thicken the epoxy and prevent drainage of the epoxy from the mixture. Mixture A was designed using the guidelines and design process as outlined for open-graded friction courses as published by NCHRP (10). This mixture was placed by hand, resulting in a very high air-void content, as illustrated in table 8.

Mixtures B and C were placed with a vibratory compactor; the gradations and maximum aggregate size were selected to account for the increased compaction and to give a range in air voids and MTD. The compactor, developed as part of this study, consisted of a 0.30-m square by 25.4-mm thick steel plate with an air vibrator mounted on top of the plate. The vibrator is used commercially for applications such as vibrating granular materials from storage bins. It is rated at 2,400 cycles per minute with 7.2 kN of applied force per cycle. The entire assembly weighed 580 N. A photograph of the assembly is shown in figure 20.

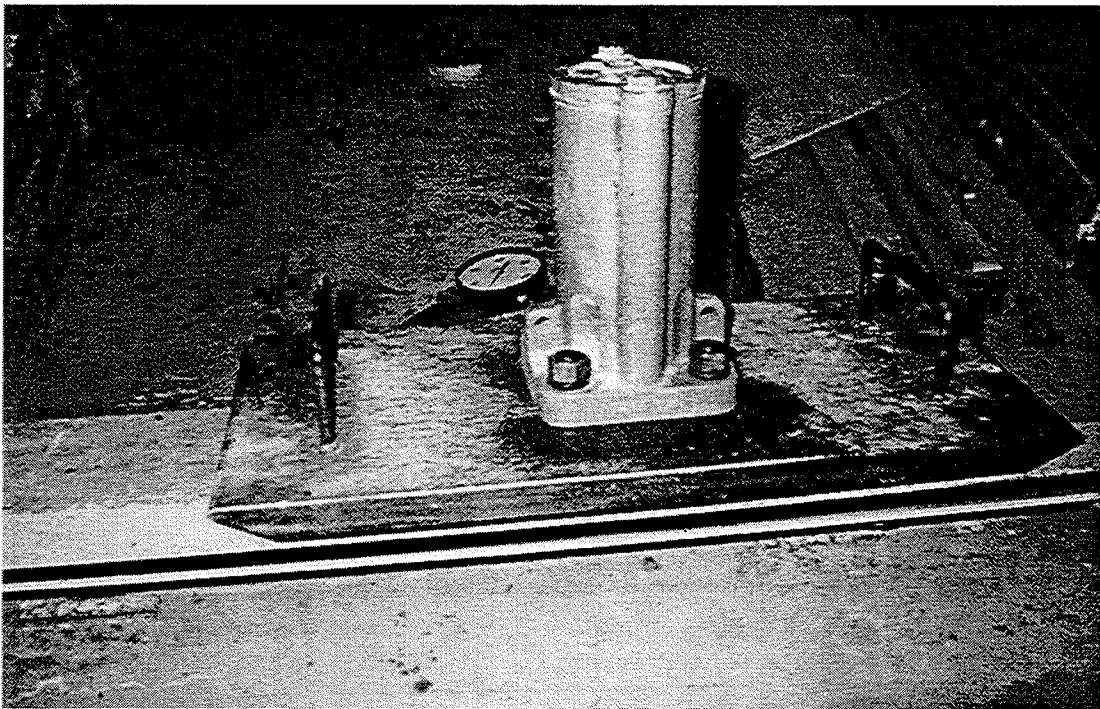


Figure 20. Photograph of vibratory compactor.

Cores were taken from the mixtures placed in the channel, and sections were removed for sand patch and profile testing. Air void content was determined for each mix in accordance with ASTM D 3203-88, "Standard Test Method for Percent Air Voids in Compacted Dense and Open Bituminous Paving Mixtures, and the results are shown in table 9.

Table 9. Air voids in laboratory porous asphalt mixes.

Distance along Channel (m)	% Air voids		
	Mix A	Mix B	Mix C
0.9	32.1	23.0	19.5
1.8	33.7	--	20.2
2.7	34.6	23.7	23.4
3.7	29.0	22.9	19.8
4.6	32.5	22.9	21.8
5.5	32.5	22.5	20.0
6.4	33.1	25.5	20.7
7.3	33.0	--	--
Avg.	32.6	23.4	20.8
Maximum Theoretical Specific Gravity	2.460	2.467	2.504

Outdoor Test Facilities

Full-scale field skid testing was needed to verify the hydroplaning potential of the open-graded asphalt concrete and grooved portland cement concrete surfaces. Initially, this testing

was scheduled for the Wallops Flight Facility, and full-scale porous pavement sections were to be installed at the facility. The facility offered a large flat area for testing at high speed with excellent support services. Unfortunately, after considerable planning, it became logistically impossible to place the test sections at the Wallops Flight Facility. After careful consideration of the alternatives, a decision was made to install four porous asphalt sections at the Penn State Pavement Durability Research Facility. However, it was decided that the research would continue to include the testing of the grooved and un-grooved PCC pavement at the Wallops Flight Facility, given that this pavement was in place, and no new construction would be required. Thus, the field skid testing was conducted on two PCC sections (broomed and broomed with grooving) at the Wallops Flight Facility and on four open-graded asphalt concrete sections at the Penn State Pavement Durability Research Facility.

Penn State Pavement Durability Research Facility

The existing surface on which the mixes were to be placed required leveling because the surface was rutted and had a large cross-slope. The testing area was a tangent section at the facility with an average longitudinal slope of one percent, approximately 3.65 m (12 ft) wide and 200 m (600 ft) long. First, the surface was milled to eliminate the existing cross-slope. Next, a typical PennDOT dense-graded ID-2 surface overlay (dense-graded with 9.0-mm top size) was placed over the test area to further eliminate any cross-slope and to provide a smooth testing area. The 2-m (6-ft) wide middle portion of the new overlay was then milled to a depth of approximately 40 mm (1.5 in). This, in essence, created a 2-m wide and 200-m long “bath tub” in which the porous asphalt mixes were placed, as presented in figure 21.

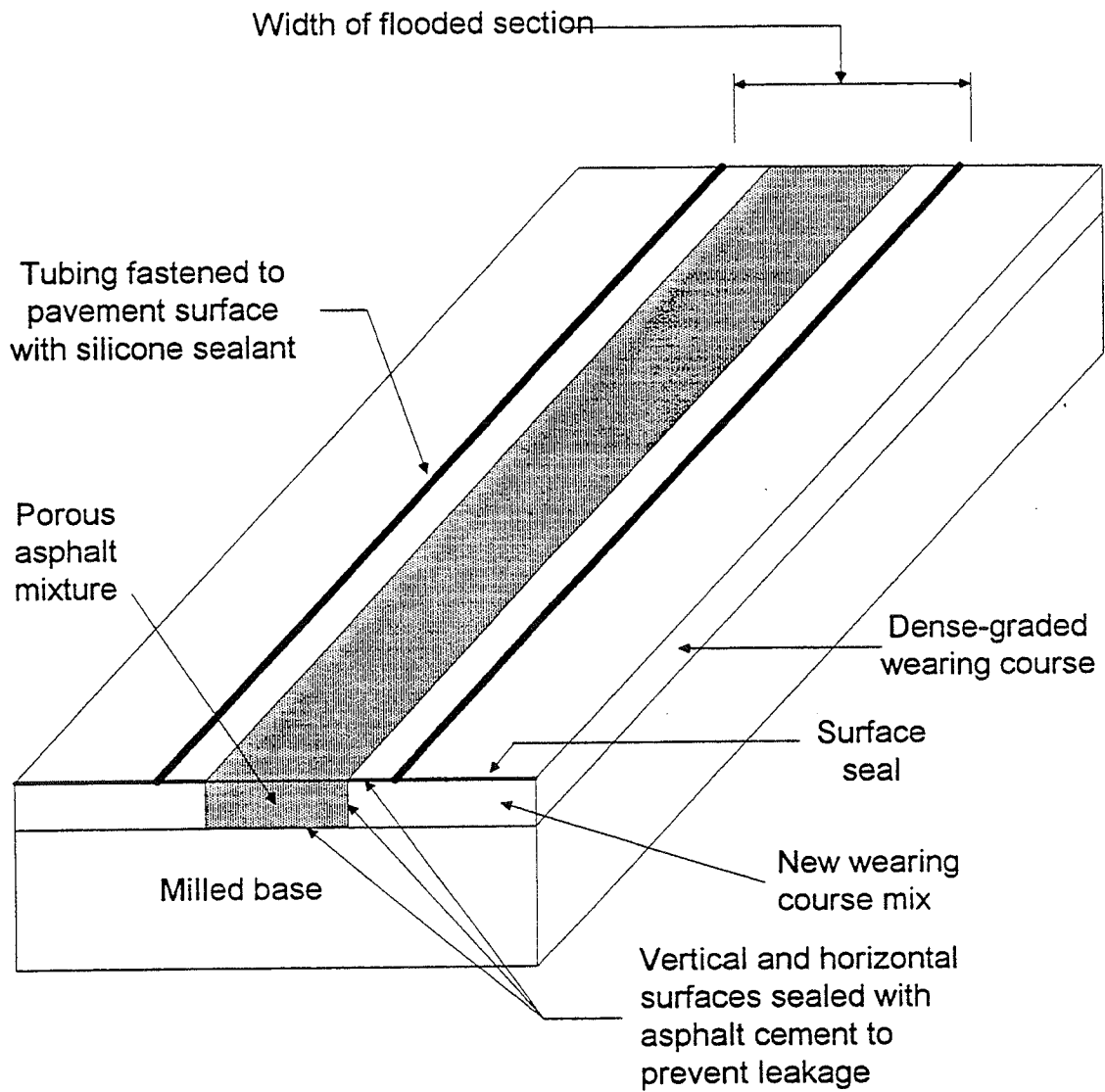


Figure 21. Schematic of test sections at the Penn State Pavement Durability Research Facility.

Four porous asphalt mixes were designed and placed at the test track facility with the cooperation of a local hot-mix contractor. A 40-m transition zone was established between each test section to allow the mixes to “run out” of the paver as the mix design was changed during the paving operation. This procedure was to ensure that the material in each test section was representative of the desired mix and not contaminated with material from an adjacent section. Wooden 2-ft-by-4-ft boards were placed across the 4-m (12-ft) lane width at the end of each test section to separate the test section from the transition sections. These boards were later removed, leaving a small trench across the pavement at the ends of each test section. The gradation used for each of the mixtures is presented in table 10.

The coarse aggregate was a local limestone, and the sand was from a siliceous glacial river deposit (same material as used in the laboratory mixtures). The mixtures were designed to yield a range of air void contents and maximum aggregate size. Mixture 1 is based on the FHWA mixture design procedure for open-graded asphalt mixes as outlined in NCHRP Synthesis 49 (10). Mixture 2 was based on a gradation reported by Huddleston et al. (9). Mixtures 3 and 4 were designed to represent typical gradations as being performed by transportation agencies in France (16). Polyester fibers were added to each mixture to minimize any tendency for drainage of the asphalt binder during construction. The binder content was selected in accordance with the standard design procedures detailed elsewhere, resulting in the binder contents shown in table 10 (10).

Table 10. Porous asphalt mix designs at the Penn State Pavement Durability Research Facility.

Sieve Size	Percent Passing			
	Mix 1	Mix 2	Mix 3	Mix 4
38 mm	100	100	100	100
25 mm	100	100	100	100
19 mm	100	99	100	100
13 mm	100	62	100	100
9 mm	97	27	97	100
No. 4	28	6.9	29	76
No. 8	13	4.9	7.1	16
No.16	7.0	3.2	3.3	8.3
No. 30	4.4	2.2	2.4	5.5
No. 50	3.0	1.7	1.9	4.0
No. 100	2.0	1.4	1.5	2.9
No. 200	1.0	0.6	0.8	1.2
Asphalt Cement (%) ¹	6.5	5.0	6.0	6.5
Polyester Fibers ^{(%)2}	0.5	0.4	0.4	0.4

¹Based on total weight of aggregate.

²Based on total weight of mixture.

The objective of the testing at Penn State was to determine the effect of the water film thickness on the hydroplaning potential, which required that the test sections be flooded during the testing. Applying water in the conventional manner with the standard ASTM E 274-90 (“Standard Test Method for Skid Resistance of Paved Surfaces Using a Full-Scale Tire”) skid trailer would not give controlled or measurable water film thicknesses, and therefore, it was necessary to flood the test sections. Water was introduced in the trough formed by the four

wooden boards at the head of each section. The water was then allowed to flow over the entire length of the section, as depicted in figure 22. The depth of flow was controlled by adjusting the rate at which water was added to the trough. The longitudinal slope, approximately one percent, provided a reasonably uniform flow over the length of the section except at the beginning and end of the sections. The test sections were designed so that the flow of water through the pavement could be measured, thereby obtaining in-situ permeability measurements. This proved impractical because, in spite of being sealed with hot asphalt cement, leaks occurred in the depressed section. Water film thickness measurements were obtained just prior to each skid test using a color-indicating gauge as described later in this chapter. Sand patch and profile measurements were also acquired for each section, and cores were obtained for laboratory permeability testing.

The skid tester used for this project is a Penn State design, in which a single-wheel trailer is affixed to the rear of a modified heavy-duty pickup truck. The tester, commonly referred to as the single-wheel skid tester, incorporates a six-force transducer into its design. This enables horizontal, vertical, and side force measurements. For this project, the single-wheel skid tester was mounted in the center of the pickup to eliminate the effects of the truck tires on the waterfilm thickness. The testing was performed in accordance with ASTM Standard E 274. A photograph of the tester can be found in figure 23.



Figure 22. Introduction of water onto test section at the Penn State Pavement Durability Research Facility.



Figure 23. Skid test in progress at the Penn State Pavement Durability Research Facility.

Wallops Flight Facility

The testing at the Wallops Flight Facility was performed in much the same manner as at Penn State. The sections were dammed, and water was flooded over the sections.

Unfortunately, the water film thickness was not as controlled as at the Penn State site, and only one water film thickness was reliably obtained. A photograph of a test in progress is shown in figure 24, and a photograph of the portland cement concrete surface is presented in figure 25.

MEASUREMENT TECHNIQUES

Measurement of Water Film Thickness

A point gauge was used to measure water film thicknesses in the laboratory (29). A point gauge is a pointed probe that is lowered from a stand until it comes in contact with the water surface. WFT measurements were made at 0.3-m increments along the length of the channel. Three measurements, located at the mid-width and at the quarter-widths of the surface, were obtained at 0.3-m increments along the length of the surface. The three measurements were then averaged to obtain one WFT measurement for each 0.30-m increment along the length of the surface.



Figure 24. Test in progress at the Wallops Flight Facility.

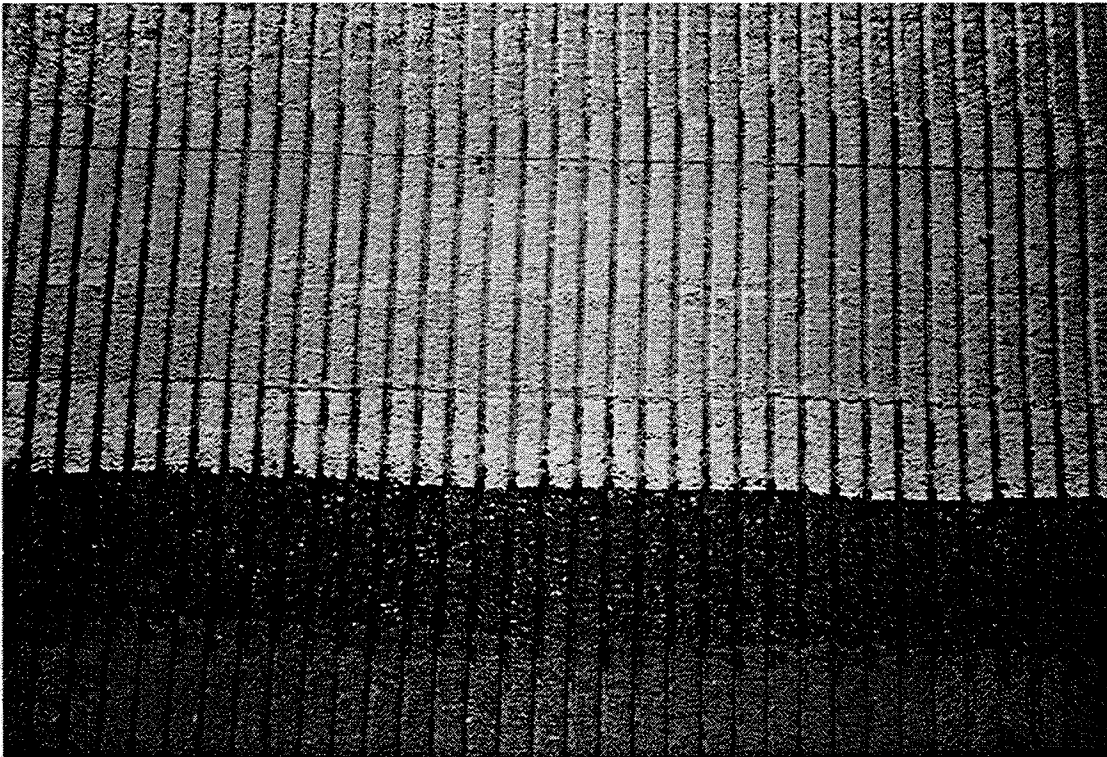


Figure 25. Grooved concrete surface at the Wallops Flight Facility.

below the top of the asperities of the aggregates. The use of a flow datum is discussed by Reed et al. (29). To obtain the data, a 25-mm-diameter metal disc was first placed on the pavement surface at the measurement location, and a point gauge reading was obtained on the top of the disc. Next, a reading was taken on the surface of the flowing water, and the thickness of the washer plus one MTD were subtracted from the point gauge reading on the water surface to obtain the flow depth. The method is illustrated in figure 26.

In order to relate the hydroplaning speed to the water film thickness and to validate the water film thickness model, the water film thicknesses had to be measured in the field and in the laboratory during rainfall. The point gauge and other devices available for making these measurements were judged unacceptable for field use because the measurements are slow and tedious to perform and cannot be obtained during rainfall. Therefore, alternate procedures for measuring the WFT were considered.

The gauge that was ultimately adopted consists of a sheet-metal fixture bent in the form of an inverted "U," as shown in figure 27. The legs of the U are approximately 50 mm high, and spaced 30 mm apart. The fixture is approximately 150 mm in length. To make a water film thickness measurement, the "legs" of the fixture were coated with a paint-like coating that changes color when wet. To obtain the data, the fixture was placed on the pavement with its "legs" immersed in the water film. The water film thickness is then determined as the dimension over which the coating changes color.

Note: Measured water film thickness is the difference between point gauge reading on water film and washer plus thickness of washer as follows:

$$WFT = (RPG_1 - RPG_W) + t_w$$

where

WFT = Water film thickness

RPG_1 = Reading of point gauge in contact with surface of water film

RPG_W = Reading of point gauge in contact with top of metal disk

t_w = Thickness of metal disk

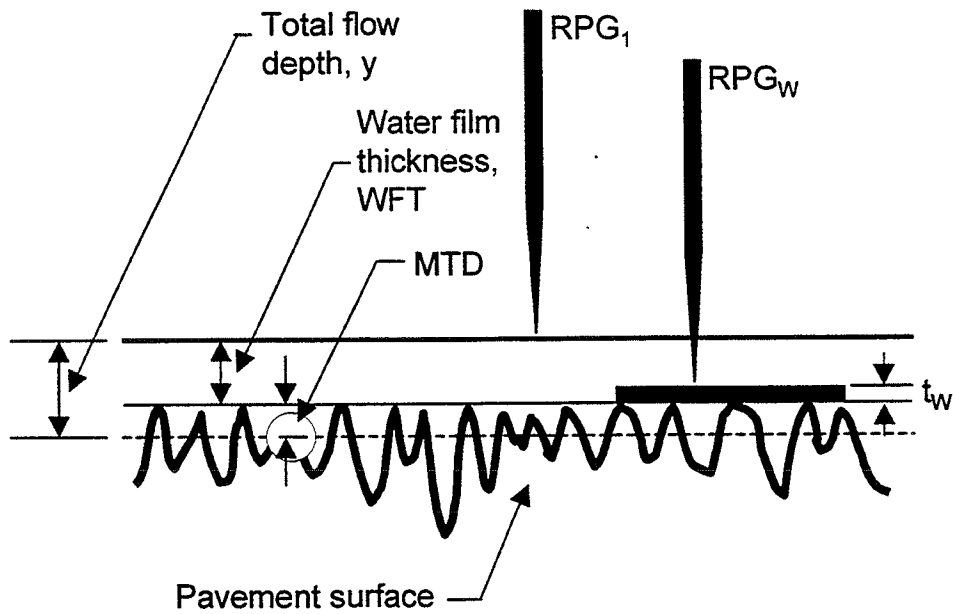


Figure 26. Measurement of water film thickness with point gauge on a porous asphalt surface in laboratory.

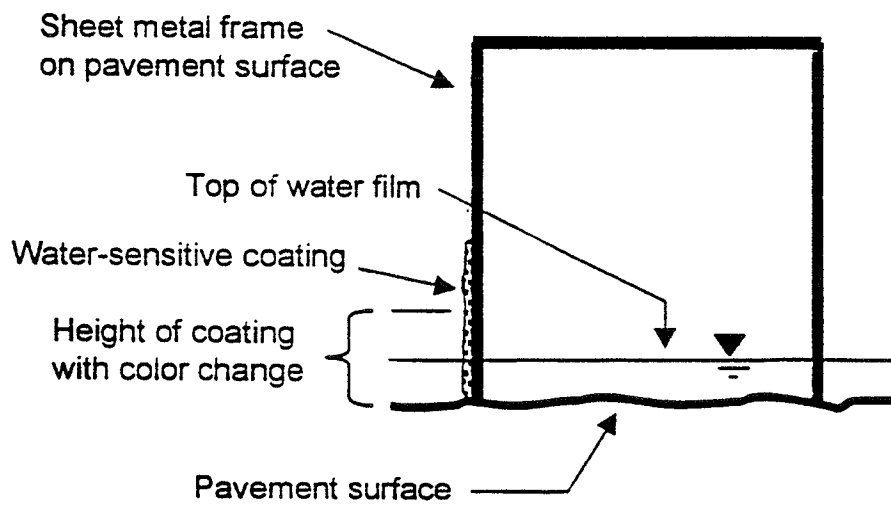


Figure 27. Schematic of the color-indicating water film thickness gauge.

The coating is initially yellow but turns bright red when it comes in contact with water. The device was calibrated in the laboratory by comparing water depths from the portland cement concrete surface measured with the point gauge and the color-indicating gauge. The water film thickness measurements were obtained with a point gauge and with the color-indicating gauge. The water film thickness values measured with the color-indicating gauge were larger than the water film thickness values measured with the point gauge because water “wicks” up the coating when the coating is wet. Sixty pairs of data points were obtained in the laboratory, with the color-indicating gauge and the point gauge. A regression of the data points resulted in the relationship:

$$KK = 0.907 \text{ WFT} + 3.81 \quad (26)$$

where

KK = Color-indicating gauge reading (mm)

WFT = Actual water film thickness value (mm)

with a correlation coefficient (R^2) of 0.85. This relationship is displayed graphically in figure 28. The color-indicating gauge was used for all of the field testing conducted at the Penn State Pavement Durability Research Facility and the Wallops Flight Facility.

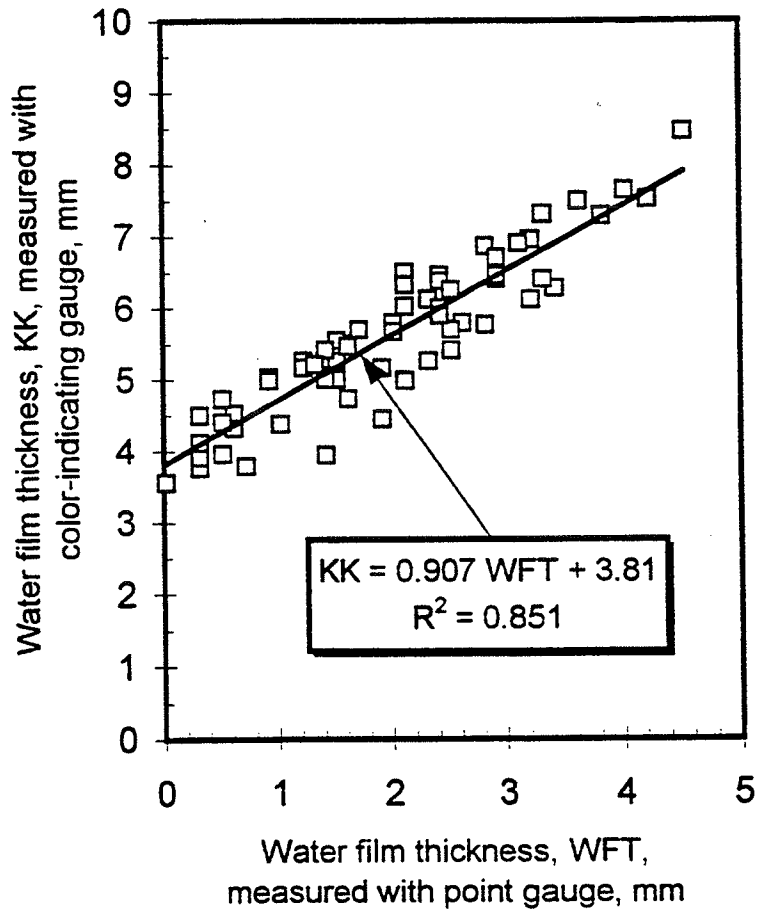


Figure 28. Correlation of water film thickness measurements obtained with the color-indicating gauge and point gauge.

Measurement of Surface Texture

A portable texture measuring device was used to perform surface texture profiles for the laboratory and field mixtures. The device produces an analog profile of the surface that can be digitized and analyzed statistically. The device is essentially a probe that is moved along the surface of the pavement and is described in detail elsewhere (40). A motor and appropriate electronic circuitry cause the probe to follow the pavement surface as the probe is moved horizontally over the surface.

The procedure for using this device has been standardized by ASTM as Designation E 1845-96, "Standard Practice for Calculating Mean Profile Depth." The procedure requires that two profile segments, each 100 mm in length, be obtained. The mean profile depth (MPD) for each of these profile segments is calculated by regressing the profile depth versus profile length, and the two values are then averaged to obtain the mean profile depth. The process is summarized in figure 29. The mean profile depth can be used to estimate the mean texture depth (ETD in equation 27) by a linear transformation (41):

$$\text{MTD}=\text{ETD} = 0.2 + 0.8 \text{ MPD (mm)} \quad (27)$$

The mean texture depth is by definition obtained with the "sand patch" (volumetric) method, ASTM E 965, "Standard Method for Measuring Surface Macrottexture Depth Using a Volumetric Technique." The ETD is an estimate of the MTD. Mean texture depths were also obtained from sand patch testing (ASTM E 965) performed in the field and on laboratory

1. *Profile measurements*
Calibrate the measuring system (when appropriate) and measure the profile of the surface.
2. *Handling of invalid readings*
Readings of this profile that are invalid (drop-outs) shall be eliminated or corrected.
3. *High-pass filtering*
Unless slope suppression according to point 6 in the following is used, high-pass filtering should be performed. It consists of removing spatial frequency component that are below the specified passband.
4. *Low-pass filtering*
Remove frequency components that are above the specified passband. This can be accomplished either by analog filtering or averaging of adjacent samples, or automatically met through the performance of the sensor.
5. *Baseline limiting*
Pick out a part of the profile that has a satisfactory baseline.
6. *Slope suppression*
The slope will be suppressed by the calculation of the regression line and subsequent subtraction of this line. An alternative is to apply appropriate high-pass filtering (see point 3 above).
7. *Peak determination*
The peak value of the profile over the baseline length is detected.
8. *MPD determination*
The mean profile depth (MPD) is calculated as the peak according to point 7 above minus the profile average, which will be 0 according to points 3 or 6 above.
9. *ETD calculation*
The MPD value is transformed to an estimated texture depth (ETD) by applying a transformation equation, $ETD = 0.2 + 0.8 MPD$.
10. *Averaging of MPD and ETD values*
Individual values measured on a site or a number of laboratory samples are averaged. This includes the calculation of the standard deviation.

Figure 29. Steps in determining texture depth using the profiling method (42).

samples. In this test, a known weight of glass beads is placed on the pavement surface and spread by hand with a rigid scrapper until the surface voids are filled. The area of the resulting “patch” of glass beads is related to the MTD.

Measurement of Manning’s n

Manning’s n for the portland cement concrete surface and for the porous asphalt surface was calculated by measuring the water film thickness on these surfaces with varying rainfall rates and surface slope. The theoretical base for the calculation is given in Appendix C, and the results of the calculations are presented in Chapter 3.

Measurement of Permeability

The static coefficient of permeability of porous asphalt concrete mixtures is a necessary input for the PAVDRN model. The customary procedure for measuring the in situ permeability of porous asphalt mixtures is to use an outflow meter. The outflow meter does not give permeability values in fundamental units, but instead provides an empirical measurement of the permeability in terms of the quantity of flow per unit of time. Because the flow is unconfined in a radial direction, it is not possible to calculate a coefficient of permeability from the conventional outflow meter. Further, for OGAC, the flow is partially in the macrotexture and partially within the mix. Therefore, a direct measurement of static permeability was used for the mixtures that were tested as part of this project. Because of the

large coefficient of permeability of porous asphalt mixtures, a standard falling head parameter cannot be used. In order to obtain a measurable flow, a large quantity of water would be required and the rate of flow would be excessive, certainly in the turbulent region.

Consequently, a drainage lag permeameter, originally described by Barker et al. (43) was used for the permeability measurements. The device, as shown in figure 30, consists of a tank, a sample container that confines the flow to the vertical direction, and a quick-release valve.

Full thickness samples from the artificial rain facility were cut into squares approximately 80 mm by 80 mm in length and width, and sheet metal was exposed to the sides of the samples to constrain the flow in the vertical direction. The permeability of the samples was measured in both the vertical and horizontal direction by testing samples oriented in both directions. Separate samples were used for each direction. This procedure ensured that there was no leakage around the periphery of the samples and that the flow occurred in the vertical direction.

Six-inch cores were obtained from the test track facility, and the lower layer of hot mix was trimmed from the cores, yielding a section that consisted of only the permeable asphalt mixture. These cores were sealed around their circumference to confine the flow to the vertical direction. The cores were then inserted in a 6-in diameter sheet metal tube and sealed around their circumference using silicone sealant, in the same manner as the rectangular samples from the indoor rain facility. Once the cores were tested in the vertical direction, they were removed from the container, and rectangular-shaped sections for testing in the horizontal direction were sawn from the cores. These cores were tested in the same manner as the

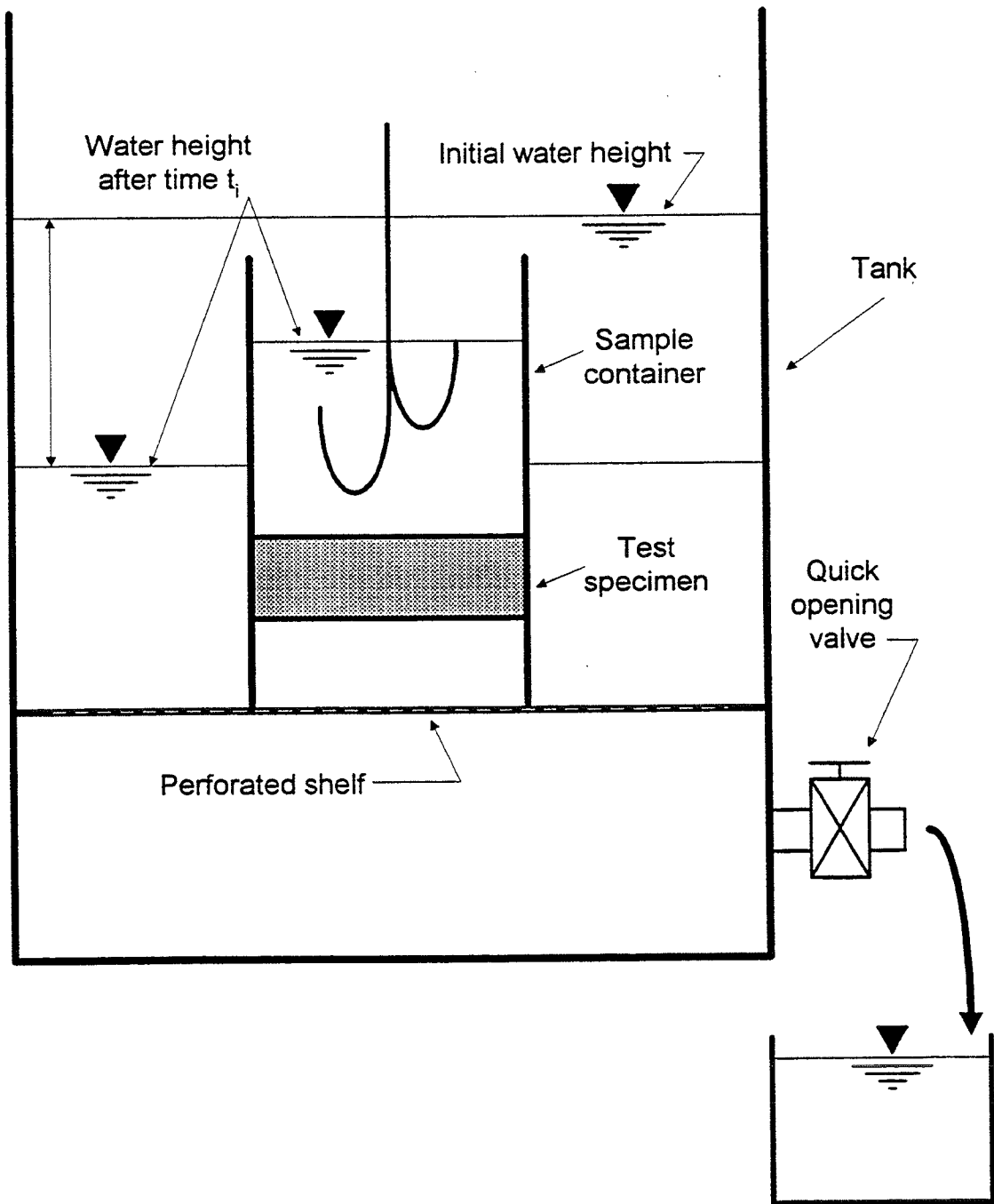


Figure 30. Schematic of drainage lag permeameter.

rectangular-shaped cores from the artificial rain facility. This procedure provided a vertical and horizontal coefficient of permeability for the field cores.

All of the samples were vacuum-saturated prior to testing. The samples were immersed in a flooded transfer vessel to a level above the sheet metal containers and placed in a vacuum chamber. A vacuum was applied to the samples until they ceased bubbling, using techniques similar to those used in measuring the maximum specific gravity for asphalt concrete, as specified ASTM D 3203-94, "Standard Test Method for Percent Air Voids in Compacted Dense and Open Bituminous Paving Mixtures." Once the samples were saturated, they were placed in the tank, the quick opening valve was opened, and the water draining from the tank was collected in a container during the time interval when the water level in the tank intersected successive points on the hook gauge. This provided sufficient data to calculate the coefficient of permeability in accordance with the equation reported by Barker (43), where:

$$k = \frac{276 ad}{At} \log \frac{h_1}{h_2} \quad (28)$$

$$Q = k A \frac{h}{d} \quad (29)$$

where

- Q = Rate of flow (ft³/s) (1 ft³/s = 0.028 m³/s)
- k = Coefficient of permeability
- A = Gross area of sample perpendicular to direction of flow (ft²)
(1 ft² = 0.093 m²)
- h = h₁-h₂, Head loss at distance d in sample in direction of flow (ft)
(1 ft = 0.305m)

Three tests were performed on each core in both the vertical and horizontal flow direction. Measured permeability values for the porous asphalt mixes from the field (mixtures 1 through 4) and the laboratory mixtures (mixtures A through C) ranged from 20 to 40 mm/s. Given the narrow range of the measured values and the likelihood of reduced permeability resulting from plugging due to road detritus, the use of the drainage lag parameter is not recommended for routine testing or as a design procedure.

TEST RESULTS

Flow on Porous Asphalt Sections

In order to determine the surface flow rate for the porous mixtures it was necessary to determine the flow rate through each mixture that would saturate the mixture to a height of one MTD. This "base flow" was subtracted from the total flow to yield only the surface flow as illustrated in figure 31. In order to determine the base flow, a plot of flow depth versus total flow was constructed as shown in figure 32. These plots were prepared for each surface and

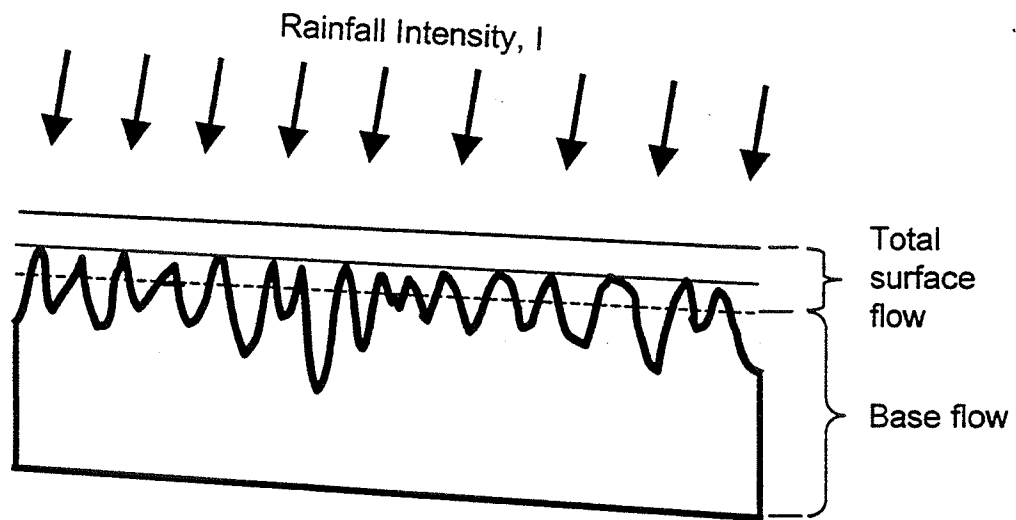


Figure 31. Definition of base and surface flow in porous asphalt sections.

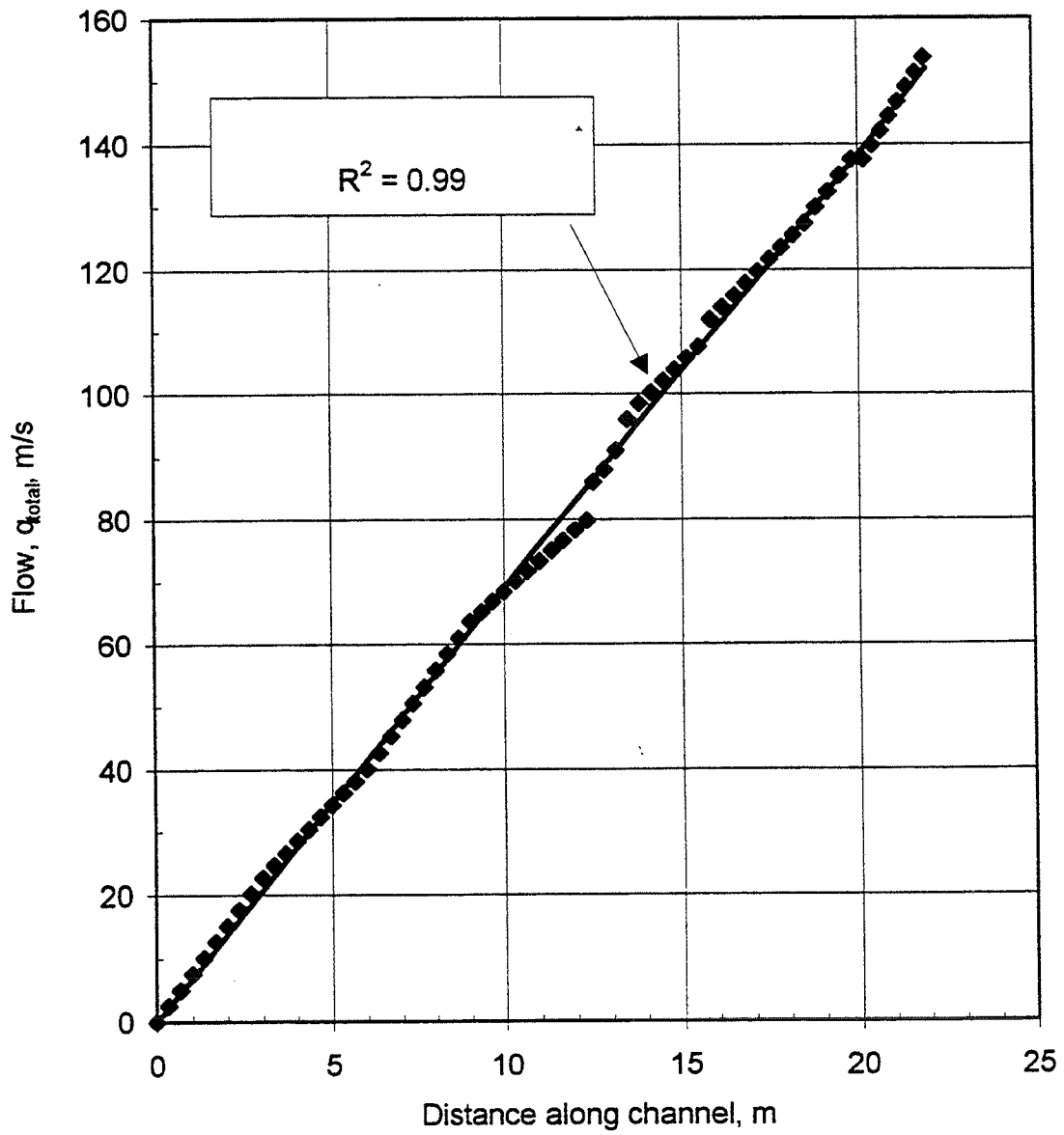


Figure 32. Plot of total flow versus flow path to determine flow depth.

for each rainfall rate and slope. The base flow rate depended on the mix, the slope of the channel, and the rainfall intensity and varied from 1.5 ml/s for mixture B (25 mm/h) to 53 ml/s for mixture A (75 mm/h). The use of the water film thickness values corrected for the base flow is discussed in detail in Appendix C where the development surface-specific equations for Manning's n is presented.

Texture Measurements

Texture measurements were made on the surfaces tested in the laboratory and field. The conventional sand patch technique causes problems with highly open mixtures because the glass beads flow into the internal voids in the mixture, giving a false value of texture depth. To overcome this problem, texture measurements were made on the laboratory porous mixtures using the conventional sand patch procedure on a cast of the surface. Texture depths were also estimated from profile measurements made on the original surfaces as presented in table 11. The casts, or replicates, were made by first placing silicone rubber on the original surface over an area of approximately 0.30 m by 0.30 m (1 ft by 1 ft). A plate was placed over the silicone rubber in order to force the rubber into the surface texture. Once the silicone had cured, it was removed and placed into a second form. A polyester casting resin was then poured over the surface of the silicone rubber and, on curing, separated from the rubber. The casting resin gave a positive replicate of the original surface.

Casts were obtained from each porous asphalt surface, spaced at equal intervals down the length of the test surface that was 7.3 m long by 0.3 m wide, and sand patch measurements were made on the casts. The results of this procedure are shown in table 11. The mean

texture depths of mixtures A, B, and C are visibly different and fall within the expected range of 1 mm (0.04 in) to 3 mm (0.12 in). Profile traces were used to calculate estimated texture depth (ETD) according to ASTM E 1845-96, "Standard Method for Measuring Surface Macrottexture Depth Using a Volumetric Technique," ISO standard as described in figure 29 (42). The results are presented in table 11. The sand patch measurements on the original surface are suspect, especially for mixture A. The profile measurements were difficult to obtain because the probe constantly stalled in the deep voids. Based on these facts, sand patch measurements on replicates of the surface are the recommended technique for making texture measurements even though it may not be convenient for field testing, particularly on highly trafficked pavements. Texture measurements made at the Penn State Pavement Durability Research Facility are found in table 12.

Table 11. Texture depth measurements on laboratory porous asphalt sections.

Distance along channel (m)	MTD Values (mm)		
	Mix A	Mix B	Mix C
0.3	1.45	1.04	2.34
1.5	1.60	--	-
3.2	2.13	1.07	2.24
3.6	1.57	1.45	--
4.8	-	1.24	1.98
6.3	--	1.47	1.93
Average	1.70	1.24	2.13
Sand patch directly on surface, Average (mm)	5.1	1.9	2.3
MTD estimated from profile measurements directly on surface (see figure 29)	2.54	2.26	2.92

Table 12. Sand patch data obtained at the Penn State Pavement Durability Research Facility.

Mix	Station	Sand Patch Diameter (mm)							Mean Texture Depth	
		1	2	3	4	Average	(mm)			
							Average		Station	Section
1	105	149.2	136.5	139.7	139.7	141			1.55	
	75	139.7	139.7	146.1	136.5	140			1.60	
	45	146.1	146.1	146.1	139.7	144			1.55	
	15	152.4	158.8	158.8	158.8	157	145	1.27	1.5	
2	105	88.9	95.3	88.9	88.9	90			3.66	
	75	95.3	95.3	88.9	88.9	92			3.66	
	45	101.6	101.6	101.6	88.9	98			3.12	
	15	88.9	88.9	82.6	82.6	85	91	4.11	3.6	
3	105	133.4	133.4	133.4	136.5	134			1.73	
	75	136.5	139.7	133.4	139.7	137			1.65	
	45	146.1	146.1	139.7	139.7	142			1.55	
	15	146.1	127.0	139.7	146.1	139	138	1.60	1.6	
4	105	165.1	165.1	158.8	168.3	164			1.14	
	75	177.8	165.1	171.5	177.8	173			1.04	
	45	177.8	165.1	177.8	177.8	174			1.02	
	15	171.5	158.8	165.1	171.5	166	169	1.12	1.1	

Full-Scale Skid Testing

Full-scale skid testing was done at the Penn State Pavement Durability Research Facility and at the Wallops Flight Facility. The results of the testing performed at the Penn

State Durability Research Facility are presented in figures 33 through 36 for the four test sections. A great effort was required to obtain these results. The sections were dammed along their side and flooded (one section at a time) as described previously in this chapter. The skid trailer was driven at different speeds down the track, and the tire, a bald ASTM E 524-88 (“Standard Specification for Standard Smooth Tire for pavement Skid-Resistance Tests”) tire, was locked over the flooded middle portion of the section. Water film thickness measurements were taken with the color-indicating gauge at intervals along the section immediately before each test as described previously. This resulted in nearly 50 sets of skid resistance-water film thickness data. In general, relatively uniform water film measurements were obtained, and only a few of the data sets were discarded. Analog traces of wheel friction recorded by the tester were examined for anomalous data. In order to obtain a zero thickness value of skid resistance, the wheel of the trailer was locked on each section with no flooding but with a damp surface. In general, replicate runs were made at each water film thickness and speed.

Although there is considerable variability in the data, several conclusions can be drawn from the test results. For the water film thicknesses that were tested, the skid resistance values were less than the “zero thickness” values. For each section, the skid resistance decreased as the water film thickness increased. However, the skid resistance typically reached a minimum and then unexpectedly increased with increasing water film thickness. After some thought, this was considered reasonable, explained by the “ploughing” effect of the wave of water pushed by the locked tire. Minimum skid resistance values were in the range of four to ten depending on the test section. Hydroplaning occurred on all of the test sections at 60 and 90 km/h when the water film thickness became high.

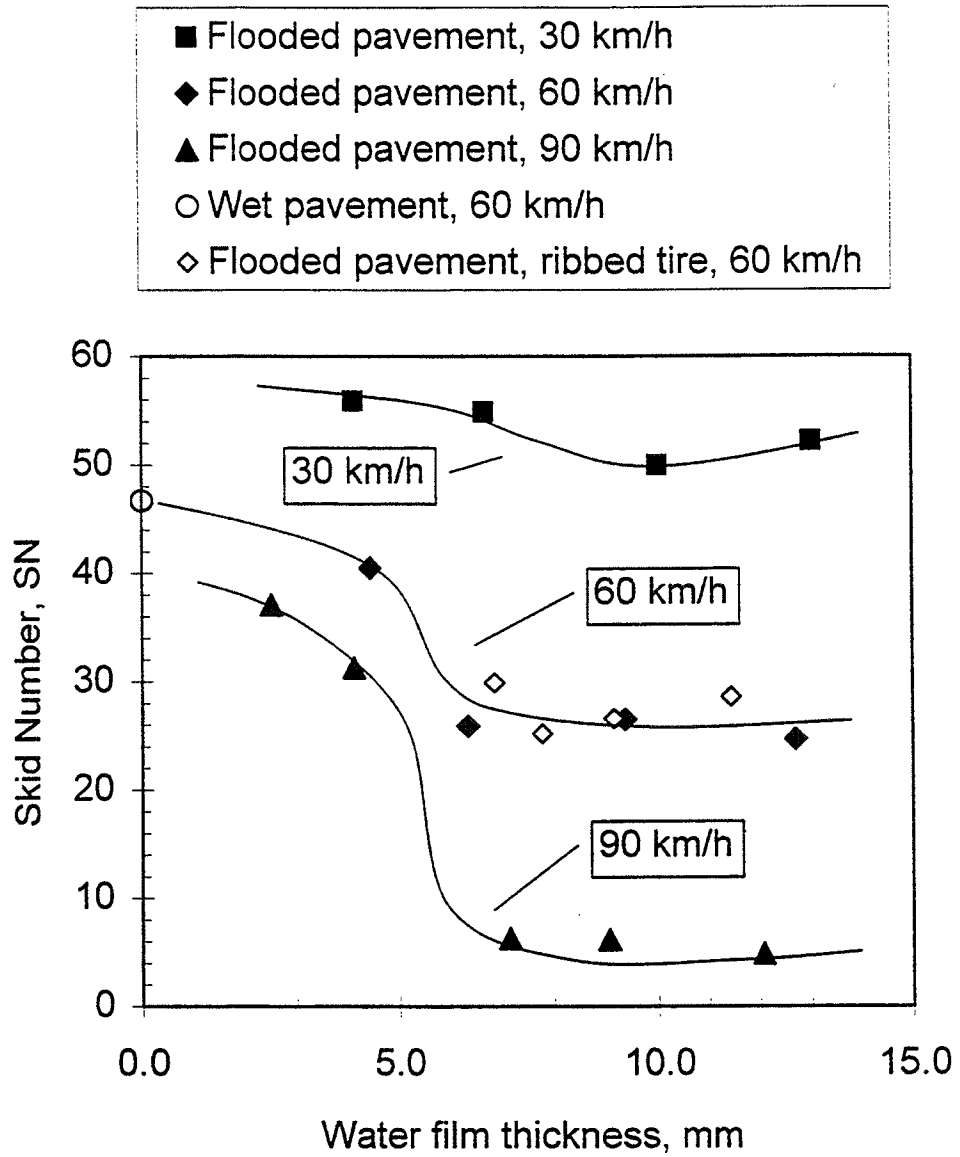


Figure 33. Skid resistance measurements at the Penn State Pavement Durability Research Facility, mixture 1.

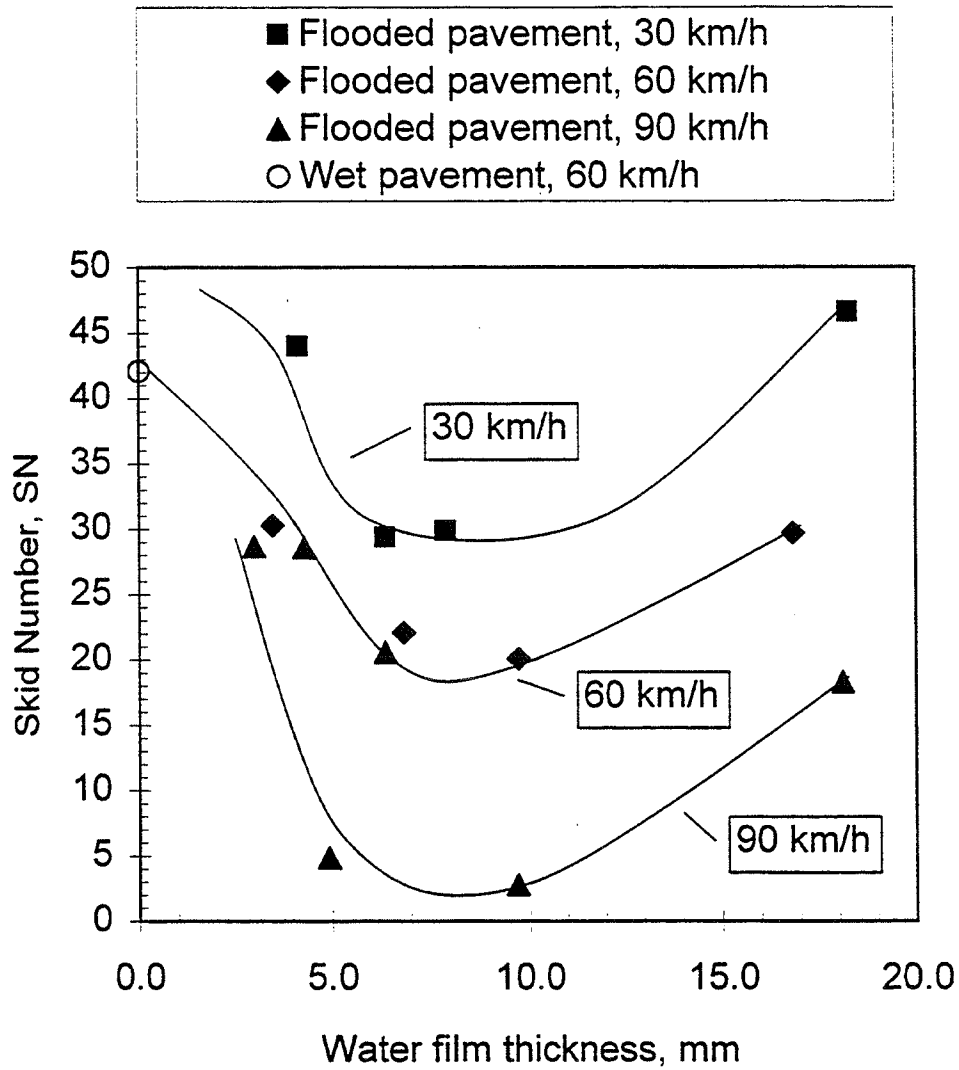


Figure 34. Skid resistance measurements at the Penn State Pavement Durability Research Facility, mixture 2.

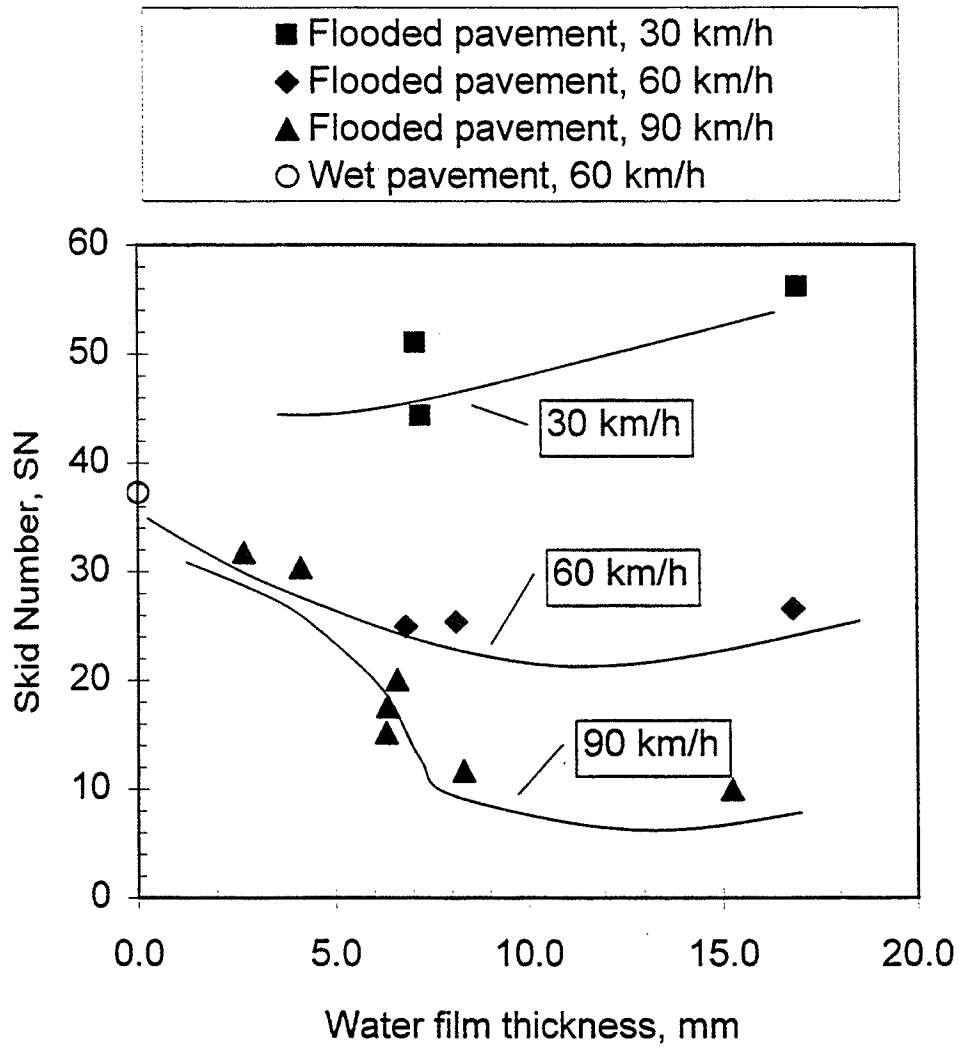


Figure 35. Skid resistance measurements at the Penn State Pavement Durability Research Facility, mixture 3.

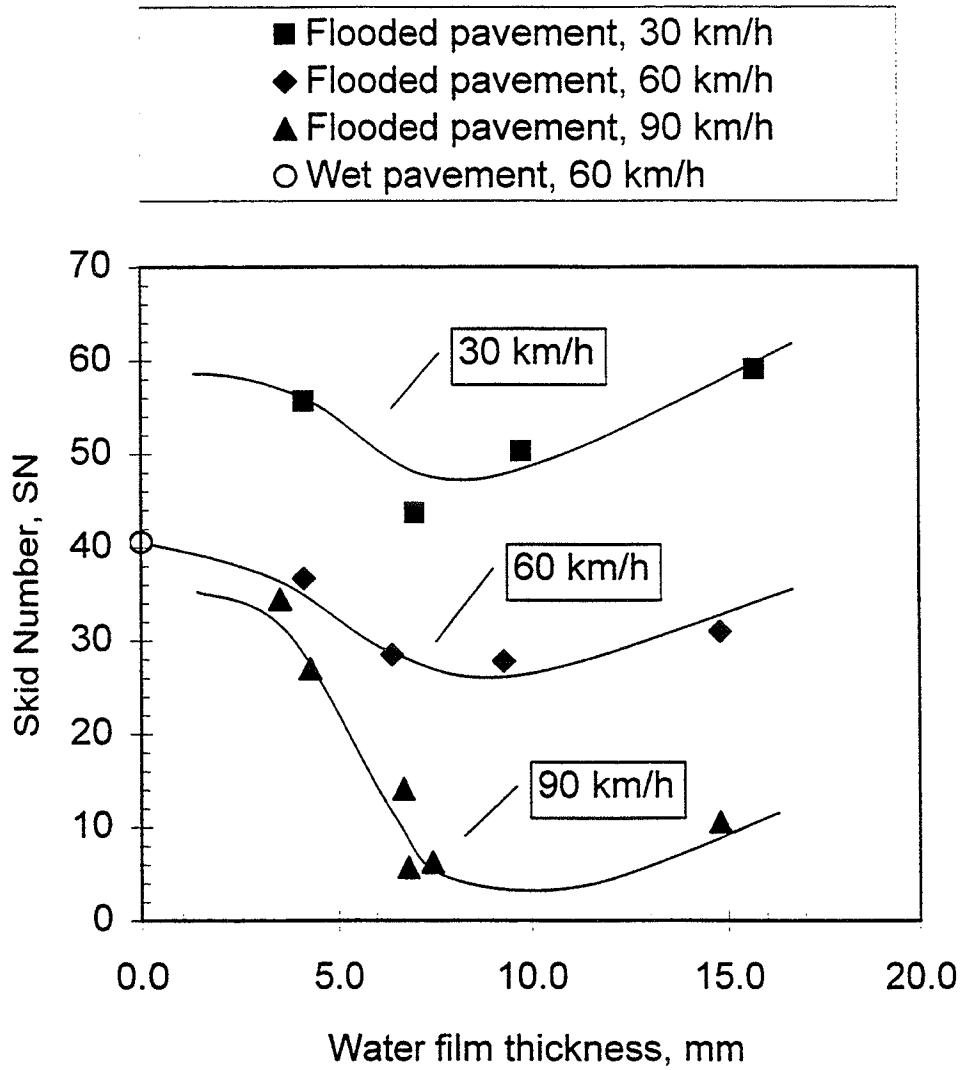


Figure 36. Skid resistance measurements at the Penn State Pavement Durability Research Facility, mixture 4.

The results from the testing in the grooved and plain portland cement concrete at the Wallops Flight Facility are shown in table 13 and figures 37 and 38. Quite surprisingly, the skid resistance versus water film thickness relationship for the grooved versus the plain portland cement concrete surface was very similar when the mean texture depth is calculated using the surface at the top of the grooves as the datum. Thus, although the grooves are a definite aid in removing water from the pavement surface, they do little to relieve the water film from beneath the tire. This effect is not apparent in the standard ASTM E 274 test as illustrated in figures 34 and 35. In the opinion of the researchers, this is also the case with porous asphalt surfaces. In other words, the main contribution offered by porous asphalt pavement surfaces to the lowering of hydroplaning speed, even though it is a very significant contribution, is the increase in the mean texture depth that these surfaces offer.

These findings do not agree with many practitioners who feel that the grooving and large texture in porous mixtures allows the water to drain from beneath the tire. Of course, the findings here are for the locked bald tire according to ASTM E 274, and the findings may be different for more heavily loaded truck tires or grooved passenger tires.

Table 13. Skid resistance test data obtained at the Wallops Flight Facility.

Pavement	Water Film Thickness (mm)	Speed (km/h)	Skid Number	Average Skid Number
Brushed Concrete	12.5 ⁽¹⁾	60	14.8	14.8
	12.5	75	9.6	9.6
	12.5	90	6.1	6.1
	12.5	82	7.1	7.1
	12.5	100	4.6	4.6
Grooved Concrete	12.5	60	17.3	17.3
	12.5	80	12.7	12.7
	12.5	90	6.0	6.0
Brushed Concrete	ASTM ⁽²⁾	30	26.9	
	ASTM	30	31.5	
	ASTM	30	31.8	30.1
	ASTM	60	18.6	
	ASTM	60	20.3	
	ASTM	60	24.2	23.2
	ASTM	90	13.8	
	ASTM	90	15.3	
	ASTM	90	17.0	15.4
Grooved Concrete	ASTM	30	30.9	
	ASTM	30	32.9	31.9
	ASTM	60	22.4	
	ASTM	60	22.6	
	ASTM	60	46.2	30.4
	ASTM	90	30.1	30.1

⁽¹⁾Flooded with water prior to testing.

⁽²⁾Water applied in front of tire in accordance with ASTM E 274.

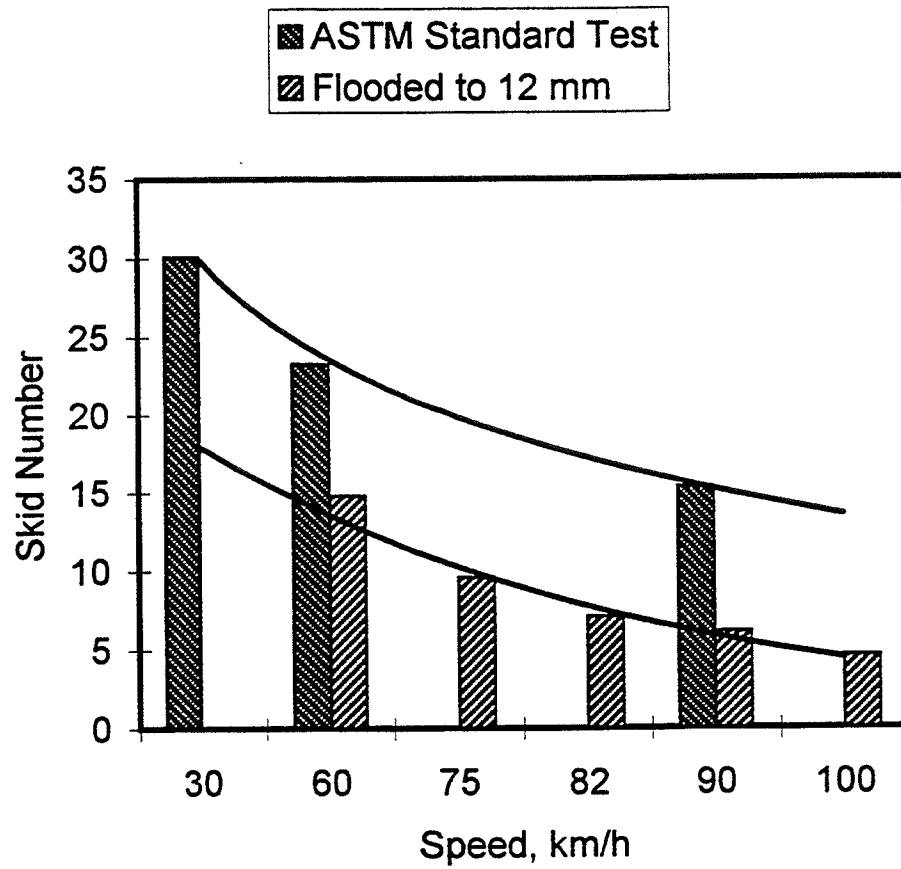


Figure 37. Test results for plain concrete sections at the Wallops Flight Facility.

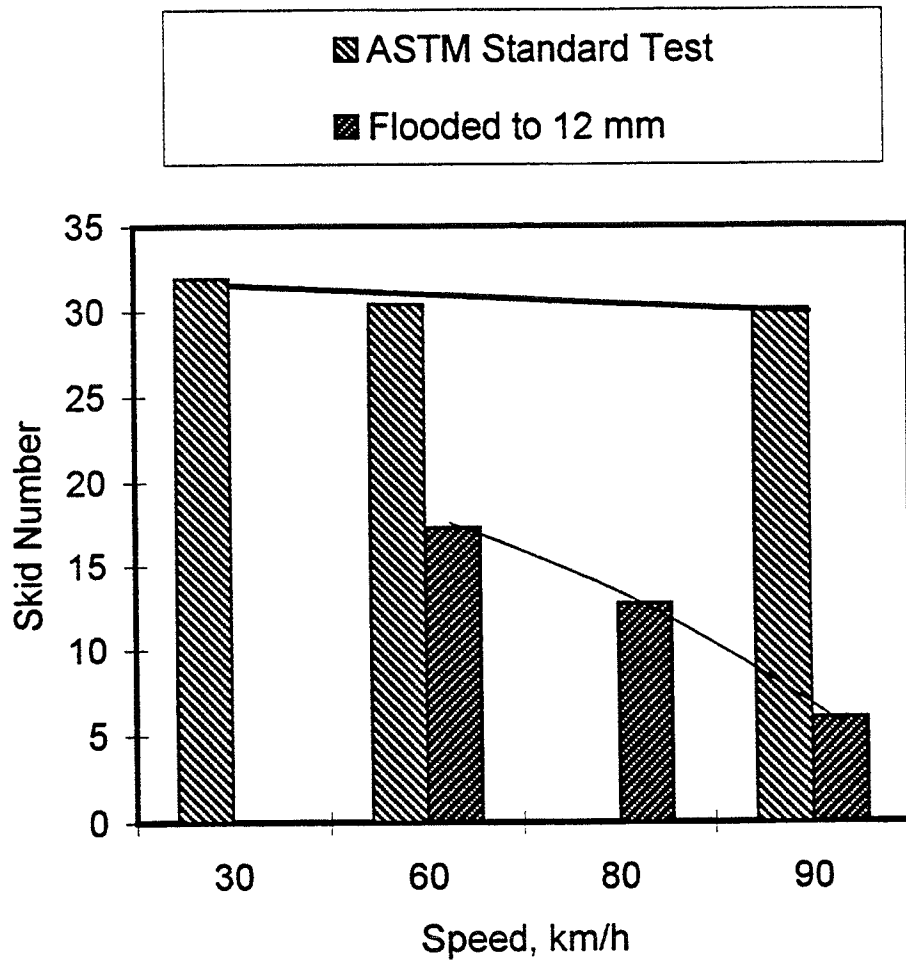


Figure 38. Test results for grooved concrete sections at the Wallops Flight Facility.

CHAPTER 5

SUMMARY, FINDINGS, AND RECOMMENDATIONS

SUMMARY

The primary objective of this research was to identify improved methods for draining rainwater from the surface of multi-lane pavements and to develop guidelines for their use. The guidelines, along with details on the rationale for their development, are presented in a separate document, "Proposed Design Guidelines for Improving Pavement Surface Drainage" (2). The guidelines support an interactive computer program, PAVDRN, that can be used by practicing engineers in the process of designing new pavements or rehabilitating old pavements, is outlined in figure 39. The intended audience for the guidelines is practicing highway design engineers that work for transportation agencies or consulting firms.

Improved pavement surface drainage is needed for two reasons: (1) to minimize splash and spray and (2) to control the tendency for hydroplaning. Both issues are primary safety concerns. At the request of the advisory panel for the project, the main focus of this study was on improving surface drainage to minimize the tendency for hydroplaning. In terms of reducing the tendency for hydroplaning, the needed level of drainage is defined in terms of the thickness of the film of water on the pavement. Therefore, the guidelines were developed within the context of reducing the thickness of the water film on pavement surfaces to the extent that hydroplaning is unlikely at highway design speeds. Since hydroplaning is

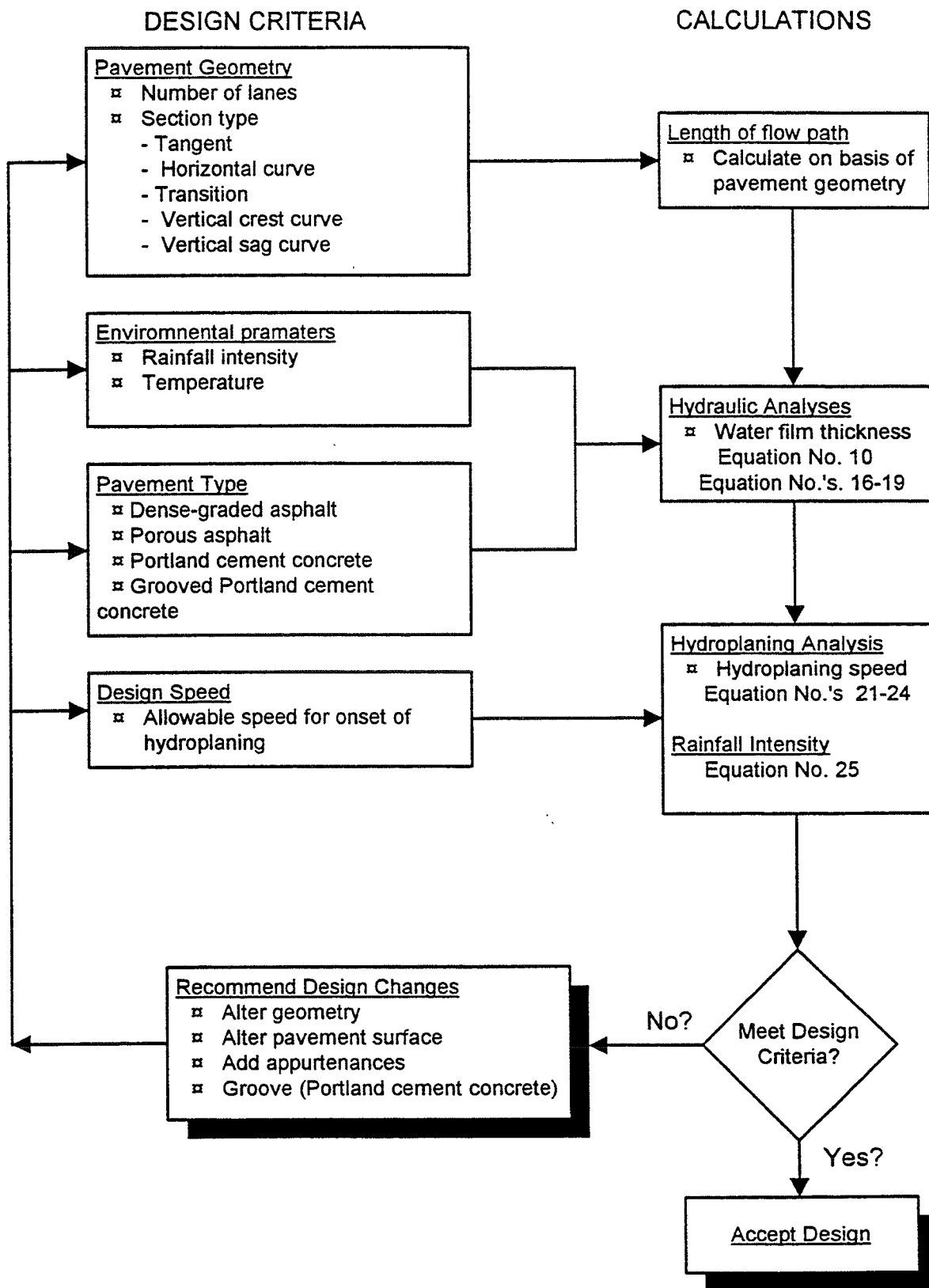


Figure 39. Flow diagram representing PAVDRN design process in “Proposed Guidelines for Improving Pavement Surface Drainage” (2).

controlled primarily by the thickness of the water film on the pavement surface, the design guidelines focus on the prediction and control of the depth of water flowing across the pavement surface as a result of rainfall, often referred to as sheet flow.

Water film thickness on highway pavements can be controlled in three fundamental ways, by:

1. Minimizing the length of the longest flow path of the water over the pavement and thereby the distance over which the flow can develop;
2. Increasing the texture of the pavement surface; and
3. Removing water from the pavement's surface.

In the process of using PAVDRN to implement the design guidelines, the designer is guided to (1) minimize the longest drainage path length of the section under design by altering the pavement geometry and (2) reduce the resultant water film thickness that will develop along that drainage path length by increasing the mean texture depth, choosing a surface that maximizes texture, or using permeable pavements, grooving, and appurtenances to remove water from the surface.

Through the course of a typical design project, four key areas need to be considered in order to analyze and eventually reduce the potential for hydroplaning. These areas are:

1. Environmental conditions;
2. Geometry of the roadway surface;
3. Pavement surface (texture) properties; and
4. Appurtenances.

Each of these areas and their influence on the resulting hydroplaning speed of the designed section are discussed in detail in the guidelines (2).

The environmental conditions considered are rainfall intensity and water temperature, which determines the kinematic viscosity of the water. The designer has no real control over these environmental factors but needs to select appropriate values when analyzing the effect of flow over the pavement surface and hydroplaning potential.

Five section types, one for each of the basic geometric configurations used in highway design, are examined. These section are:

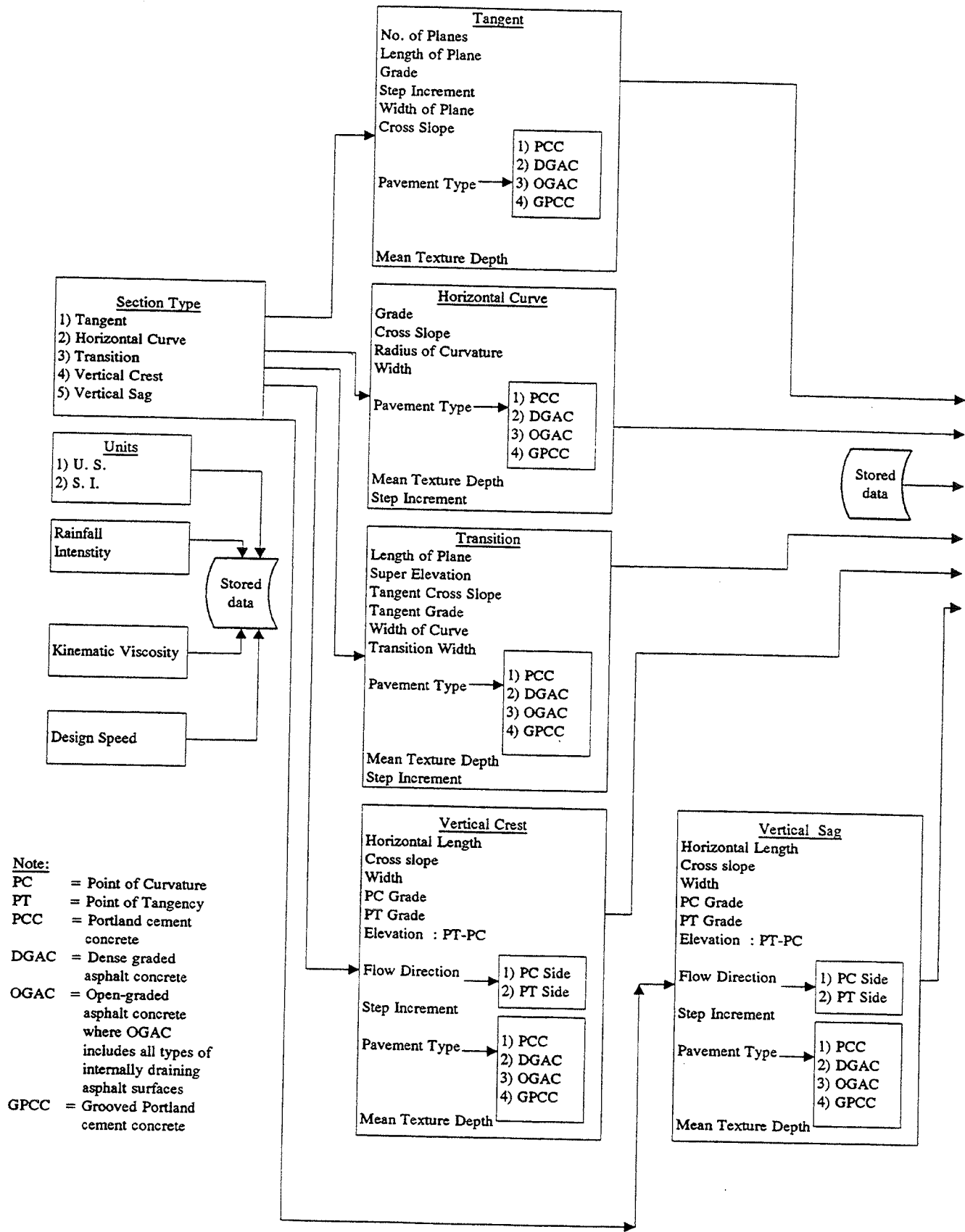
1. Tangent;
2. Superelevated curve;
3. Transition;
4. Vertical crest curve; and
5. Vertical sag curve.

Pavement properties that affect the water film thickness include surface characteristics, such as mean texture depth and grooving of portland cement concrete surfaces, are considered in the process of applying PAVDRN. Porous asphalt pavement surfaces can also reduce the water film thickness and thereby contribute to the reduction of hydroplaning tendency and their presence can also be accounted for when using PAVDRN. Finally, PAVDRN also allows the design engineer to consider the effect of drainage appurtenances, such as slotted drain inlets. A complete description of the various elements that are considered in the PAVDRN program is illustrated in figure 40. A more complete description of the design process, the parameters used in the design process, and typical values for the parameters is presented in the "Proposed Design Guidelines for Improving Pavement Surface Drainage" (2) and in Appendix A.

FINDINGS

The following findings are based on the research accomplished during the project, a survey of the literature, and a state-of-the-art survey of current practice.

1. **Model.** The one-dimensional model is adequate as a design tool. The simplicity and stability of the one-dimensional model offsets any increased accuracy afforded by a two-dimensional model. The one-dimensional model as a predictor of water film thickness and flow path length was verified by using data from a previous study (11).



- Note:**
- PC = Point of Curvature
 - PT = Point of Tangency
 - PCC = Portland cement concrete
 - DGAC = Dense graded asphalt concrete
 - OGAC = Open-graded asphalt concrete where OGAC includes all types of internally draining asphalt surfaces
 - GPCC = Grooved Portland cement concrete

Figure 40. Factors considered in PAVDRN program.

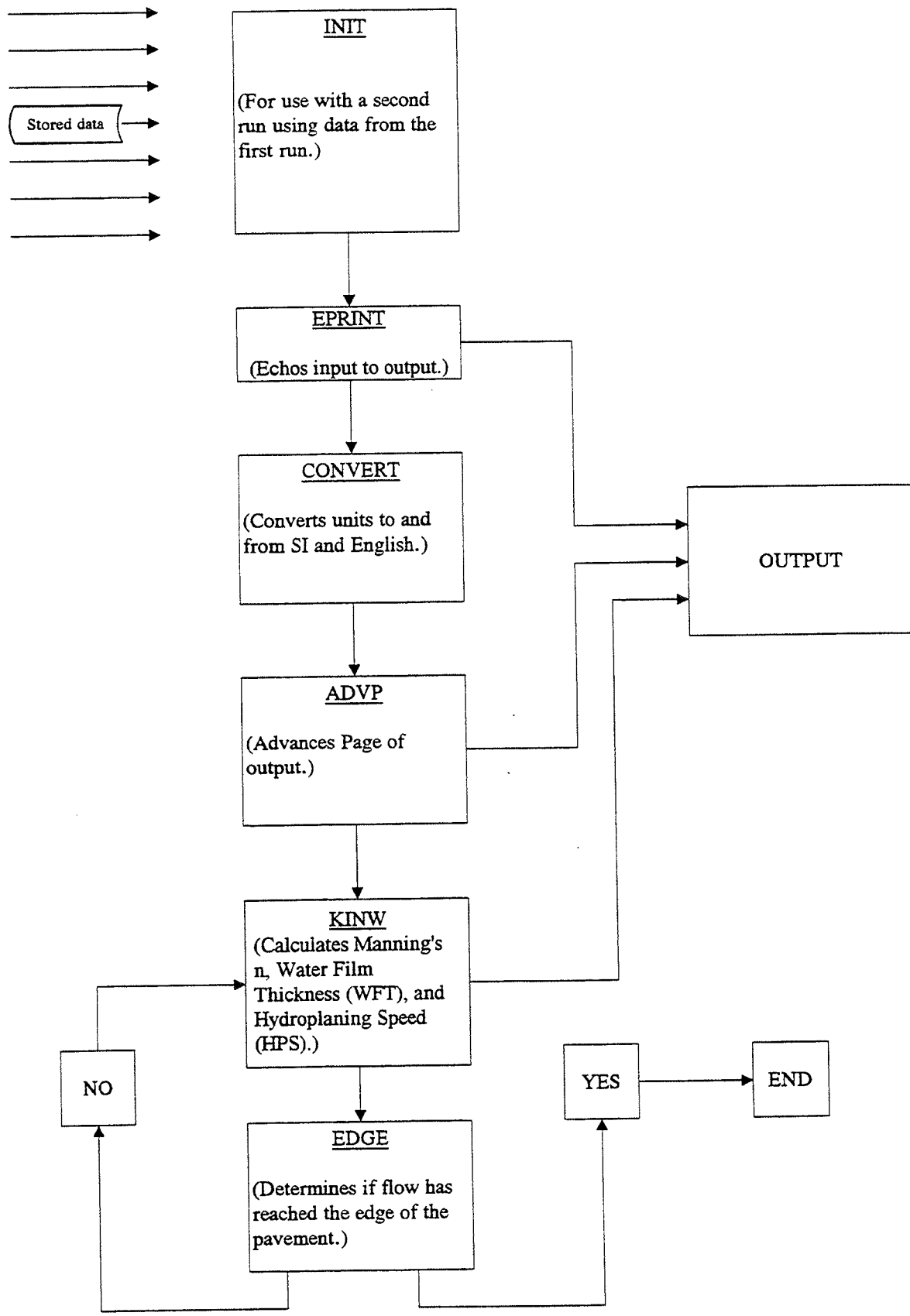


Figure 40. Factors considered in PAVDRN program (continued).

2. Occurrence of Hydroplaning. In general, based on the PAVDRN model and the assumptions inherent in its development, hydroplaning can be expected at speeds below roadway design speeds if the length of the flow path exceeds two lane widths.
3. Water Film Thickness. Hydroplaning is initiated primarily by the depth of the water film thickness. Therefore, the primary design objective when controlling hydroplaning must be to limit the depth of the water film.
4. Reducing Water Film Thickness. There are no simple means for controlling water film thickness, but a number of methods can effectively reduce water film thickness and consequently hydroplaning potential. These include:
 - Optimizing pavement geometry, especially cross-slope.
 - Providing some means of additional drainage, such as use of grooved surfaces (PCC) or porous mixtures (HMA).
 - Including slotted drains within the roadway.
5. Tests Needed for Design. The design guidelines require an estimate of the surface texture (MTD) and the coefficient of permeability (porous asphalt only). The sand patch is an acceptable test method for measuring surface texture, except for the more open (20-percent air voids) porous asphalt mixes. In these cases, an estimate of the surface texture, based on tabulated data, is sufficient. As an alternative,

sand patch measurements can be made on cast replicas of the surface. For the open mixes, the glass beads flow into the voids within the mixture, giving an inaccurate measure of surface texture.

Based on the measurements obtained in the laboratory, the coefficient of permeability for the open-graded asphalt concrete does not exhibit a wide range of values, and values of k may be selected for design purposes from tabulated design data (k versus air voids). Given the uncertainty of this property resulting from compaction under traffic and clogging from contaminants and anti-skid material, a direct measurement (e.g., drainage lag permeameter) of k is not warranted.

Based on the previous discussion, no new test procedures are needed to adopt the design guidelines developed during this project.

6. Grooving. Grooving of PCC pavements provides a reservoir for surface water and can facilitate the removal of water if the grooves are placed parallel to the flow path. Parallel orientation is generally not practical because the flow on highway pavements is typically not transverse to the pavement. Thus, the primary contribution offered by grooving is to provide a surface reservoir unless the grooves connect with drainage at the edge of the pavement. Once the grooves are filled with water, the tops of the grooves are the datum for the WFT and do not contribute to the reduction in the hydroplaning potential.

7. Porous Pavements. These mixtures can enhance the water removal and thereby reduce water film thickness. They merit more consideration by highway agencies in the United States, but they are not a panacea for eliminating hydroplaning. As with grooved PCC pavements, the internal voids do not contribute to the reduction of hydroplaning; based on the field tests done in this study, hydroplaning can be expected on these mixtures given sufficient water film thickness. Other than their ability to conduct water through internal flow, the large MTD offered by porous asphalt is the main contribution offered by the mixtures to the reduction of hydroplaning potential. The high-void (> 20 percent), modified binder mixes used in Europe merit further evaluation in the United States. They should be used in areas where damage from freezing water and the problems of black ice are not likely.

8. Slotted Drains. These fixtures, when installed between travel lanes, offer perhaps the most effective means of controlling water film thickness from a hydraulics standpoint. They have not been used extensively in the traveled lanes and questions remain unanswered with respect to their installation (especially in rehabilitation situations) and maintenance. The ability to support traffic loads and still maintain surface smoothness has not been demonstrated and they may be susceptible to clogging from roadway debris, ice, or snow.

RECOMMENDATIONS AND CONCLUSIONS

The following recommendations are offered based on the work accomplished during this project and on the conclusions given previously:

1. **Implementation.** The PAVDRN program and associated guidelines need to be field tested and revised as needed. The program and the guidelines are sufficiently complete so that they can be used in a design office. Some of the parameters and algorithms will likely need to be modified as experience is gained with the program.
2. **Database of Material Properties.** A database of material properties should be gathered to supplement the information contained in PAVDRN. This information should include typical values for the permeability of porous asphalt and typical values for the surface texture (MTD) for different pavement surfaces to include tined portland cement concrete surfaces. A series of photographs of typical pavement sections and their associated texture depths should be considered as an addition to the design guide (2).
3. **Pavement Geometry.** The AASHTO design guidelines (1) should be re-evaluated in terms of current design criteria to determine if they can be modified to enhance drainage without adversely affecting vehicle handling or safety.

4. Use of appurtenances. Slotted drains should be evaluated in the field to determine if they are practical when installed in the traveled way. Manufacturers should reconsider the design of slotted drains and their installation recommendations currently in force to maximize them for use in multi-lane pavements and to determine if slotted drains are suitable for installations in the traveled right of way.
5. Porous Asphalt Mixtures. More use should be made of these mixtures, especially the modified high air-void mixtures as used in France. Field trials should be conducted to monitor HPS and the long-term effectiveness of these mixtures and to validate the MPS and WDT predicted by PAVDRN.
6. Two-Dimensional Model. Further work should be done with two-dimensional models to determine if they improve accuracy of PAVDRN and to determine if they are practical from a computational standpoint.

ADDITIONAL STUDIES

On the basis of the work done during this study, a number of additional items warrant further study. These include:

1. Full-scale skid resistance studies to validate PAVDRN in general and the relationship between water film thickness and hydroplaning potential in particular are needed in light of the unexpectedly low hydroplaning speeds predicted during

this study. The effect of water infiltration into pavement cracks and loss of water by splash and spray need to be accounted for in the prediction of water film thickness. Surface irregularities, especially rutting, need to be considered in the prediction models.

2. Field trials are needed to confirm the effectiveness of alternative asphalt and portland cement concrete surfaces. These include porous portland cement concrete surfaces, porous asphalt concrete, and various asphalt micro-surfaces.
3. The permeability of porous surface mixtures needs to be confirmed with samples removed from the field, and the practicality of a simplified method for measuring in-situ permeability must be investigated and compared to alternative measurements, such as the outflow meter.
4. For measuring pavement texture, alternatives to the sand patch method should be investigated, especially for use with porous asphalt mixtures.

THIS PAGE INTENTIONALLY LEFT BLANK

REFERENCES

1. *A Policy on Geometric Design of Highways and Streets*. American Association of State Highway and Transportation Officials (1990) 1087 pp.
2. "Proposed Design Guidelines for Improving Pavement Surface Drainage." The Pennsylvania Transportation Institute, The Pennsylvania State University (1998).
3. Gallaway, B. M., Schiller, R. E., and Rose, J. G., "The Effects of Rainfall Intensity, Pavement Cross Slope, Surface Texture, and Drainage Length on Pavement Water Depths." *Federal Highway Administration Research Report No. 138-5* (1971) 69 pp.
4. Gallaway, B. M., Ivey, D. L., Hayes, G. G., Ledbetter, W. G., Olson, R. M., Woods, D. L., and Schiller, R. E., "Pavement and Geometric Design Criteria for Minimizing Hydroplaning." *Federal Highway Administration Report No. FHWA-RD-79-31* (1979) 278 pp.
5. *Highway Drainage Guidelines*. American Association of State Highway and Transportation Officials (1992) 250 pp.
6. *Hydraulic Design of Highway Culverts*, Hydraulic Design Series No. 5, Federal Highway Administration, FHWA-IP-85-15 (1985).

7. Jens, S. W., "Design of Urban Highway Drainage." Federal Highway Administration Report No. FHWA-TS-79-225 (August 1979) 272 pp.
8. Johnson, F. L. and Chang, F. M., "Drainage of Highway Pavements." Federal Highway Administration Report No. FHWA-TS-84-202 (March 1984) 136 pp.
9. Huddleston, I. J., Zhou, H. and Hicks, R. G., "Performance Evaluation of Open-Graded Asphalt Concrete Mixtures Used in Oregon." *Asphalt Paving Technology*, Vol. 60 (March 1991) pp. 19-43.
10. "Open-Graded Friction Courses for Highways." National Cooperative Highway Research Program Synthesis No. 49 (1978) 50 pp.
11. Brown, J. R., "Pervious Bitumen-Macadam Surfacing Laid to Reduce Splash and Spray at Stonebridge, Warwickshire." Transportation and Road Research Laboratory Report No. LR 563 (1973) 23 pp.
12. Zwan, J. T. van der, Goeman, T., Gruis, H. J., Swart, J. H., and Oldenburger, R. H., "Porous Asphalt Wearing Courses in the Netherlands: State of the Art Review." *Porous Asphalt Pavements: An International Perspective*, Transportation Research Record 1265 (1990) pp. 95-110.

13. Isenring, T., Koster, H., and Scazziga, I., "Experiences With Porous Asphalts in Switzerland." *Porous Asphalt Pavements: An International Perspective*, Transportation Research Record 1265 (1990) pp. 41-53.
14. Heystraeten, G. van, "The Winter Behaviour of Porous Asphalt in Belgium." Marrakech XIXth World Road Congress, PIARC Technical Committees on Flexible Roads and Surface Characteristics, Workshop on Pervious Macadam, Proc. (September 1991) pp. 289-291.
15. Talirz, H., "Drainage Asphalt - From the Economic Point of View a Reasonable Investment." Marrakech XIXth World Road Congress, PIARC Technical Committees on Flexible Roads and Surface Characteristics, Workshop on Pervious Coated Macadam, Proc. (September 1991) pp. 285-288.
16. Delanne, Y, Goyon, V., and Poirier, J. P., "Experimental Sites for Testing Thin Layer Drainage Asphalt Performances: First Results." Marrakech XIXth World Road Congress, PIARC Technical Committees on Flexible Roads and Surface Characteristics, Workshop on Pervious Coated Macadam, Proc. (September 1991) pp. 278-281.
17. Lefebvre, G., *Porous Asphalt*. Permanent International Association of Road Congresses, Technical Committee on Flexible Roads, Technical Committee on Surface Characteristics, Belgium (1993) 161 pp.

18. Decoene, Y., "Contribution of Cellulose Fibers to the Performance of Porous Asphalts." *Porous Asphalt Pavements: An International Perspective*, Transportation Research Record 1265 (1990) pp. 82-86.
19. Sainton, A., "Advantages of Asphalt Rubber Binder for Porous Asphalt Concrete." *Porous Asphalt Pavements: An International Perspective*, Transportation Research Record 1265 (1990) pp. 69-81.
20. Tappeiner, W. J., "Open-Graded Asphalt Friction Course." *National Asphalt Pavement Association No. IS 115* (1993) 15 pp.
21. Surchamp, A., "Collecteur par enrobés drainants sur périphérique parisien." *Route Actualités*, No. 4 (1995) p. 34.
22. The Ministry for Verkeer en Waterstaat, "Structuurschema Verkeer." *Vervoer* (1991).
23. Kirsch, J. W., "Informal Comments on the Road Spray Problem." *Systems, Science, and Software*, Document No. SSR-IR-72-1352, La Jolla, CA, (1972).
24. Camomilla, G., Malgarini, M., and Gervasio, S., "Sound Absorption and Winter Performance of Porous Asphalt Pavement." *Porous Asphalt Pavements: An International Perspective*, Transportation Research Record No.1265 (1990) pp. 1-8.

25. Sherard, T. D., "Suppression of Vehicle Splash and Spray." Society of Automotive Engineers Paper No. 730718 (1973).
26. Brosseaud, Y., Poirier, J. C., and Roche, J. P., "Draining Asphalts—Conclusions Drawn From the Performance Assessment of the Two Experimental Road Sites." AIPCR-PIARC, Montreal, Canada (1996).
27. Michael, L. L., Regional Engineer, Western Regional Laboratory, Maryland Department of Transportation, Personal Communication (1996).
28. Brosseaud, Y., "Evaluation of the Experimental Site of Porous Asphalt on Motorway A63 After 8 Years of Traffic." European Conference on Porous Asphalt, Madrid, Spain (March 1997).
29. Reed, J. R., Proctor, M. L., Kibler, D. F., and Agrawal, S. K., "Measurements of Runoff Depths From a Grooved Laboratory Slab." *Transportation Research Board Circular No. 274* (April 1984) pp. 25-35.
30. Reed, J. R., Kibler, D. F., and Proctor, M. L., "Analytical and Experimental Study of Grooved Pavement Runoff, Final Report." Federal Aviation Administration Report No. DOT/FAA/PM-83/84 (August 1983) 65 pp.

31. Reed, J. R., Kibler, D. F., and Krallis, G. A., "Analytical and Experimental Study of Runway Runoff With Wind Effects. Final Report." Federal Aviation Administration Report No. DOT/FAA/CT- TN89/59 (October 1989) 64 pp.
32. Lewis, A. E., Lewis, S. B., and Lee, K. W., *Correlation of Pavement Surface Texture to Hydraulic Roughness*. TRR 1471 (1994) pp 10-17.
33. Zhang, W. and Cundy, T. W., "Modeling of Two Dimensional Overland Flow." *Water Resources Research*, Vol. 25, No. 9 (September 1989) pp. 2019-2035.
34. Russam, K. and Ross, N. F., "The Depth of Rain Water on Road Surfaces." Road Research Laboratory, Ministry of Transport Report No. LR 236 (1968) 25 pp.
35. Reed, J. R. and Stong, J. B., "Resistance Variables for Sheet Flows on Portland Cement Concrete Surfaces." Mid-Atlantic Universities Transportation Center Report No. III-9207 (1992) 127 pp.
36. Stong, J. B., "Resistance Variables for Sheet Flows on Portland Cement Concrete Surfaces." Ph.D. Dissertation, The Pennsylvania State University, 1992.
37. Henry, J. J., and Meyer W. E., "The Simulation of Tire Traction on Wet Pavements." 18th International Automobile Technical Congress, Hamburg, Germany, Proc., No. 369 (1980) pp. 121-128.

38. Huebner, R. S., Reed, J. R., and Henry, J. J., "Criteria for Predicting Hydroplaning Potential." *American Society of Civil Engineers Journal of Transportation Engineering*, Vol. 112, No. 5 (September 1986) pp. 549-553.
39. Izzard, C. F., "Hydraulics of Runoff From Developed Surfaces." Highway Research Board, Proc. Vol. 26 (1946) pp. 129-150.
40. Dahir, S. H., Henry, J. J., and Meyer, W. E., *Seasonal Skid-Resistance Variations*. NTIS: PB80-222441 (1979).
41. Wambold, J. C., "Road Characteristics and Skid Testing." Transportation Research Record No. 1196 (1988) pp. 294-299.
42. American Society for Testing Materials, "Standard Practice for Calculating Mean Profile Depth." ASTM E 1845-96, Philadelphia, PA.
43. Barker, E. S., and Sawyer, C. L., "Highway Subdrainage." *Public Roads*, Vol. 26, No. 12 (1952), pp. 251-270.
44. Agrawal, S. K., and Henry J. J., "Experimental Investigation of the Transient Aspect of Hydroplaning." Annual Meeting of the Transportation Research Board, Washington, D. C., Proc. (January 1980) pp. 35.

45. G. G. Hayers, D. L. Ivey, and Gallaway, B. M., "Hydroplaning, Hydrodynamic Drag, and Vehicle Stability." ASTM Special Technical Publication No. 793, American Society for Testing and Materials, Philadelphia, PA (1983), pp. 151-66.
46. Gallaway, B. M., Ivey, D. L., Ross, H. E. Jr, Ledbetter, W. B., Woods, D. L., and Schiller, R. E., "Tentative Pavement and Geometric Design Criteria for Minimizing Hydroplaning." *Federal Highway Administration Report No. FHWA-RD-75-11* (1975) 191 pp.
47. Tayfur, G., Kavvas, M. L., Govindaraju, R. S., and Stone, D. E., "Applicability of St. Venant Equations for Two-Dimensional Overland Flows Over Rough Infiltrating Surfaces." *American Society of Civil Engineers Journal of Hydraulic Engineering*, Vol. 119, No. 1 (January 1993).
48. Froehlich, D. C., "Finite Element Surface Water Modeling System: Two-Dimensional Flow in a Horizontal Plane User's Manual." Federal Highway Administration Report No. FHWA-RD-88-177 (April 1989).
49. Huebner, R. S., "Overland Flow on Highway Pavements: Comparison of a One-Dimensional Kinematic Model and a Two-Dimensional Finite Element Model." Ph. D. Dissertation, The Pennsylvania State University (1990) 290 pp.

50. Woolhiser, D. A. and Liggett, J. A., "One-Dimensional Flow Over a Plane: The Rising Hydrograph." *Water Resources Research*, Vol. 3, No. 3 (September 1967) pp. 753-771.

51. Morris, E . M. and Woolhiser, D. A., "Unsteady one-dimensional flow over a plane: partial equilibrium and recession hydrographs." *Water Resources Research*, Vol. 16, No. 2, (April 1980) pp. 355-360.

52. Reed, J. R., Warner, J. C., and Huebner, R. S., "Sheet Flow Resistance of Asphalt Pavements." 1994 ASCE National Conference on Hydraulic Engineering, Buffalo, NY, Proc. (August 1994) pp.1100-1104.

THIS PAGE INTENTIONALLY LEFT BLANK

APPENDIX A

PROGRAM OVERVIEW

GENERAL DESCRIPTION

PAVDRN is a program package that was developed at The Pennsylvania State University's Pennsylvania Transportation Institute. The work was sponsored by the National Cooperative Highway Research Program Project 1-29, "Improved Surface Drainage of Pavements."

PAVDRN is intended for use by highway design engineers and determines the likelihood of hydroplaning on various highway pavement sections. It does this by computing the longest flow path length over a given pavement section and determining the water film thickness (depth of water above the roughness asperities of the pavement surface) at points along the path. The water film thickness is used to estimate the speed at which hydroplaning will occur. A worst-case scenario is examined by determining the water film thickness and hydroplaning speeds along the longest flow path length under steady-state conditions with a uniform rainfall rate. The predicted hydroplaning speed is compared to the design speed of the facility established by the engineer. Results are printed in a summary report format.

INSTALLATION

PAVDRN is distributed on two disks. The program runs under WindowsTM 3.1x or higher. (A FORTRAN version of the program is also available.) At a minimum, the computer used to run PAVDRN should have the following characteristics:

- 80386SX or DX processor or above
- MS-DOS 6.2 or above
- WindowsTM 3.1x running in standard or enhanced mode or above

The following steps describe the installation process:

1. Insert distribution diskette 1 into a floppy disk drive.
2. From the WindowsTM menu bar at the top of the screen, use the mouse and the left-hand mouse button to click on **File**.
3. From the **File** pull-down menu, click on **Run**.
4. In the dialog box for **Run**, type **a:setup** or **b:setup** (depending upon which floppy drive you have inserted distribution diskette 1 into).
5. Press **Enter** or click on **OK**.
6. Follow the directions shown on the Setup screens that follow. One of the first steps will be to provide the drive and subdirectory in which you want the program files installed. Certain files will also be copied to other subdirectories like the `\WINDOWS\SYSTEM` subdirectory in addition to the files copied to the directory

you indicated for the program files. Only the most current versions of files will be copied. This is intentional.

The installation process creates a program group in the Program Manager window labeled **PAVDRN**. When the group is opened, three program icons are displayed. The one that most users will use routinely is the PAVDRN program whose icon is a rain cloud. The PAVDRN program is started by double-clicking the left mouse button on this icon. The other two programs, **SHARE.EXE** and **GSW.EXE**, are only needed if a message appears on the user's screen prompting the user to start these programs. In most cases, they are not needed.

USING PAVDRN

After starting the PAVDRN program by double-clicking on the rain cloud icon labeled PAVDRN in the PAVDRN program group, the user should see the first of three screens that make up the user interface for the PAVDRN program. **Screen 1** requires the user to input general information about the simulation. Detailed information on each of the data items required for the first screen appears in the following. **Screen 2** requires the user to input data concerning the specific section with which he or she is working or designing. The third screen is a screen used for displaying the data set constructed using Screens 1 and 2. It is also used to display the output from the PAVDRN program, which includes information about water film thickness and hydroplaning speeds along the length of the flow path.

In general, the steps taken to use PAVDRN are:

1. Open the PAVDRN program group.
2. Double-click on the PAVDRN rain cloud icon.
3. Edit the values and text on Screen 1 for the current pavement section or simulation.
4. Go to Screen 2.
5. Edit the values on Screen 2 for the current pavement section or simulation.
6. Return to Screen 1.
7. Click on **File** on the menu bar at the top of the screen.
8. Click on **Save** on the drop down File menu and enter the name of the file in which you wish to save the data. (Another subdirectory can be selected at this point if desired).
9. Select **Run PAVDRN** from the File drop down menu or the Analysis drop-down menu on the menu bar at the top of the screen.
10. Select **View PAVDRN results** from the Analysis drop-down menu or the View drop-down menu on the menu at the top of the screen.
11. Print the output report or exit the viewing screen by clicking on one of the buttons at the bottom of the viewing screen.

By using the View drop down menu, the output report or the data file can be examined; **neither file can be edited using this screen.** The output file cannot be edited; the data file can be changed only by making changes to values in Screens 1 and/or 2. The output file and the data file are ASCII files and can be edited using a text editor such as the Notebook editor found in the Accessories group of Windows™.

SCREEN 1 - DATA INPUT AND EDITING

The input data described in the following are required in Screen 1, as displayed in figure A-1. They can be changed by using standard Windows™ editing techniques or by using the spin or option buttons where provided. An example of an option button is the option for the Section Type, as described in the following. Spin buttons are used for the design speed and rainfall intensity on Screen 1.

The tangent section is the only section that accommodates different texture depths, cross-slopes, and pavement types within a single section. All other sections have only one value for each of these variables in the PAVDRN model. Note that Screen 1 is initiated with default values that should be edited for the specific pavement section being analyzed. Also, Screen 1 is the only screen that contains the menu bar at the top of the screen.

Section Description

This part of the screen allows the user to provide a description of the design sections. Three lines, 72 characters each, are used to describe the section and any other unique aspects of the simulation.

Data Input - Screen 1

Section Description

Enter descriptive information
for this analysis here

(Use up to three lines to describe or label the analysis of this section)

Section Type

- Tangent
- Curve
- Transition
- Vertical Crest
- Vertical Sag

Rainfall Intensity

1

Water Temperature

50

Kinematic Viscosity

.00001406

Design Speed

55

System of Units

- US
- Metric (SI)

Use data from upstream pavement section

Go to Screen 2

Figure A-1. Example of PAVDRN input screen 1, environmental and section type.

Section Type

Five different design sections are considered (see figure A-2 for the plan and profile views of each type of section).

Tangent Section. A tangent section is a straight section that may consist of up to ten planes (sections with varying slope) that have unique cross-slopes, widths, texture depths, and/or pavement types.

Horizontal Curve Section. A horizontal curve section contains a circular curve with both the grade and superelevation specified.

Transition Section. A transition section is a straight section with a grade in which the cross-slope at the tangent end changes to meet the superelevation of the curved section.

Crest Vertical Curve Section. A vertical curve section is a section with a cross-slope that crests between point of curvature (PC) and point of tangency (PT).

Sag Vertical Curve Section. A sag vertical curve section contains a cross-slope that sags between the PC and the PT.

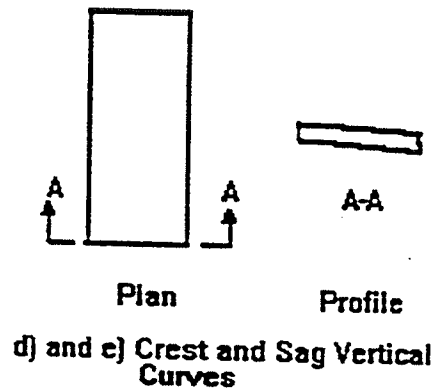
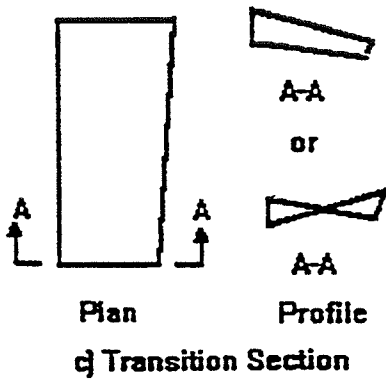
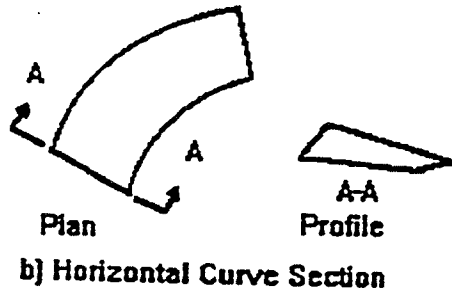
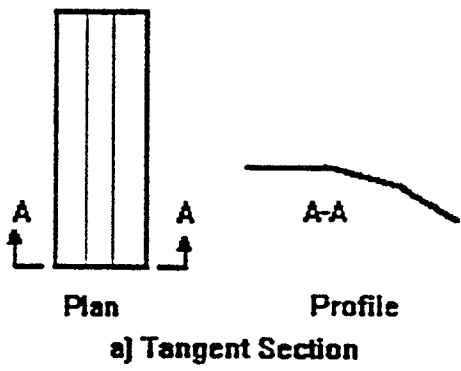


Figure A-2. Pavement cross sections included in PAVDRN.

System of Units

The system of units used for input and output (SI or English) may be chosen at the option of the user.

Rainfall Intensity

The rainfall intensity must be selected by the user in units of in/h or mm/h. The selection of a value for the rainfall intensity is discussed in the following.

Water Temperature

The temperature of water flowing over the pavement surface must be selected by the user in units of °F or °C.

Kinematic Viscosity of Water

The kinematic viscosity used in this simulation is expressed in units of ft^2/s , m^2/s . The value for the kinematic viscosity is calculated by an algorithm within PAVDRN as a function of the water temperature. The lowest possible water temperature should be used, keeping in mind the rainfall intensity and the season of the year. The temperature of the water may be

different than the ambient air temperature depending on pavement temperature and rainfall duration.

Design Speed

The design speed for the pavement section being analyzed must be specified by the user in either mi/h or km/h.

Multiple (Joined) Sections

If the simulation is set up for a pavement section that is downstream from a previously analyzed section, and if the program output for the previously analyzed section indicates that the flow path extended to the end of the section, click on the box. This option allows the conditions existing at the end of the previous section to be linked to the new section. A typical screen for a portland cement concrete pavement and a porous asphalt pavement are shown in figures A-3 and A-4.

Data Input - Screen 2

Tangent Section

Number of Planes

Section Length

Pavement Grade

Step Size

Plane Properties

Pavement Type

DG-AC PCC
 OG-AC G-PCC

Cross-slope

Plane Width

Texture Depth

Return to Screen 1

Figure A-3. Example of PAVDRN input screen 2, geometric requirements for portland cement concrete pavement.

Data Input - Screen 2

Tangent Section

<p>Number of Planes</p> <p>1</p>	<p>Plane Properties</p> <p>Plane 1</p> <p>OG-AC Permeability</p> <p>0</p> <p>Plane Width</p> <p>12</p> <p>Pavement Type</p> <p><input type="radio"/> DG-AC <input type="radio"/> PCC</p> <p><input checked="" type="radio"/> OG-AC <input type="radio"/> G-PCC</p> <p>Cross-slope</p> <p>.015</p> <p>Texture Depth</p> <p>.02</p>
<p>Section Length</p> <p>1000</p>	
<p>Pavement Grade</p> <p>.01</p>	
<p>Step Size</p> <p>3</p>	
<p>Return to Screen 1</p>	

Figure A-4. Example of PAVDRN input screen 3, geometric requirements for porous asphalt.

SCREEN 2 - DATA INPUT AND EDITING

Each of the different types of sections (selected from Screen 1) has a unique Screen 2 because of the different types of information required for each section type. The data required for each of these screens are described in the following according to the type of section.

Tangent Section

Number of planes. This section is used to define the number of planes sloped in one direction that form a series of planes over which flow will cascade until it reaches the edge or end of the pavement. This feature allows the user to simulate the effect of using different pavement materials and cross-slopes in different lanes of pavement. Up to ten different planes can be included.

Section Length. This entry defines the length of pavement section in the direction of travel (ft, m).

Pavement grade. This entry defines the longitudinal slope or grade of the pavement in the direction of travel (ft/ft, m/m).

Step Size. The computational step size (ft, m) determines the points along the flow path at which the water film thickness and hydroplaning speeds are computed. These values are reported in the summary tables of the output.

Plane Properties. For each plane, the pavement type, cross-slope, mean texture depth, and plane width are required. First, use the drop down list showing the plane number for which input data will be edited, and click on the appropriate plane number in the drop down list.

Pavement Type Four types of pavements are used in PAVDRN; they are:

- PCC: Portland cement concrete,
- GPCC: Grooved portland cement concrete,
- DGAC: Dense-graded asphaltic concrete, and
- OGAC: Open-graded or porous asphaltic concrete.

When grooved PCC is selected as the pavement type, text boxes for the groove spacing, the groove width, and the groove depth are displayed. This information is used to effectively increase the mean texture depth of the pavement.

If open-graded or porous asphaltic concrete is selected as the pavement type, an additional text box is displayed to provide a place for entering a value for the permeability of the pavement (mm/h, in/h). This value is used to reduce the amount of water available for surface runoff. The value for pavement permeability is set to zero for all other pavement types.

In general, porous pavements, if they and their bases are designed and constructed correctly and not clogged, will remove all runoff water from the surface. Isenring et al. (13) found permeabilities that ranged from 0.75 to 3.5 mm/s. This rate far exceeds a maximum design rainfall rate for surface runoff of 150 mm/h. The OGAC permeability then should be the “effective” permeability of the pavement.

Cross-slope. This entry defines the cross-slope of the pavement surface (ft/ft, m/m).

Texture Depth. The texture depth is the mean texture depth using a standard sand patch test (ASTM E 965) or equivalent (in, mm). The following are typical values for the mean texture depth and may be used if texture depth or sand patch measurements are not available.

- PCC 0.25 - 1.1 mm 0.01 - 0.044 in
- DGAC 0.23 - 1.0 mm 0.009 - 0.065 in
- OGAC 1.0 - 4.1 mm 0.04 - 0.161 in

Plane Width. This entry defines the width of the pavement section (ft, m).

Horizontal Curve Section

Section Grade. A longitudinal slope or grade in the direction of travel along the center line of the pavement is defined in this entry (ft/ft, m/m).

Superelevation. In this entry, the superelevation or cross-slope of the curve (ft/ft, m/m) is defined. The values are always positive.

Radius. In this entry the radius of curvature (ft, m) is defined.

Pavement Width. This entry defines the width of the curved pavement section (ft, m).

Pavement Type. There are four types of pavements are used in PAVDRN; they are:

- PCC: Portland cement concrete,
- GPCC: Grooved portland cement concrete,
- DGAC: Dense-graded asphaltic concrete, and
- OGAC: Open-graded or porous asphaltic concrete.

When grooved PCC is selected as the pavement type, text boxes for the groove spacing, the groove width and the groove depth are displayed. This information is used to effectively increase the mean texture depth of the pavement.

If open-graded or porous asphaltic concrete is selected as the pavement type, an additional text appears to provide a place for entering a value for the permeability of the pavement. This value is used to reduce the amount of water available for surface runoff. The value for pavement permeability is set to zero for all other pavement types.

Texture Depth. The mean texture depth is selected in this entry. The value used may be based on using a standard sand patch test or a profile measurement (in, mm).

Step Size. The computational step size (ft, m) determines the points along the flow path at which the water film thickness and hydroplaning speeds are computed. These values are reported in the summary tables of the output.

Transition Section

Three categories of data are required for the transition section in PAVDRN: data for the tangent section end, data for the curved section end, and data for the transition section itself.

Tangent End of Transition Section

Information provided about the tangent end of the transition section include values for grade, runout length, cross-slope, and pavement width.

Grade. This is the longitudinal slope or grade of the transition section in the direction of travel (ft/ft, m/m).

Runout Length. This is the length of the transition section in the direction of travel (ft, m).

Pavement Width. This is the width of the transition section pavement at the tangent end of the transition (ft, m).

Cross-slope. This is the cross-slope of the transition section pavement at the tangent end of the transition (ft/ft, m/m). The cross-slope value can be positive or negative (adverse to the superelevation of the curve end of the transition).

Curve End of Transition Section

Information provided about the curve end of the transition section include values for pavement width and superelevation.

Pavement Width. This is the width of the transition section pavement at the curve end of the transition (ft, m).

Superelevation. Superelevation or cross-slope of the curve at the curve end of the transition section (ft/ft, m/m). The value is always positive.

General Data for Transition Section

Three items, pavement type, texture depth, and step size apply to the entire transition section.

Pavement Type. Four types of pavements are used in PAVDRN; they are:

- PCC: Portland cement concrete,
- GPCC: Grooved portland cement concrete,
- DGAC: Dense-graded asphaltic concrete, and
- OGAC: Open-graded or porous asphaltic concrete.

When grooved PCC is selected as the pavement type, text boxes for the groove spacing, the groove width and the groove depth are displayed. This information is used to effectively increase the mean texture depth of the pavement.

If open-graded or porous asphaltic concrete is selected as the pavement type, an additional text box appears to provide a place to enter a value for the permeability of the pavement. This value is used to reduce the amount of water available for surface runoff. The value for pavement permeability is set to zero for all other pavement types.

Texture Depth. Mean texture depth using a standard sand patch test or equivalent (in, mm).

Step Size. Computational step size (ft, m). This value determines the points along the flow path at which the water film thickness and hydroplaning speeds are computed. These values are reported in the summary tables of the output.

Crest Vertical Curve Section

Length of Vertical Curve. Horizontal length of the vertical curve (ft,m).

Pavement Width. Width of the pavement (all lanes sloping in one direction toward the edge of the pavement) (ft, m).

Cross-slope. Cross-slope of the pavement (ft/ft, m/m). The cross-slope value is always positive.

Grade at PT. Longitudinal grade or slope at the point of tangency (PT) (ft/ft, m/m). The grade is negative if elevations decrease from left to right.

Grade at PC. Longitudinal grade or slope at the point of curvature (PC) (ft/ft, m/m). The grade is positive if elevations increase from left to right.

Relative Elevation. Relative elevation of the PT to the PC (ft, m). The relative elevation is negative if the PT is lower than the PC.

Texture Depth. Mean texture depth using a standard sand patch test or equivalent (in, mm).

Step Size. Computational step size (ft, m). This value determines the points along the flow path at which the water film thickness and hydroplaning speeds are computed. These values are reported in the summary tables of the output.

Pavement Type. Four types of pavements are used in PAVDRN; they are:

- PCC: Portland cement concrete,
- GPCC: Grooved portland cement concrete,
- DGAC: Dense-graded asphaltic concrete, and
- OGAC: Open-graded or porous asphaltic concrete.

When grooved PCC is selected as the pavement type, text boxes for the groove spacing, the groove width and the groove depth are displayed. This information is used to effectively increase the mean texture depth of the pavement.

If open-graded or porous asphaltic concrete is selected as the pavement type, an additional text box is displayed to provide a place for entering a value for the permeability of the pavement. This value is used to reduce the amount of water available for surface runoff. The value for the pavement permeability is set to zero for all other pavement types.

Direction of Flow from the Crest. This item requires that the user determine for which side of the crest vertical curve PAVDRN will calculate the water film thickness and hydroplaning speeds. In some cases (i.e., where the PT or the PC is the crest point) only one selection makes sense.

Sag Vertical Curve

Length of Vertical Curve. Horizontal length of the vertical curve (ft,m).

Pavement Width. Width of the pavement (all lanes sloping in one direction toward the edge of the pavement) (ft, m).

Cross-slope. Cross-slope of the pavement (ft/ft, m/m). The cross-slope value is always positive.

Grade at PT. Longitudinal grade or slope at the point of tangency (PT) (ft/ft, m/m). The grade value is negative if elevations decrease from left to right.

Grade at PC. Longitudinal grade or slope at the point of curvature (PC) (ft/ft, m/m). The grade value is positive if elevations increase from left to right.

Relative Elevation. Relative elevation of the PT to the PC (ft, m). The relative elevation is negative if the PT is lower than the PC.

Texture Depth. Mean texture depth using a standard sand patch test or equivalent (in, mm).

Step Size. Computational step size (ft, m). This value determines the points along the flow path at which the water film thickness and hydroplaning speeds are computed. These values are reported in the summary tables of the output.

Pavement Type. Four types of pavements are used in PAVDRN; they are:

- PCC: Portland cement concrete,
- GPCC: Grooved portland cement concrete,
- DGAC: Dense-graded asphaltic concrete, and
- OGAC: Open-graded or porous asphaltic concrete.

When grooved PCC is selected as the pavement type, text boxes for the groove spacing, the groove width and the groove depth appear. This information is used to effectively increase the mean texture depth of the pavement.

If open-graded or porous asphaltic concrete is selected as the pavement type, an additional text box is displayed to provide a place to enter a value for the permeability of the pavement. This value is used to reduce the amount of water available for surface runoff. The value for pavement permeability is set to zero for all other pavement types.

Direction of Flow to the Sag. This item requires that the user determine for which side of the sag vertical curve PAVDRN will calculate water film thickness and hydroplaning

speeds. In some cases (i.e., where the PT or the PC is the sag point) only one selection is meaningful.

PAVDRN RESULTS AS AN EXAMPLE

PAVDRN produces a summary report as the result of its execution. The report can be viewed on-screen by selecting **View** or **Analysis** from the menu bar on Screen 1. The report can also be printed and has two parts. The first part presents an "echo" print of the data provided by the user. It should be examined to ensure that correct values were used in the simulation of runoff over the pavement section. Table A-1 is an example of the data set produced by PAVDRN for a tangent section. Table A-2 shows part 1 of the report produced by PAVDRN.

Table A-1. PAVDRN input data set.

TEST DATA SET - USERS GUIDE

Tangent Section - 4 lane pavement with variable cross-slope

PCC Pavement

1,1,2,.00001134,55,0

2,1000,.01,3

24,.015,1,0,.02

24,.02,1,0,.02

Table A-2. PAVDRN output - Part 1: Echo print of input data.

PAVDRN - Highway Drainage Program - Version 1.0

developed by R. S. Huebner (717)948-6127
 Pennsylvania Transportation Institute
 The Pennsylvania State University
 University Park, PA 16802

Sponsored by the National Cooperative Highway Research Program
 NCHRP Project 1-29

Program started on 5/ 1/1997 at 22:55:59

TEST DATA SET - USERS GUIDE

Tangent Section - 4 lane pavement with variable cross-slope
 PCC Pavement

Type of section	Tangent
System of units for input and output	US
Number of consecutive planes	2
Rainfall intensity (in/h, mm/h)	2.00
Kinematic viscosity (sq.ft./s, sq.m./s)	.11E-04
Section length (ft, m)	1000.00
Longitudinal slope or grade (ft/ft, m/m)	.10E-01
Section design speed (mi/h, km/h)	55.
Computational step size (ft, m)	3.00

Plane No.	Length (ft, m)	Slope (ft/ft, m/m)	Pavement Type	Infiltration Rate(in/h,mm/h)	Texture Depth (in, mm)
1	24.0	.015	PCC	.000	.020
2	24.0	.020	PCC	.000	.020

The second part shows the results of the analysis in tabular form, table A-3.

Table A-3. Example of a PAVDRN analysis results screen.

Results for Plane No. 1

X	Y	Distance	WFT	Flow/width	Manning's n	Reynold's No.	Hydr. Speed
(ft,m)	(ft,m)	(ft,m)	(in,mm)	(cfs/ft,cms/m)			(mi/h,km/h)
.0	.0	.00	-.20E-01	.00E+00	.000	0.	999999
2.0	3.0	3.61	.21E-01	.17E-03	.092	15.	71
4.0	6.0	7.21	.29E-01	.33E-03	.064	29.	65
6.0	9.0	10.82	.35E-01	.50E-03	.051	44.	62
8.0	12.0	14.42	.40E-01	.67E-03	.044	59.	60
10.0	15.0	18.03	.44E-01	.83E-03	.039	74.	59
12.0	18.0	21.63	.47E-01	.10E-02	.035	88.	57
14.0	21.0	25.24	.50E-01	.12E-02	.032	103.	57
16.0	24.0	28.84	.53E-01	.13E-02	.030	118.	56

Notes: 1) + denotes Reynold's numbers greater than 1000.

(Manning's n may be in error)

2) * denotes hydroplaning speeds less than the facility design speed of 55. (mi/h, km/h)

3) Hydroplaning speed is equal to 999999. for water film thickness less than or equal to 0.0

Time to equilibrium for plane 1 is 2.19 min.

Total time to equilibrium at the end of this plane is 2.19 min.

Table A-3. (Continued)

Results for Plane No. 2

X (ft,m)	Y (ft,m)	Distance (ft,m)	WFT (in,mm)	Flow/width (cfs/ft,cms/m)	Manning's n	Reynold's No.	Hydr. Speed (mi/h,km/h)
16.0	24.0	28.84	.48E-01	.13E-02	.030	118.	57
17.5	27.0	32.20	.50E-01	.15E-02	.029	131.	56
19.0	30.0	35.55	.52E-01	.16E-02	.027	145.	56
20.5	33.0	38.91	.54E-01	.18E-02	.026	159.	55
22.0	36.0	42.26	.56E-01	.20E-02	.025	173.	55
23.5	39.0	45.61	.58E-01	.21E-02	.024	186.	55
25.0	42.0	48.97	.59E-01	.23E-02	.023	200.	54*
26.5	45.0	52.32	.61E-01	.24E-02	.022	214.	54*
28.0	48.0	55.68	.62E-01	.26E-02	.021	227.	53*

Notes: 1) + denotes Reynold's numbers greater than 1000.

(Manning's n may be in error)

2) * denotes hydroplaning speeds less than the facility design speed of 55. (mi/h, km/h)

3) Hydroplaning speed is equal to 999999. for water film thickness less than or equal to 0.0

Time to equilibrium for plane 2 is 2.46 min.

Total time to equilibrium at the end of this plane is 4.65 min.

Program completed successfully at 22:55:59

The table contains X and Y coordinates for the flow path length, as well as the length of the flow path. X and Y are zero at the beginning of the flow path. This location varies with different pavement section types as described in the following section. The water film thickness above the pavement roughness asperities and the flow-per-unit width of the plane along the flow path are also displayed. The far right column shows the predicted hydroplaning speed. (The basis for this value is described in the following). Manning's n and Reynold's

number at each point are also presented. A number of notes that pertain to the results conclude the output report. An estimate of the time of concentration for the pavement section is also reported. This value is useful in selecting an appropriate rainfall intensity for the analysis.

A comma-delimited, ASCII text file with the extension *filename.ASC* contains the data shown in table A-1. These data can be incorporated into a third-party plotting package to aid in the interpretation of the results.

The origin of the flow path can be identified as follows:

Tangent Section

The origin can be located anywhere along the upper edge of the pavement section (i.e., the inside edge of the first plane).

Horizontal Curve Section

The origin is difficult to identify; however, the terminal point of the flow path is the lowest point in the curve. Assuming a grade and superelevation, this would be at the corner of the inside edge of the lower part of the curve. If the curve has no grade, the origin can be located at any point along the upper or outside edge of the curve. The flow should be directly across the pavement to the inside edge.

Transition Section

If the tangent end of the transition and the curve end of the transition have slopes in the same direction, the origin is located up from the end with the mildest slope and along the upper edge of the pavement.

If the tangent end and the curve end of the transition section have adverse slopes, the origin is located at the point of zero cross-slope along the length of the section. This point should be accurately located by the x-coordinate shown in the printout. The flow path extends from this point toward the end of the section with the mildest cross-slope. This is not necessarily the end with the smallest slope but, rather, the end where the change in cross-slope per unit per length is the smallest.

Crest Vertical Curve Section

The outlet of the flow path is located at the lower edge of the pavement section at the PC or PT, depending upon which side of the vertical curve is being analyzed. The origin is located up-gradient from the outlet point. The x-coordinate of the origin is located using the value shown in the printout. The flow path extends from this point toward the end of the section with the mildest cross-slope. It is not necessarily the end with the smallest slope but, rather, the end where the change in cross-slope per unit length is the smallest.

Crest Vertical Curve Section

The outlet of the flow path is located at the lower edge of the pavement section at the PC or PT, depending upon which side of the vertical curve is being analyzed. The origin is located up-gradient from the outlet point. The x-coordinate of the origin is located using the value shown in the printout.

Sag Vertical Curve Section

The outlet of the flow path is located at the lower edge of the pavement section, i.e., the sag, where the longitudinal slope is zero. The origin is located up-gradient from this outlet point. The x-coordinate of the origin is located using the value shown in the printout.

BASIS OF CALCULATION

The basis for the value computed for the predicted hydroplaning speed is described in detail in an article by Huebner, Reed, and Henry (38). The algorithm uses two expressions for computing the hydroplaning speed. The first is based on data collected by Agrawal and Henry (44) and is based on a regression expression of their data (water film thickness versus hydroplaning speed) to predict the hydroplaning speeds for water film thicknesses less than 2.4 mm (0.095 in). The second is used for water film thicknesses greater than 2.4 mm (0.095 in) and is based on an expression developed by Gallaway et al. (4), where the hydroplaning speed

is a function of water film thickness, tire tread depth, pavement mean texture depth, and tire pressure. Conservative values of the tire pressure, 165 kPa (24 lb/in²), and tire tread depth, 2.4 mm (3/32 in), were used in the PAVDRN model to generalize Gallaway's expression.

One method for the selecting the design rainfall intensity for the hydroplaning analysis is based on the frequency and duration of an event. It is recommended that a frequency of 100 years (100-year return period) be used representing a one-percent risk or chance, so the intensity will be exceeded. The duration should be based upon the pavement's time of concentration. The time of concentration can be determined using output from the PAVDRN model. In summary, the key parameters for selecting a value of rainfall intensity based on hydrologic considerations in order to estimate the hydroplaning potential of a pavement surface are: (1) location, (2) risk level, and (3) time of concentration.

A second method of selecting a rainfall intensity for hydroplaning analysis is by examining the effect of driver response. Table A-4 was developed based upon work done by Hayers et al. (45) and AASHTO.

Clearly, the selection of the design rainfall intensity for analyzing the hydroplaning potential of a highway section needs to consider both driver response and the likelihood of an event or risk. It is recommended that the designer employ a value from table A-4 to establish a maximum rainfall intensity specifically for determining the potential for hydroplaning on the designed pavement section. The value should be compared with the rainfall information (I-D-F

curves) for the location of the project. The user should select the lesser of the two values and use it for completing the hydroplaning analysis of the pavement section.

Table A-4. Rainfall intensity for stopping sight distances.

Design Speed	Stopping Sight	Maximum Rainfall Intensity,
m/h, (km/h)	Distance, ft (m)	in/h, (mm/h)
50 (80)	475 (145)	5.96 (151)
55 (88)	550 (167)	4.18 (186)
60 (96)	650 (198)	2.88 (73)
65 (104)	725 (221)	2.18 (55)
70 (112)	850 (259)	1.54 (39)

APPENDIX B

REVIEW OF MODELS

MODEL SELECTION AND DEVELOPMENT

Models that can be used to predict hydroplaning speeds and the depth of sheet flow over a roadway surface have been published in the literature. These models are identified and discussed in detail in this appendix. Several types of models are available for predicting the depth of sheet flow:

- One-dimensional models;
- Two-dimensional models;
- Depth of flow over porous pavements;
- Porous media flow models; and
- Other models.

These models were discussed in the main body of this report, and additional information regarding these models is presented here.

One-Dimensional Flow Models

Russnam and Ross (34) presented a model for one-dimensional flow over highway pavements based on equations developed by Chezy and Manning for open channel flow. Both

equations represent turbulent, one-dimensional, steady-state flow. If the slope of the energy grade line is assumed to be equal to the slope of the flow path, they represent uniform flow. The authors also noted that even at velocities and depths when flow would normally be considered to be laminar, the impact of rainfall on the fluid surface created conditions that were turbulent. The Manning equation was simplified by assuming a wide channel approximation where the hydraulic radius, R, is equivalent to the depth of flow. This resulted in the following equation, B-1:

$$h = \frac{K (L i)^m}{S^n} \quad (B-1)$$

where:

- h = Depth of flow (cm)
- K = Empirically determined constant
- L = Length of the flow path (m)
- i = Rainfall intensity (cm/h)
- m,n = Empirically determined exponents
- S = Slope of the flow path (m/m)

The values of K, m, and n were determined from data collected on a rolled asphalt pavement with chippings and on a brushed concrete pavement. This led to the general equation for both pavement surfaces, B-2:

$$h = 0.017 \frac{(L i)^{0.47}}{S^{0.20}} \quad (B-2)$$

Measurements of Manning's roughness coefficient, n , were not made, and there was no statistical evaluation of equation B-2 comparing it to the observed data. The authors also offered a discussion of the effect of cross-slope on flow over pavements, suggesting that the total length of the flow path could be determined by using the vector sum of the slopes to determine the direction of flow as presented in equation B-3:

$$L_f = L \left[1 + \left(\frac{m_1}{m_2} \right)^2 \right]^{1/2} \quad (\text{B-3})$$

where:

- L_f = Length of the flow path
- L = Width of the pavement lane
- $1/m_1$ = Cross slope of the pavement
- $1/m_2$ = Longitudinal slope of the pavement
(slope in the direction of travel)

The report also presented the results of field tests that were used to develop the previous equations. Although the relationships developed by these authors were not used in this study, their work does represent a significant contribution to the literature, and their data were used to verify the models developed during this study.

Empirical Flow Models

In 1971 and again in 1979, Gallaway et al. (3,4,46) at the Texas Transportation Institute developed a set of empirical equations for predicting water depths on road surfaces. The equations were one-dimensional, inasmuch as they were developed from data collected from surfaces with slopes in a single principal direction. The equations, based on a regression analysis, used plane length, rainfall intensity, texture depth, and pavement slope to predict water depth. Depths were observed at 20 locations on a pavement section. In the 1971 study, (3) nine pavement surfaces were used, along with six slopes and five rainfall rates. The 1979 study (4) added observations on portland cement concrete pavements to those in the 1971 study to improve the regression. The coefficients of determination, r^2 , were 0.68 and 0.83 for the regression equations reported in the two studies, respectively. The regression equation with the highest coefficient of determination and the one representing all 1,059 observations on the surfaces is shown in the following (B-4):

$$\text{WFT} = \frac{0.003726 L^{0.519} i^{0.562} \text{MTD}^{0.125}}{S^{0.364}} - \text{MTD} \quad (\text{B-4})$$

where

- WFT = Water film thickness (in) (1 in = 25.4 mm)
- L = Plane length (ft) (1 ft = 305 mm)
- i = Rainfall intensity (in/h)
- MTD = Mean texture depth (in)

S = Pavement slope (m/m)

h = Water depth (in) = WFT + MTD

To date, Gallaway's work represents the single most comprehensive set of water depth data collected on different types of pavements. The equation, however, is without a fundamental resistance variable, such as Manning's n, and has been regressed by combining pavements with different types of surfaces. These models were not used in this study.

Flow Models Based on Kinematic Wave Equation

The kinematic wave approximation was discussed in the body of this report (equations 4 through 5). To expand, steady-state or equilibrium conditions correspond to the greatest depths on a flow surface. Under these conditions, depths have increased to the point that inflow is equal to outflow. For the steady-state case, the term $\delta u/\delta t$ is zero. On impervious surfaces, such as portland cement concrete, the infiltration rate is zero, and the term f in equations 4 and 5 is dropped from the right-hand side of the equation. Thus, if infiltration is zero, the equation representing the conservation of momentum is:

$$u \frac{\delta u}{\delta x} + g \frac{\delta h}{\delta x} + \frac{i u}{h} = g (S_{ox} - S_{fx}) \quad (B-5)$$

The kinematic approximation assumes that the velocity terms in equation B-5 are negligible (i.e., gradually varied flow) and that the gravitational forces are equal to the frictional forces. Equation B-5 then reduces to the following, B-6:

$$S_{ox} = S_{fx} \quad (B-6)$$

The kinematic wave approximation has been shown to be valid for conditions when K is greater than 20, and the Froude number, N_F , is greater than 0.5, where:

$$K = \frac{S_{ox} L}{h_o N_F^2} \quad (B-7)$$

and h_o = normal depth.

Additionally, when N_F is less than 0.5,

$$N_F^2 K > 5 \quad (B-8)$$

Rainfall-induced flow on most pavement surfaces falls within the criteria established by equations B-7 and B-8. Further development results in equations 6 through 8 as discussed in the body of this report.

Two-Dimensional Flow Models

Flow on highway pavements is a two-dimensional phenomenon. A vertical component to flow exists that would add a third dimension. Yet, since the fluid depths are so small,

variations in flow in the z-direction can be averaged, and flow may be accurately represented by a two-dimensional model. Equations B-9 through B-11 present the equations of state, continuity, and conservation of momentum for two-dimensional flow.

Conservation of mass:

$$\frac{\delta h}{\delta t} + \frac{\delta(uh)}{\delta x} + \frac{\delta(vh)}{\delta y} = i - f = I \quad (\text{B-9})$$

where

- h = Depth of flow
- u = Spatially averaged velocities (x - direction)
- v = Spatially averaged velocities (y - direction)
- i = Rainfall intensity over the domain
- f = Infiltration rate
- I = Incoming rainfall minus infiltration into subsurface

Conservation of momentum in the x-direction leads to:

$$\frac{\delta u}{\delta t} + u \frac{\delta u}{\delta x} + v \frac{\delta u}{\delta y} + g \frac{\delta h}{\delta x} = g(S_{ox} - S_{fx}) - \frac{u(i-f)}{h} + \frac{\rho r \cos \theta_x}{h} + vt \quad (\text{B-10})$$

whereas conservation of momentum in the y-direction leads to:

$$\frac{\delta v}{\delta t} + u \frac{\delta v}{\delta x} + v \frac{\delta v}{\delta y} + g \frac{\delta h}{\delta y} = g (S_{oy} - S_{fy}) - \frac{v(i-f)}{h} + \frac{\rho r \cos \theta_y}{h} + vt \quad (\text{B-11})$$

where

u, v, h, i, and f are the same as described in B-9

and

- g = Acceleration due to gravity (32.17 ft/s² or 9.806 m/s²)
- S_{ox}, S_{oy} = Slope of the flow path in the x and y directions, respectively
- S_{fx}, S_{fy} = Slope of the energy grade line in the x and y directions, respectively
- v_t = Terminal rainfall velocity
- θ_x, θ_y = Angle of rainfall input with respect to the x- and y-axes

The equations are simplified, as were the one-dimensional equations, by negating the force of raindrop impact and, if appropriate, the infiltration term. In most two-dimensional models the remaining terms are retained, and the partial differential terms are approximated using either a finite difference or finite element scheme. In general, the system of nonlinear, partial differential equations has no analytical solution and must be solved by numerical methods.

Zhang and Cundy (33) developed a two-dimensional model for computing water depths and velocities on a three-dimensional surface. The model allows an inclined plane with

irregular topography and is based upon a two-step, explicit solution of the finite difference approximation of the continuity and momentum equations shown earlier in equations B-9 through B-11. The rainfall intensity was considered constant over a finite length but, like infiltration, could vary over discrete lengths. The model also allowed spatial variations in plane characteristics, including surface roughness and topography. Tayfur et al. (47) applied an implicit solution scheme to Zhang and Cundy's model to improve the number of iterations necessary to reach equilibrium conditions. The model was applied to a planar surface with a relatively steep slope (eight percent). Due to the nature of nonlinear equations, stability and convergence remained a problem. Specifically, instability at lower slopes was noted.

Froehlich (48) developed a two-dimensional, free-surface model to analyze flows affecting roadway structures, such as culverts, embankments, and bridges. It has the capacity to analyze unsteady, nonuniform flows but is limited to situations where flow enters or leaves the flow domain at the boundaries and cannot account for infiltration or flows due to a spatially distributed source, such as rainfall, on a pavement surface. Huebner (49) developed a two-dimensional, steady-state, finite element flow model for flow over highway pavements with irregular topography. The program produced acceptable results for planar surfaces but encountered problems with stability and convergence when irregular topographies were introduced. The two-dimensional models are cited here for completeness. They were considered too cumbersome for use in the drainage guidelines as developed for this project.

THIS PAGE INTENTIONALLY LEFT BLANK

APPENDIX C

DETERMINATION OF MANNING'S N

A parameter that describes the hydraulic resistance of the pavement surface must be known in order to predict the water film thickness that occurs on a pavement surface during sheet flow. Manning's n is commonly used for this purpose and was used for this purpose in the equations that were selected and developed during this study for use in the PAVDRN model. Values for Manning's n must be determined experimentally by measuring water flow depths under either natural or artificial rainfall. During the course of this study, the hydraulic resistance of three different types of pavement surface were determined:

- Portland cement concrete
- Porous asphalt
- Dense-graded asphalt concrete

A great deal of experimental data that could be used to determine Manning's n values was available in the literature, and these data were used during this project to verify values of Manning's n established by previous researchers (29-31,36,39). Additional data were also obtained as part of this project for porous pavements and for long flow paths on portland cement concrete. Both sets of data were used in the analyses to give the values of Manning's n used in PAVDRN. These analyses are described in this appendix.

GENERAL APPROACH

Manning's n was determined by first expressing the flow depth, y , as a function of independent variables such as the pavement slope (S), mean texture depth (MTD), flow path length (L), and rainfall rate (i):

$$y = f(S, \text{MTD}, L, i) \quad (\text{C-1})$$

Data from the literature, as well as data obtained during this study, were used with regression analyses to determine functional forms and coefficients for equation C-1. Variables that were not statistically significant were eliminated during the regression analyses. Separate regression equations for y were established for each of the pavement surfaces. Once the relationships for y were determined, the equations for y were substituted into the kinematic wave equation, equation C-2 (also see equation 9), thereby eliminating the flow depth as a variable in the final expression for Manning's n . The kinematic wave equation is expressed as (35):

$$y = \left[\frac{nLi}{36.1 S^{0.5}} \right]^{0.6} \quad (\text{C-2})$$

where

- y = Hydraulic flow depth (mm)
- n = Manning's hydraulic resistance variable
- L = Drainage path length (m)

- i = Rainfall intensity (mm/h)
S = Drainage surface slope (m/m)

Since Manning's n is surface specific, the regression analyses must be considered separately for each of the surfaces of interest, in this case portland cement concrete, dense graded asphalt concrete, and porous asphalt. The analyses follow for each of these surfaces.

PORTLAND CEMENT CONCRETE SURFACES

In a previous study, Reed and Stong (35) performed experiments using the artificial rainfall simulator at Penn State to develop an expression for Manning's n for Portland cement concrete surfaces. The experiments were performed on three brushed PCC surfaces with MTD values of 0.25, 0.70, and 1.12 mm and rainfall rates of approximately 25, 50, and 75 mm/h using the same artificial rainfall facility as used in this project. The PCC surfaces were 0.30 m wide by 7.3 m long. Testing was conducted with slopes of 0.5, 1.5, and 2.5 percent. The facility and the test protocols are described in chapter 3 of this report. Reed and Stong (35) collected 2,367 data points, which represented 789 observations; each observation represented the average of three data points. During this study, 1,656 data points representing 552 observations were collected for the Reynold's number ranging from approximately 200 to 1,000.

VALIDATION OF DATA

The kinematic wave approximation is valid only when certain criteria are met, requiring that (30):

- The flow must be fully rough,
- The slope of the energy gradient (S_f) must be approximately equal to the surface slope (S) of the pavement, and
- Certain requirements must be met with respect to the Froude number.

In order to satisfy the requirement of full roughness, the data must satisfy the following relationship:

$$n \sqrt[6]{R S_f} \geq 1.05 \times 10^{-13} \quad (C-3)$$

where

- R = Hydraulic radius (mm)
- S_f = Slope of the energy gradient (m/m)

In this case the hydraulic radius is equal to the flow depth, y (30). A total of 141 observations were eliminated from the data set based on this criterion. All 141 observations that were eliminated were for either high rainfall intensities, long drainage lengths, large flow

rates, shallow pavement slopes, or combinations thereof. Under these conditions, pelting rain could add turbulence and cause a fully rough flow that is not ensured by equation C-3.

Elimination of these 141 data points ensured fully rough conditions and agreement with the kinematic wave assumption.

The second criterion that must be satisfied for the kinematic wave equation to be valid is that the energy gradeline slope, S_f be approximately equal to the surface slope, S , of the pavement. This criterion is satisfied if $N_F^2 K$ is greater than five (30):

$$N_F^2 K = \frac{S L}{y} \quad (C-4)$$

where

N_F	=	Froude number
K	=	Kinematic wave number
y	=	Hydraulic flow depth (m)
S	=	Runoff surface slope (m/m)
L	=	Drainage path length (m)

The Froude number, N_F , is defined as:

$$N_F = \frac{v}{\sqrt{g y}} \quad (C-5)$$

where

- v = Flow velocity (m/s)
g = Gravitational constant, 9.81 m/s²

One additional criterion must be met for subcritical flow when the Froude number is less than 0.5 (50,51):

$$N_F^2 K = \frac{S L}{y} > 5 \quad (C-6)$$

where the variables are as previously described. A total of 76 of 1,341 observations were eliminated because they did not meet the criterion of equation C-6.

Manning's n for $500 < N_R < 1,000$

Before an equation for Manning's n could be established, it was necessary to establish the relationship between the flow depth and the experimental variables. The flow depth for the 1,124 valid data points was regressed versus the flow rate, q, the mean texture depth, MTD, and the surface slope, S, with the following results ($R^2 = 0.926$):

$$y = \frac{122.43 q^{0.308} \text{MTD}^{0.0316}}{S^{0.286}} \quad (C-7)$$

Mean texture depth, runoff surface slope, and flow rate were the only statistically significant parameters. Removing MTD from equation C-7 resulted in equation C-8 with an R^2 of 0.92.

$$y = \frac{126.66 q^{0.312}}{S^{0.285}} \quad (C-8)$$

Similar results were observed by Reed and Stong (35). On the basis of these results, it appears that MTD has little effect on flow depth. However, hydraulic flow depth, y , is the sum of the water film thickness and mean texture depth. Therefore, the MTD parameter was retained in the relationship and equation C-8 was used in the work that follows.

The next step was to combine equation C-8 with equation C-2. In equation C-2, S is raised to a very small power and, according to equation C-2, appears to not be very important in determining the Manning's n value over a range of typical drainage slope values.

Therefore, the smallest and largest slopes from the data set, 0.005 and 0.025 respectively, were used to calculate an average value of $S^{0.025}$, 0.90. The maximum error introduced by replacing $S^{0.025}$ in this manner was 2.1 percent. The kinematic viscosity, ν , was also replaced with a constant value. Since the data from Reed and Stong were measured at a temperature of approximately 18 °C ($\nu = 1.057 \times 10^{-6} \text{ m}^2/\text{s}$) and the data taken from this study were measured at 9 °C ($\nu = 1.35 \times 10^{-6} \text{ m}^2/\text{s}$), a weighted average was used for the kinematic viscosity. In other words, 714 of 1,124 total data points were from the study by Reed and Stong (35), and the kinematic viscosity used in equation C-8 was weighted more toward a ν of 1.057×10^{-6}

m²/s. Upon replacing S and v in equation C-8 with the appropriate constants, equation C-9 was obtained:

$$n = \frac{0.319}{N_R^{0.480}} \quad (C-9)$$

Figure C-1 is a log-log plot of equation C-9 and the calculated Manning's n values from 1,124 experimental observations, and there is a good degree of scatter around equation C-9. On the other hand, the figure shows that as the Reynold's number increases, the experimental data appear to be underestimated, especially as the Reynold's number approaches 1,000. Therefore, because of the apparent dependency of Manning's n on the Reynold's number, equation C-9 was reevaluated by considering Manning's n independently within several different ranges in the Reynold's number.

Manning's n for Reynold's Numbers Less Than 500

Equation C-9 underestimates Manning's n as the Reynold's number approaches 1,000, as shown in figure C-1. This was a major reason for the experimentation that was done on portland cement concrete surfaces during this study. The authors also reviewed the transition region for open channel flow, which is commonly accepted to occur within the range of Reynold's numbers of 500 to 1,000. It is important to note the commonly assumed transition region is for flow without pelting rainfall. Two regions were considered, $N_R < 500$ and $500 < N_R < 1,000$. The 500 value was an important dividing point because below 500 flow is

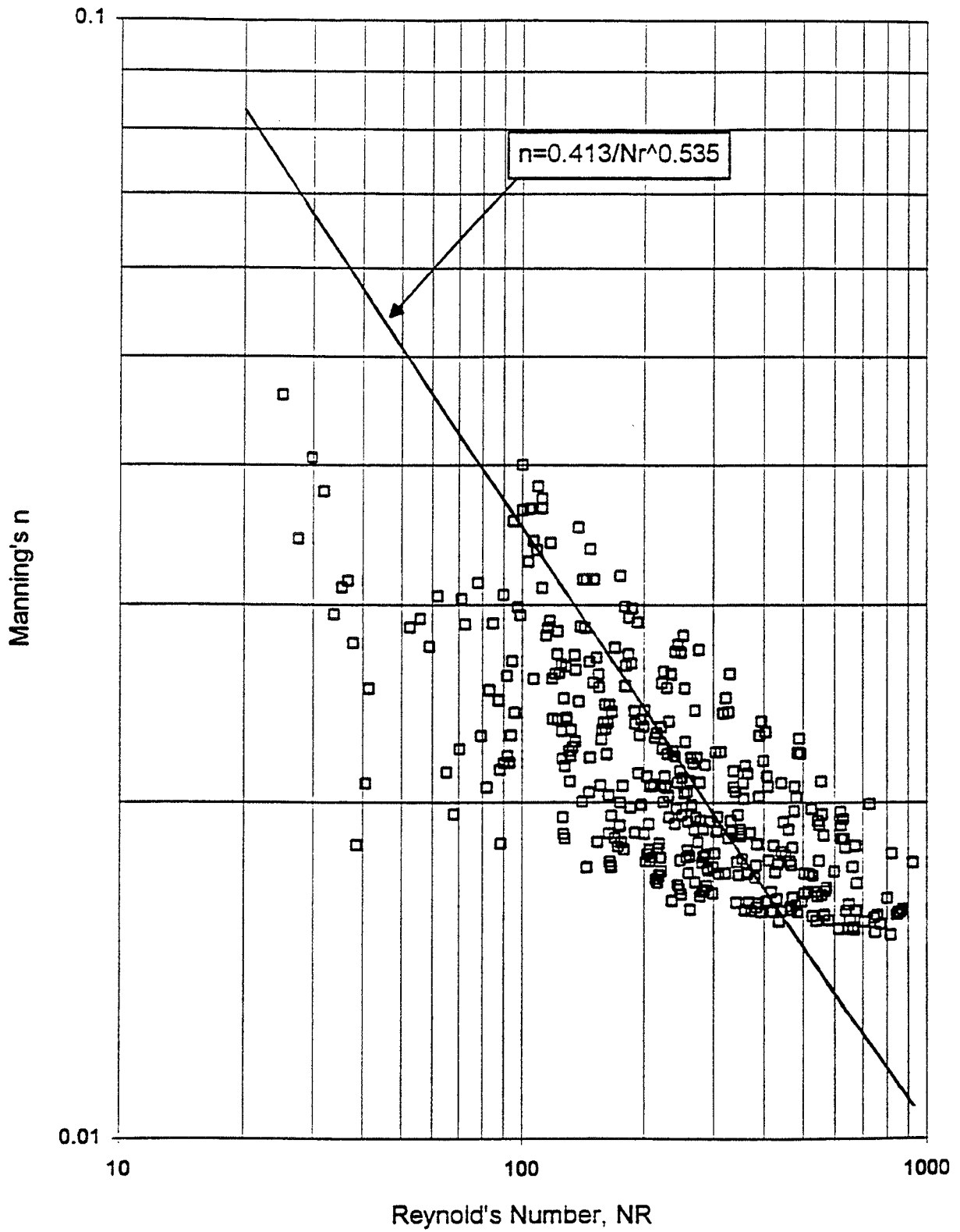


Figure C-1. Manning's n on PCC surfaces for Reynolds' numbers less than 1,000 (Eq.C-9).

traditionally assumed to be laminar. However, in the case of shallow flow with pelting rain, as is the case on a pavement surface, the flow is disturbed, possibly creating turbulent flow at Reynold's numbers less than 240.

The first step was to reduce the data set so that it contained only Reynold's numbers less than 500. A total of 1,070 of 1,124 observations had Reynold's numbers less than 500 and were used in the subsequent analysis. The procedure applied was identical to the one implemented for Reynold's numbers less than 1,000. A regression equation was performed and MTD, S, and v were removed as before. The result was the following, with $R^2 = 0.916$:

$$n = \frac{0.345}{N_R^{0.502}} \quad (C-10)$$

Figure C-2 is a log-log plot of equation C-10 and the calculated Manning's n values from 1,070 observations. Once again, there is degree of scatter around equation C-10 in Figure C-2. On the other hand, equation C-10 still appeared to overestimate Manning's n as the Reynold's number approaches 500. Also of concern was the manner in which the data points appear to level off prior to a Reynold's number of 500. Figure C-2 shows that the Manning's n values appear to begin to level off at approximately a Reynold's number of 240.

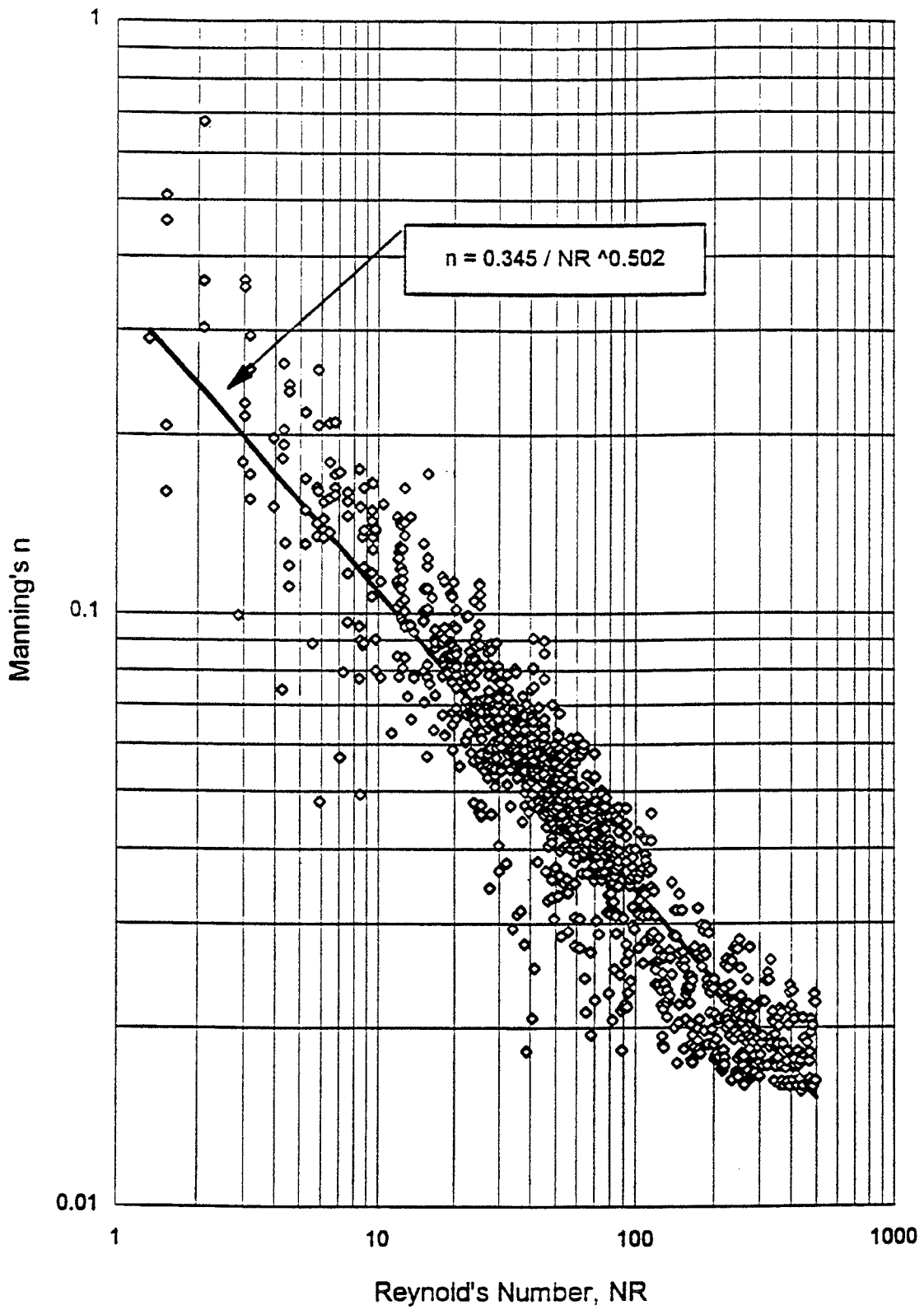


Figure C-2. Manning's n on PCC surfaces for Reynold's numbers less than 1,000 (Eq. C-10).

Manning's n for $N_R < 240$

The previous procedures were applied to a data set for Reynold's numbers less than 240. A maximum Reynold's number of 240 was chosen because it appears as though Manning's n attains a constant value when N_R is less than 240 (see figure C-2). The entire data set was first reduced to a data set of 940 observations with Reynold's numbers less than 240. A regression equation for hydraulic flow depth was completed and, with systematic substitution and elimination of variables, produced

$$n = \frac{0.388}{N_R^{0.535}} \quad (C-11)$$

with an R^2 of 0.887. Figure C-3 is a log-log plot of equation C-11 and the calculated Manning's n values from 940 observations. The points in figure C-3 appear to be consistently scattered around equation C-11. Also, equation C-11, shown in figure C-3, does not overestimate Manning's n as the Reynold's number approaches 240. It is important to remember that equation C-11 was developed under certain parameter restrictions. Equation C-11 is for rainfall runoff on PCC surfaces with MTDs between 0.25 mm and 1.12 mm, runoff surface slopes between 0.005 and 0.025 m/m, rainfall intensities between 25 and 75 mm/h, and drainage path lengths up to 40 m.

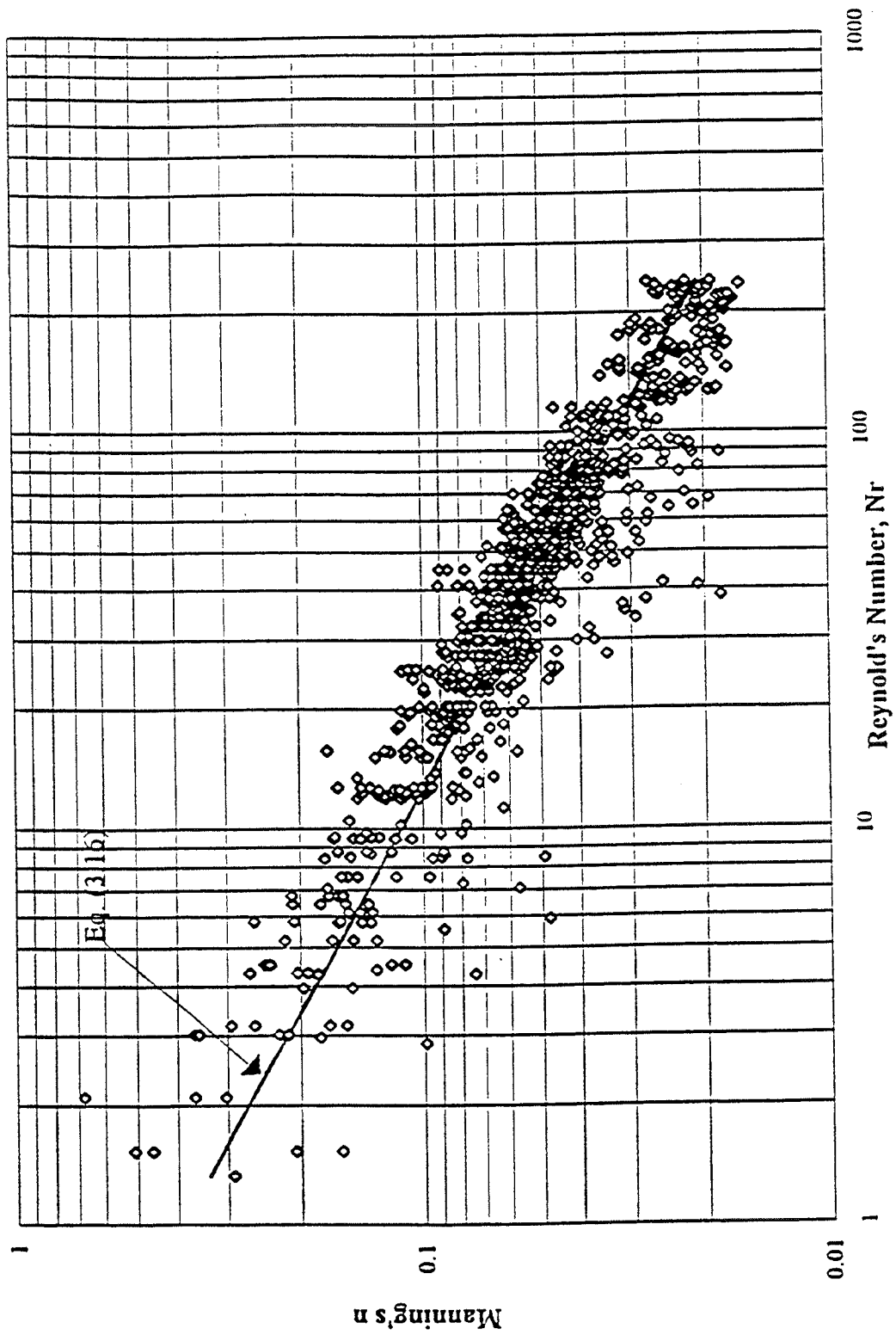


Figure C-3. Manning's n on PCC surfaces for Reynold's numbers less than 1,000 (Eq. C-11).

Summary of Manning's n on Portland Cement Concrete

The results of the previous analyses produced two observations. These observations maybe explained as follows.

1. As the upper-limit Reynold's number was reduced from 1,000 to 500 to 240, so were the R^2 values for subsequent regressions. Since data with higher Reynold's numbers were eliminated, an increased emphasis on lower Reynold's numbers was inevitable. Data with lower Reynold's numbers or hydraulic flow depths were prone to have more error due to the precision of the point gauge. The increased scatter of data for smaller Reynold's numbers can be seen in figure C-1.
2. As the upper-limit Reynold's number was reduced from 1,000 to 500 to 240, the exponent of S systematically decreased from equation C-10 to equation C-11.

Constant Manning's n for Reynold's Numbers Greater Than 500

The experimental Manning's n values appear to level off and approach a constant value beginning at a Reynold's number of approximately 500. For Reynold's numbers greater than 500, a constant value can be assumed for Manning's n, as evidenced in figure C-4 with a value of 0.017, based on one surface with a MTD of 0.91 mm.

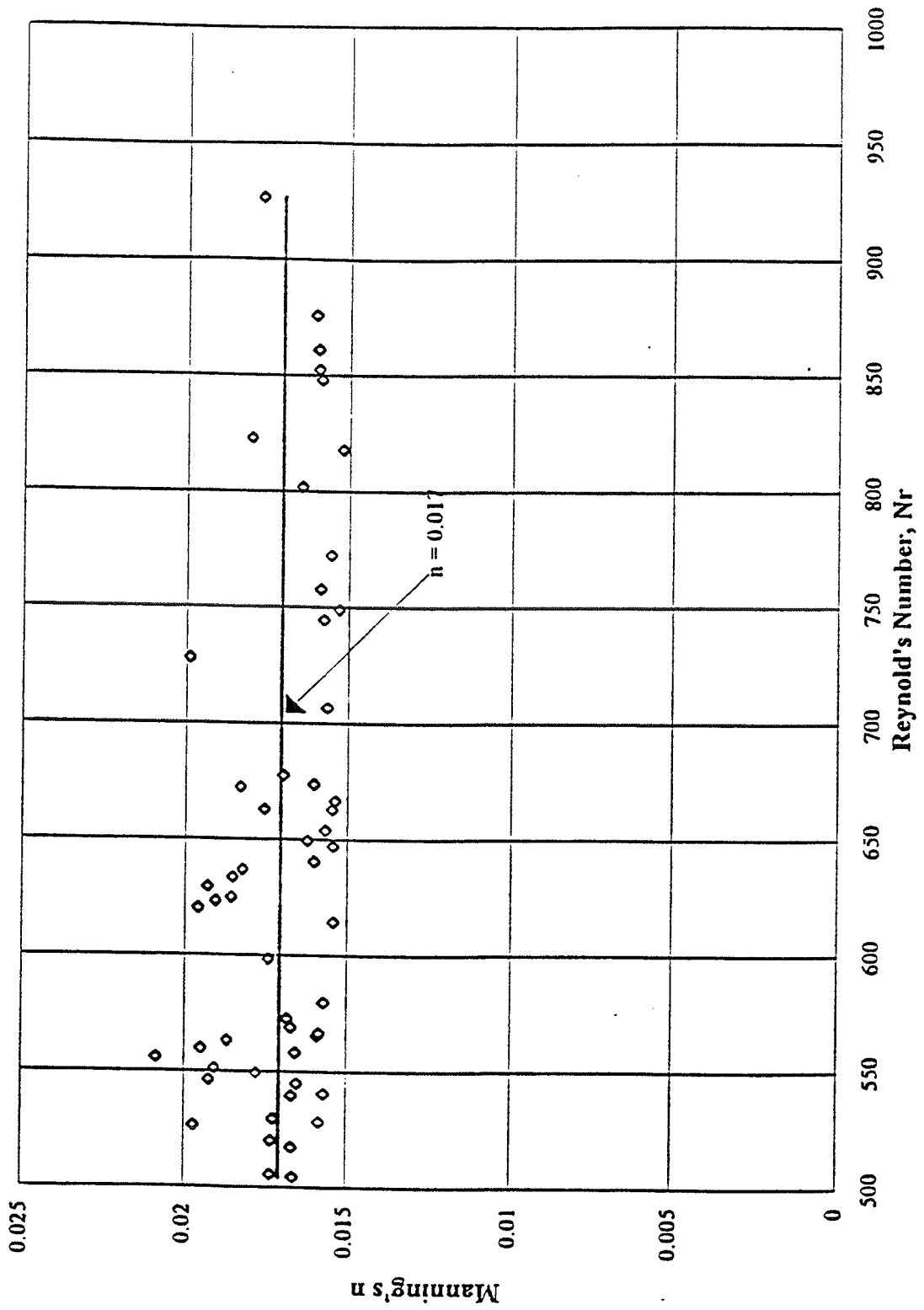


Figure C-4. Manning's n on PCC surfaces for Reynold's numbers greater than 500.

Equations Used in PAVDRN

The equations that were chosen for predicting Manning's n on PCC surfaces are:

$$n = \frac{0.319}{N_R^{0.480}} \quad (500 < N_R < 1000) \quad (C-12)$$

$$n = \frac{0.345}{N_R^{0.502}} \quad (240 < N_R < 500) \quad (C-13)$$

$$n = \frac{0.388}{N_R^{0.535}} \quad (N_R < 240) \quad (C-14)$$

For the Reynold's numbers equal to or greater than 1,000, hydraulic flow resistance or Manning's n on PCC surfaces is a constant of 0.012, the value of n from equation C-12 for a Reynold's number of 1,000 and a traditional value of n for concrete-lined channels.

MANNING'S N FOR POROUS PAVEMENTS

First, the criterion for fully rough flow was tested as described earlier, and of the 1,495 data points, only two sets did not satisfy this criterion. It was observed that the fully rough conditions did not prevail at high depth values with a low rainfall intensity. This enhances the

theory that the impact of the pelting rain causes internal turbulence in the flow and adds to the fully rough condition.

The second criterion requires that the friction slope be equal to the surface slope. This is satisfied if the kinematic wave number is greater than 20. All of the data sets satisfied this criterion. Additionally, for Froude numbers less than 0.5, the criterion as described by equations C-4 through C-6 must be satisfied. Analysis of the data revealed that 47 data sets did not satisfy these criteria. These data sets included low depths on shallow slopes with a high rainfall intensity, possibly reflecting the difficulty in measuring the smaller depths. Upon examination of the data, a total of 49 data sets were eliminated from the total of 1,493 data sets leaving a total of 1,444 data sets remaining for further analysis.

A regression of the data sets was performed to give:

$$y = 0.1590 \text{ MTD}^{0.150} (i L)^{0.345} S^{-0.107} \%AV^{0.072} \quad (\text{C-15})$$

where

- y = Depth of flow (mm)
- MTD = Mean texture depth (mm)
- i = Rainfall intensity (mm/h)
- L = Drainage path length (m)
- S = Channel slope (m/m)
- %AV = Percent air void content of the mixture

with an $R^2 = 0.799$. The values of percent air void content were utilized due to the fact that the permeability measurements of the mixtures were not available. With the coefficient of the air void content appearing to render the parameter negligible, a subsequent regression was performed and showed:

$$y = 0.1995 \text{ MTD}^{0.129} (\text{I L})^{0.345} \text{ S}^{-0.111} \quad (\text{C-16})$$

with an $R^2 = 0.797$.

A subsequent regression of the data showed:

$$y = 0.2080 (\text{I L})^{0.346} \text{ S}^{-0.116} \quad (\text{C-17})$$

with an $R^2 = 0.790$, a negligible decrease in the correlation.

Equation C-15 was then equated to the kinematic wave equation, as was done for the PCC surfaces previously and solved for Manning's n to produce:

$$n = \frac{1.490 \text{ S}^{0.306}}{N_R^{0.424}} \quad (\text{C-18})$$

An attempt was made to further simplify the relationship; however, the slope term appears to be a significant parameter and was retained in the relationship. Figure C-5 illustrates the observed data points and the relationship shown in equation C-18. The three curves displayed are equation C-5 solved for each of the three slopes used in the experimentation, namely 0.005, 0.015, and 0.025 m/m. It is evident from the figure that the slope term plays a significant role in the relationship. The applicability of equation C-18 is limited to porous surfaces with the following criteria: mean texture depth between 1.25 and 2.13 mm, Reynold's numbers less than 550, slopes less than 0.025 m/m, and void contents between 20 and 33 percent.

MANNING'S N FOR DENSE-GRADED ASPHALT CONCRETE

Recently, Reed, Warner, and Huebner (52) developed a similar expression for dense graded asphaltic concrete surfaces. The data were obtained from four DGAC surfaces of the Gallaway et al. (3) study with MTD values of 0.23, 0.48, 0.51, and 0.99 mm. The slopes ranged from 0.5 percent to 4 percent, with rain rates applied up to 150 mm/h and drainage lengths up to 7.3 m. A regression analysis of the data was performed and combined with the kinematic wave approximation, as described earlier for the PCC and porous pavement surfaces. This resulted with:

$$n = \frac{0.0823}{N_R^{0.174}} \quad (C-19)$$

This relationship yielded an R^2 of 0.88 and is bounded by a maximum N_R of 230 and the experimental ranges, as indicated previously.

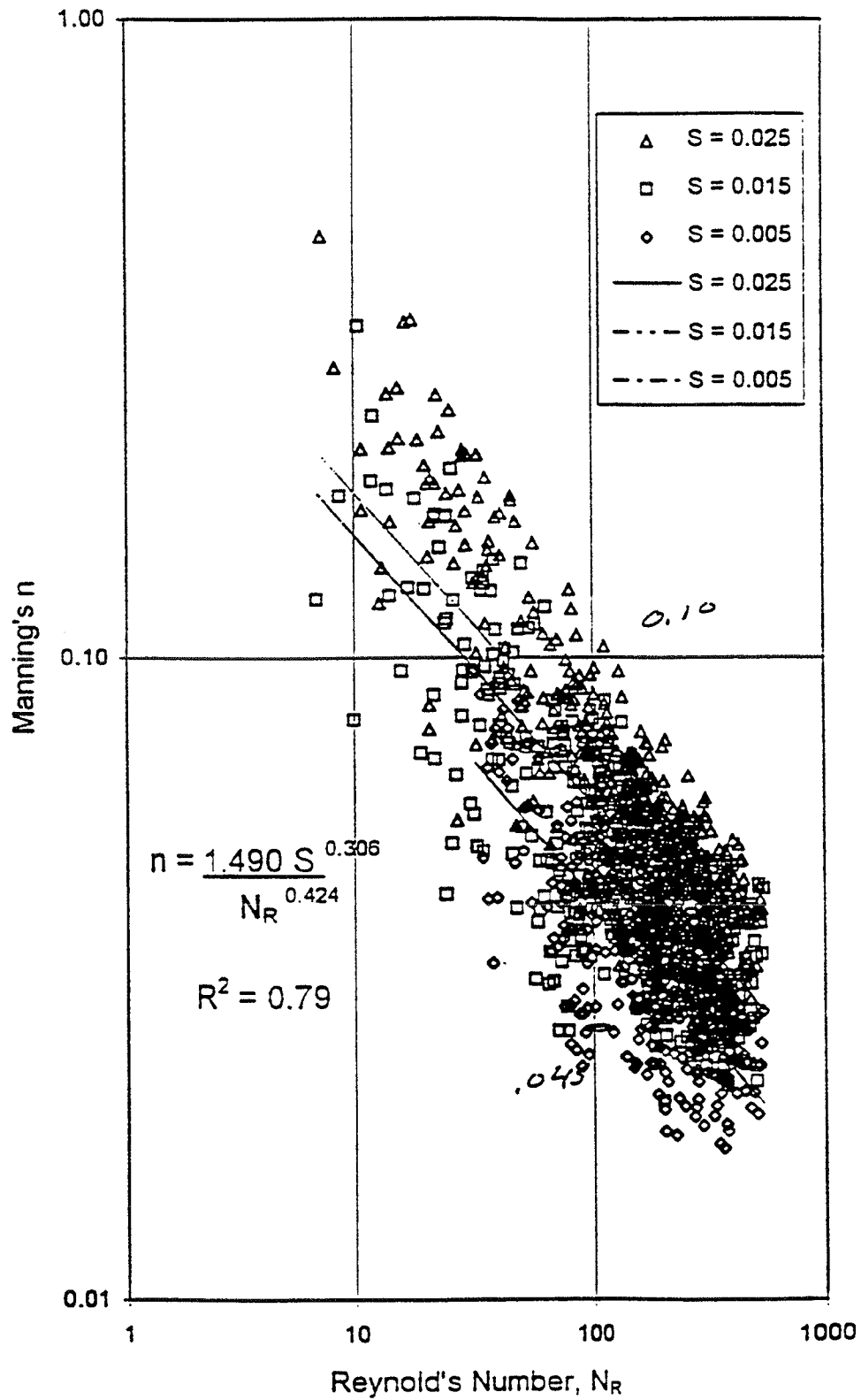


Figure C-5. Manning's n for porous asphalt surfaces.

APPENDIX D

MODEL EVALUATION

Sensitivity analyses were performed for PAVDRN and for the water film thickness and hydroplaning speed models. The purpose of the sensitivity analysis was to determine the sensitivity of PAVDRN and the models to the various input parameters, to make certain that the models behaved in a reasonable manner, and to establish the sensitivity of the response variables (predicted values) to the input parameters (design parameters). The results of the sensitivity analyses are given in this appendix.

ANALYSIS OF THE PAVDRN MODEL

The sensitivity analyses for the PAVDRN program were conducted by varying three variables: pavement slope, S ; rainfall intensity, i ; and mean texture depth, MTD. Each of these input variables was assigned three values—a low, an intermediate, and a high value—as given in table D-1. The analyses were conducted by fixing two of the input variables (S and i , S and MTD, or i and MTD) at the intermediate value and allowing the other two variables (MTD, i , and S , respectively) to assume their low, intermediate, and high values. The calculations were conducted for the four pavement types: dense-graded asphalt concrete, plain portland cement concrete, grooved portland cement concrete, and open-graded porous asphalt concrete. The values for the rainfall intensity, i , pavement slope, S , and mean texture depth, MTD, used in these calculations are given in table D-1. Note that the values for rainfall

intensity and pavement slope are the same for each of the pavement types, but the MTD is different for the open-graded asphalt concrete.

Table D-1. Values used in PAVDRN sensitivity analysis.

Variable	Minimum	Intermediate	Maximum
Rainfall, intensity, i in/h (mm/h)	1.00 (25.4)	3.0 (76)	6.0 (152)
Slope, S ft/ft (m/m)	0.0050 (0.0050)	0.015 (0.015)	0.030 (0.030)
Mean texture depth, MTD in (mm), DGAC and PCC ⁽¹⁾	0.01 (.25)	0.02 (0.51)	0.05 (1.14)

⁽¹⁾DGAC = dense-graded asphalt concrete, PCC = plain or grooved portland cement concrete, and OGAC = open-graded asphalt concrete.

Values of water film thickness versus flow path length for the four pavement types are shown in figures D-1 through D-4. The figures show how the water film thickness varies for each of the variables when the others are held at their extreme values.

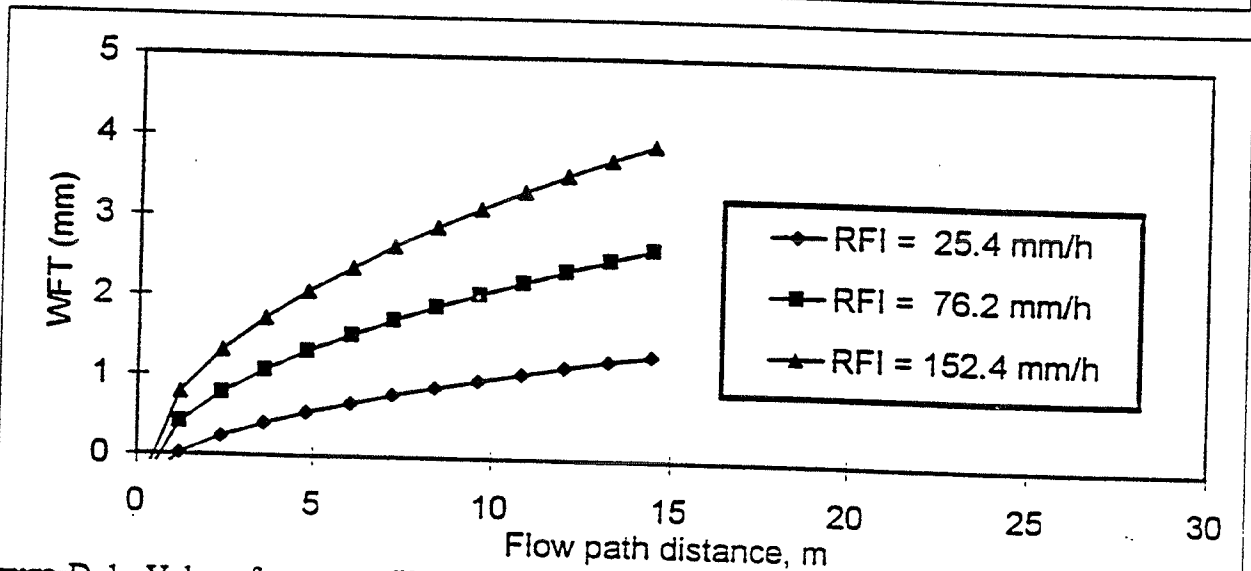
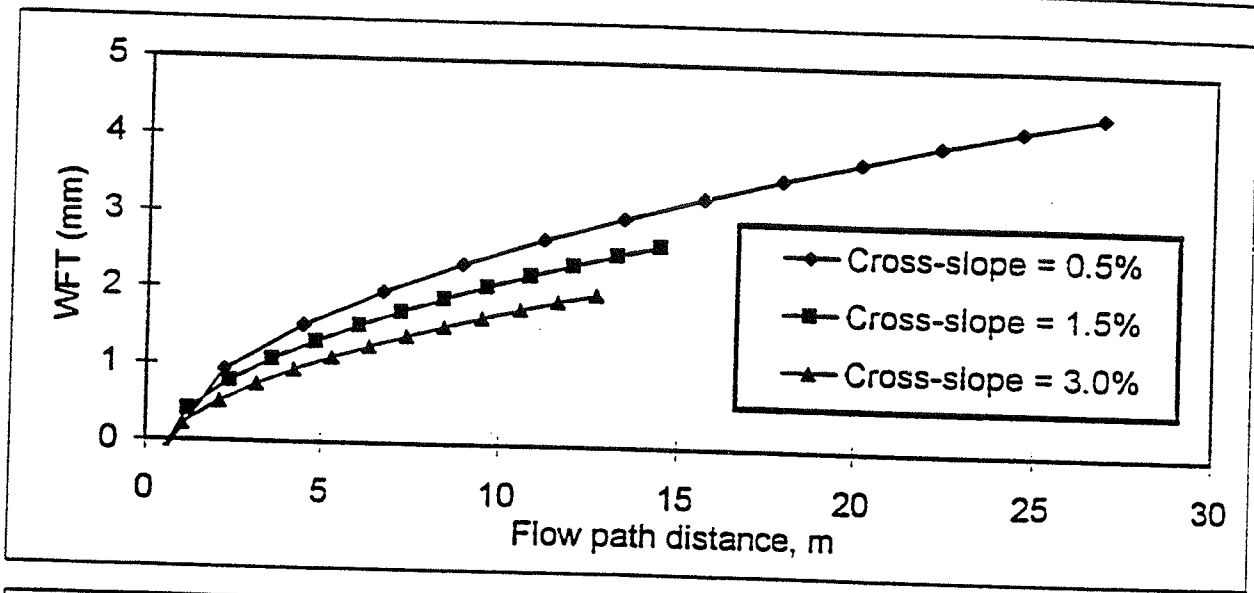
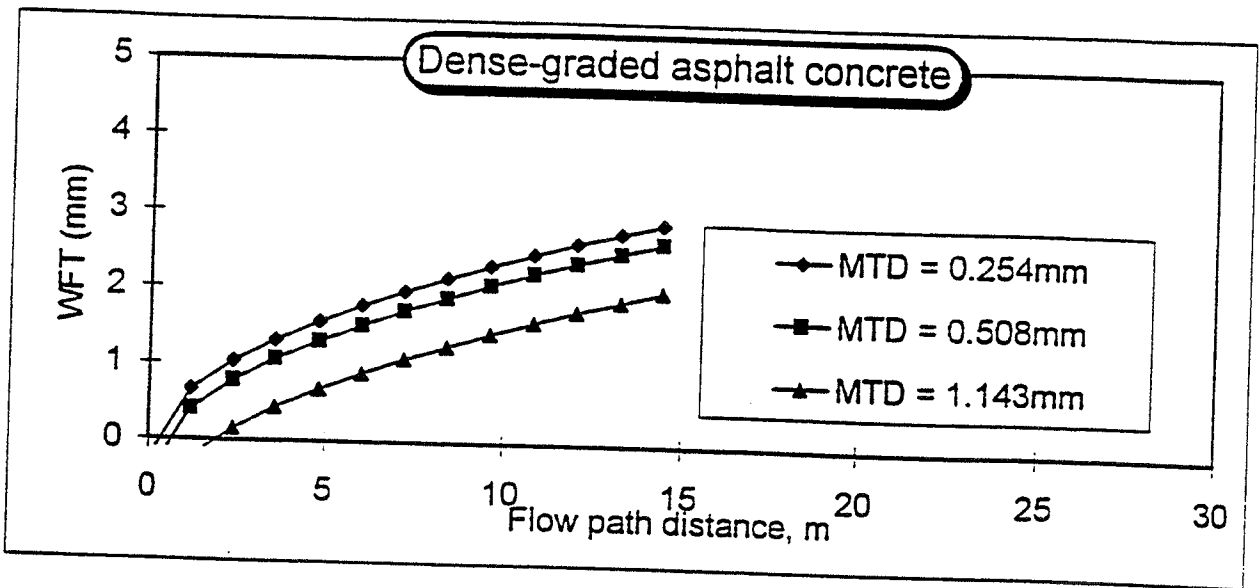


Figure D-1. Values for water film thickness versus flow path length for dense-graded asphalt concrete pavement.

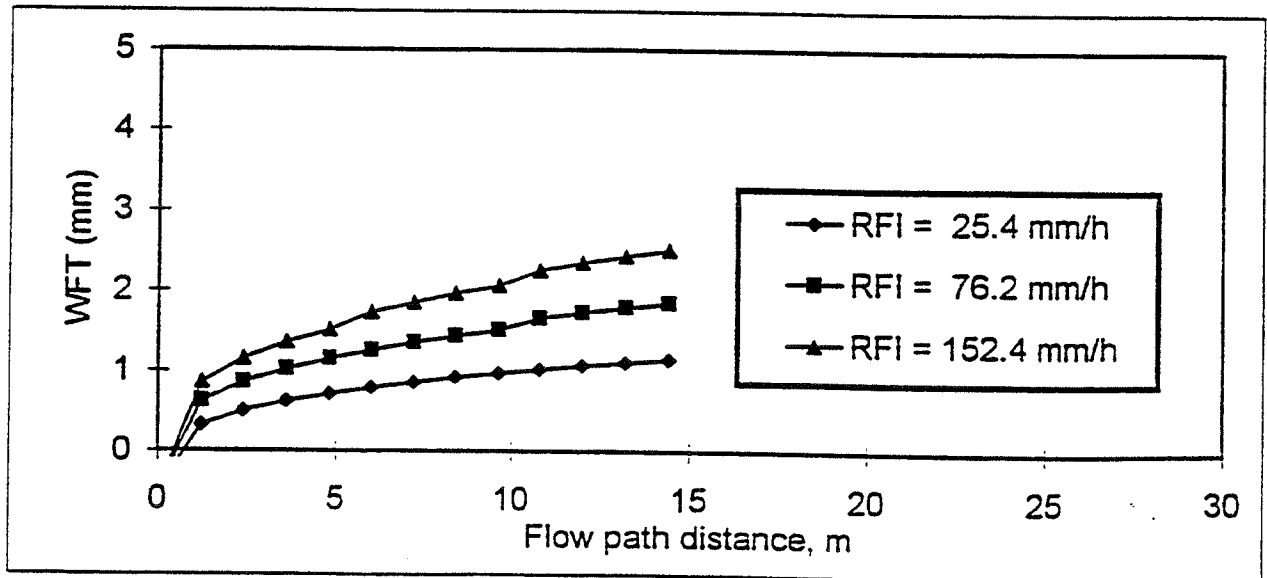
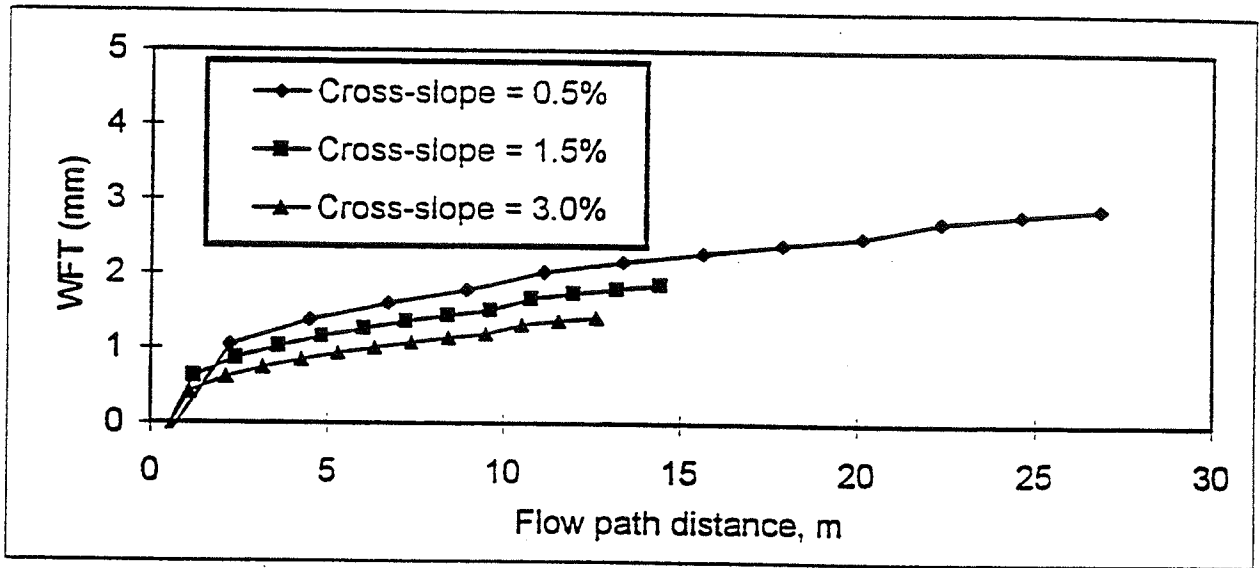
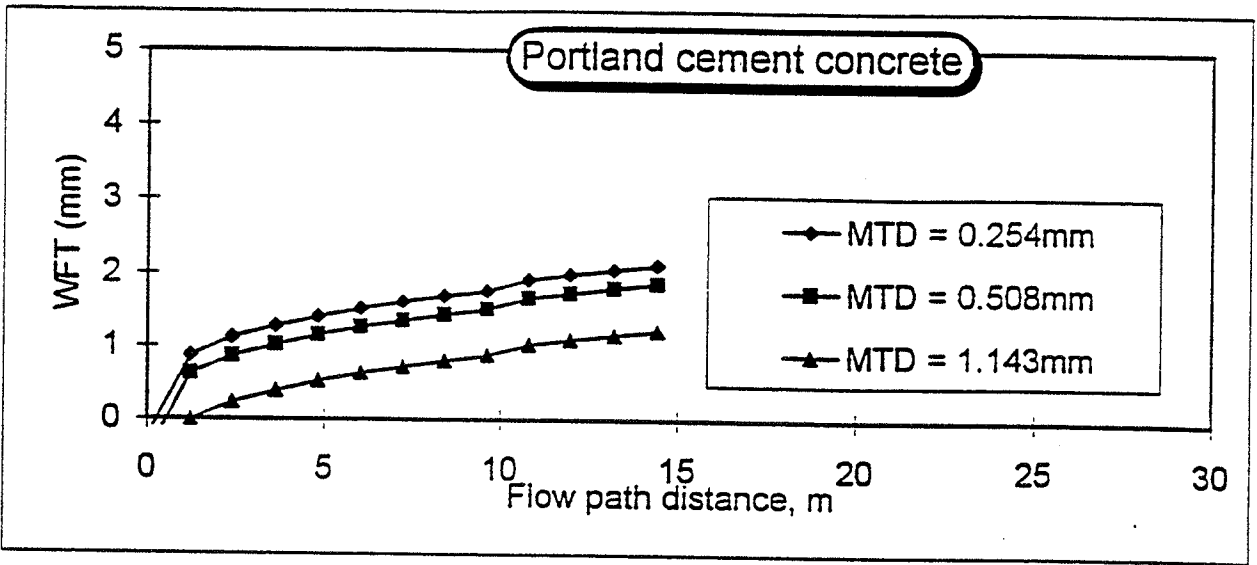


Figure D-2. Values for water film thickness versus flow path length for portland cement concrete pavement.

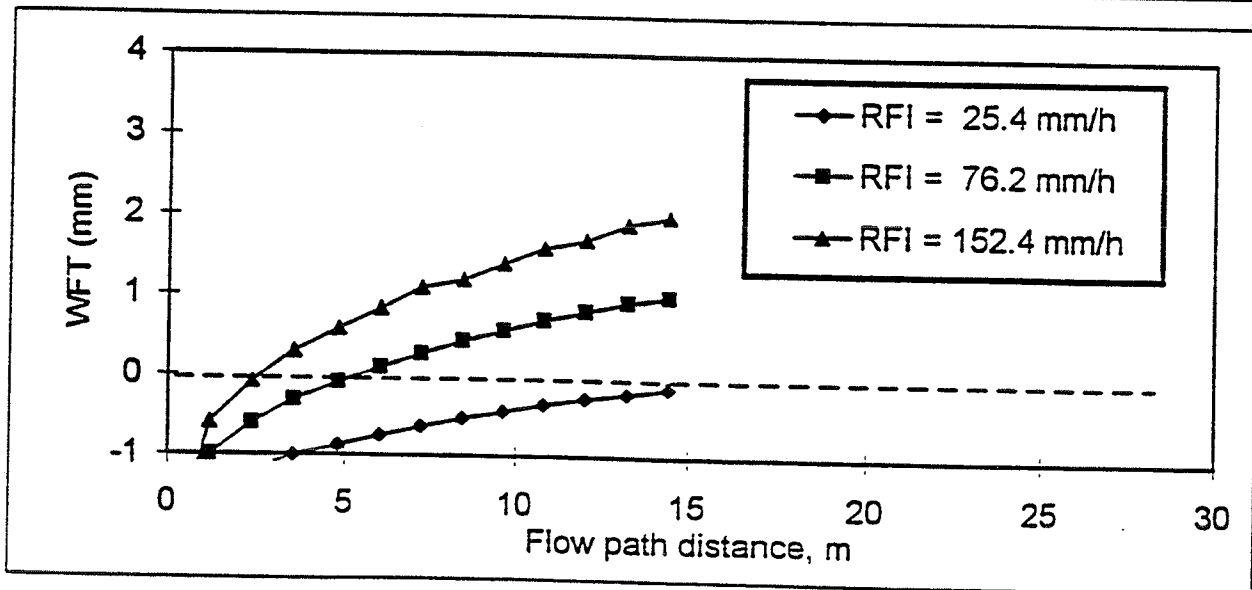
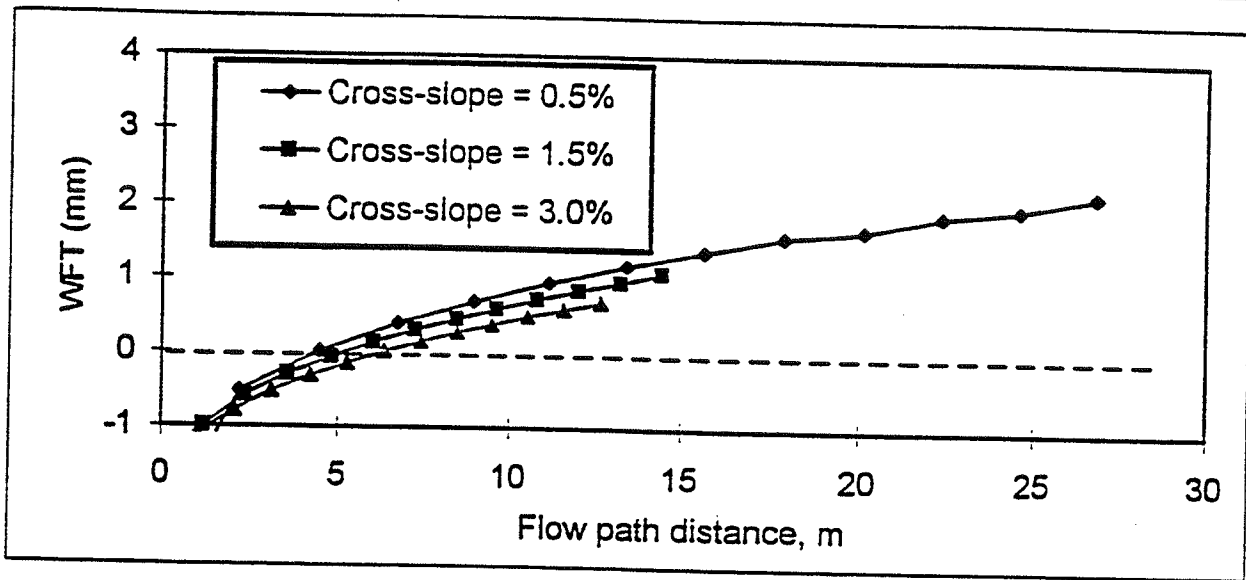
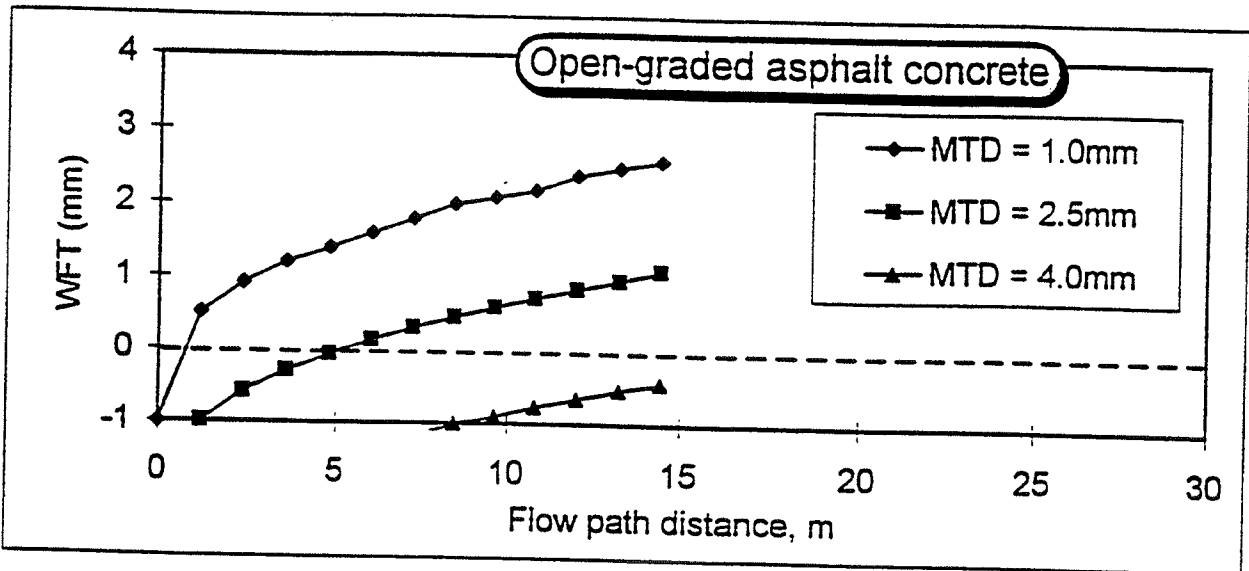


Figure D-3. Values for water film thickness versus flow path length for open-graded asphalt concrete pavement (no internal flow).

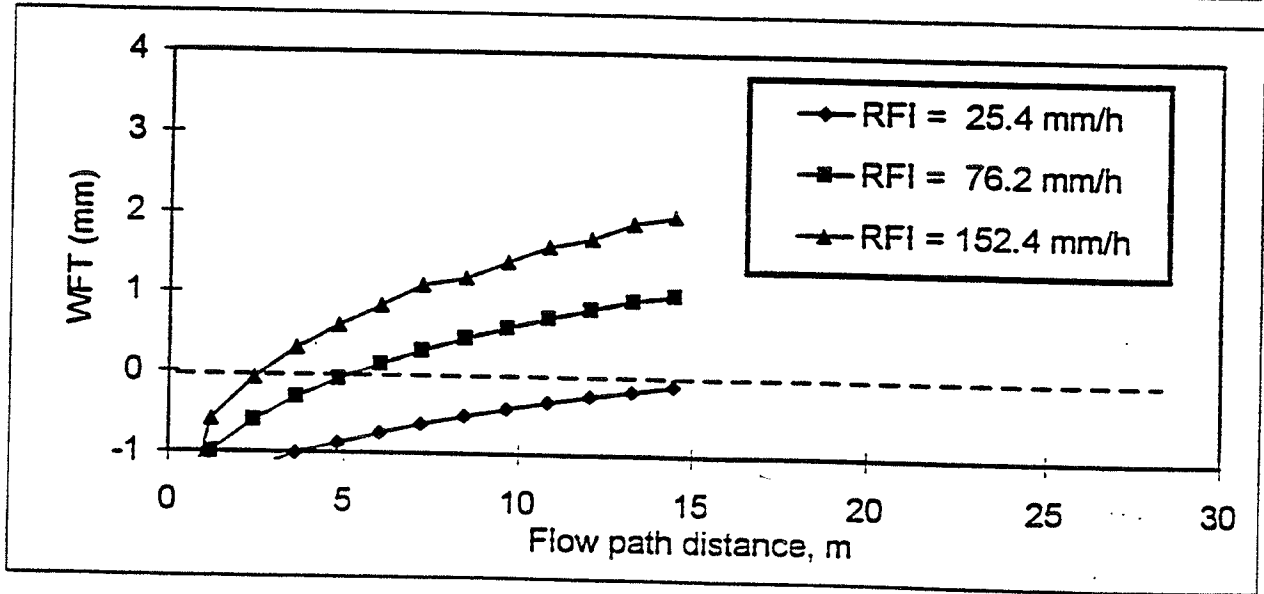
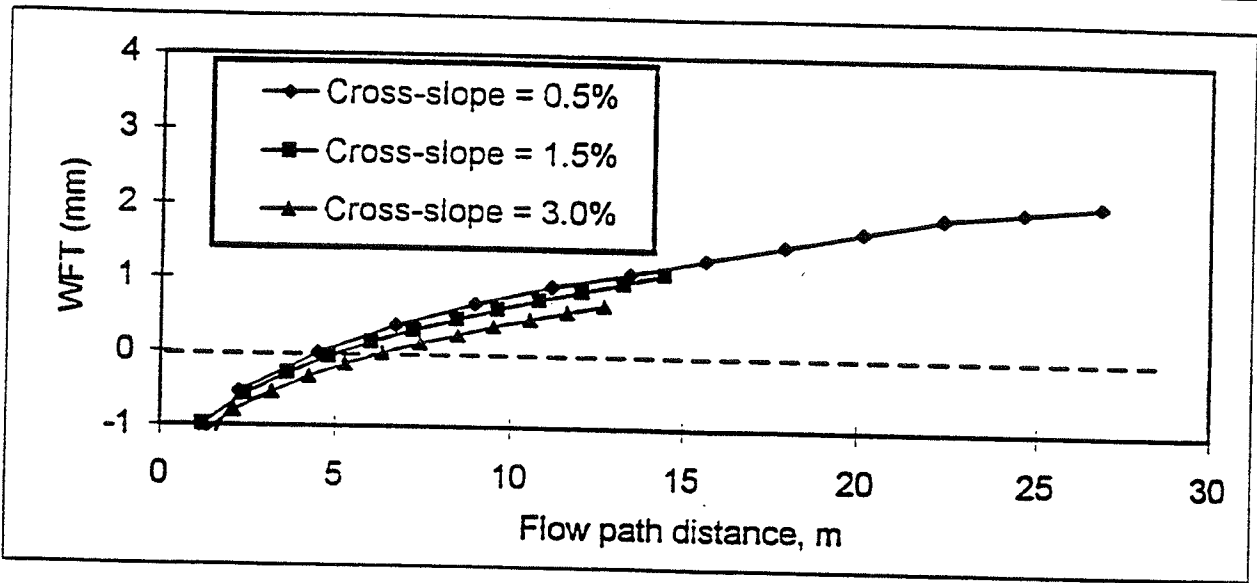
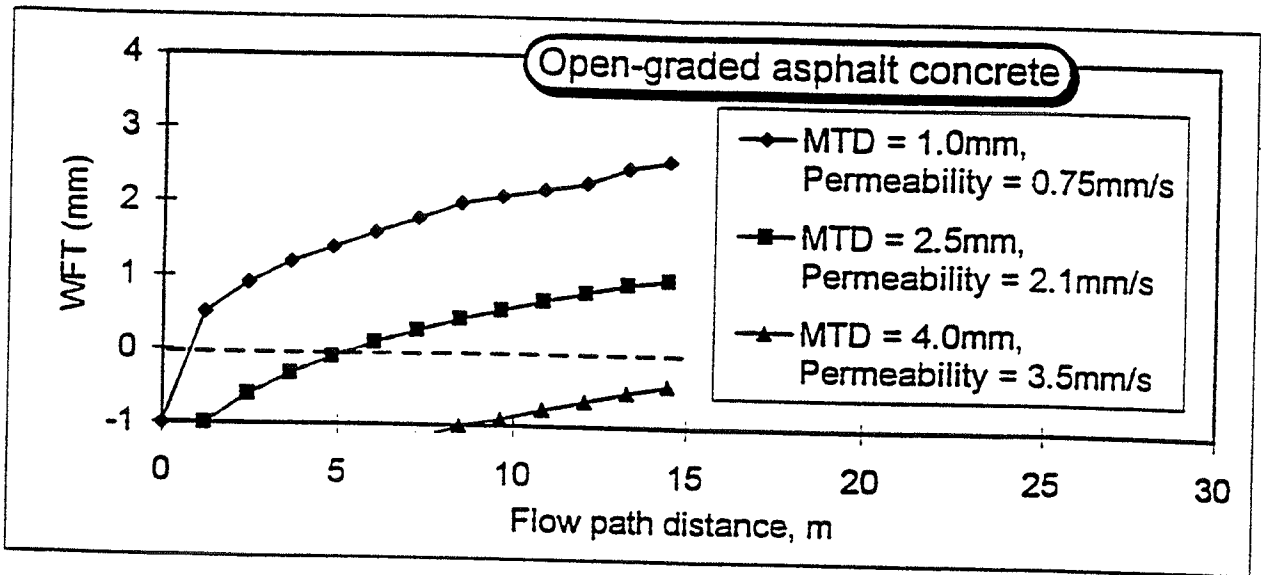


Figure D-4. Values for water film thickness versus flow path length for open-graded asphalt concrete pavement (internal flow).

SENSITIVITY ANALYSIS OF THE WATER FILM THICKNESS MODEL

The following equation is used in PAVDRN to calculate the water film thickness:

$$y = \left(\frac{42.32 n q}{S^{0.5}} \right)^{0.6} \quad (D-1)$$

where

- y = Flow depth (in)
- n = Manning's roughness coefficient
- q = Flow (ft³/s/ft)
- S = Slope of the drainage path (ft/ft)

with the values and coefficients in English units.

The water film thickness is predicted in PAVDRN using the following relationship:

$$\text{WFT} = \left[\frac{n L i}{36.1 S^{0.5}} \right]^{0.6} - \text{MTD} \quad (D-2)$$

where

- n = Manning's roughness coefficient
- L = Drainage path length (in)
- i = Rainfall rate (in/h)

S = Slope of drainage path (mm/mm)

MTD = Mean texture depth (in)

and the values and coefficients are in English units.

The sensitivity analyses were conducted using procedures outlined earlier. Low, intermediate, and high values for n, q, and S are given in table D-2, and the analyses were conducted for several flow path lengths, as given in the table.

Table D-2. Values used in kinematic wave equation sensitivity analysis.

Variable	Minimum	Intermediate	Maximum
Manning's n	0.01	0.025	0.05
Rainfall, intensity, i, in/h (mm/h)	1.00 (25.4)	3.0 (76)	6.0 (152)
Slope, S, ft/ft (m/m)	0.0050 (0.0050)	0.015 (0.015)	0.030 (0.030)
Drainage path length, L, ft (m)	3.0 (0.92)	24 (7.3)	48 (14.6)
Flow, q, ft ³ /s/ft (m ³ /h/m) ⁽¹⁾	6.94 x 10 ⁻⁵ (6.45 x 10 ⁻⁶)	3.37 x 10 ⁻³ (3.13 x 10 ⁻⁴)	6.67 x 10 ⁻³ (6.20 x 10 ⁻⁴)

⁽¹⁾The values of the flow rate, q, are the result of multiplying the drainage path length, L, by the rainfall intensity, i, and converting the units as appropriate.

SENSITIVITY OF THE MODEL TO VARIATIONS IN N

The partial derivative of the kinematic wave equation with respect to n is:

$$\frac{\partial y}{\partial n} = \frac{5.677 q^{0.6}}{n^{0.4} S^{0.3}} \quad (\text{D-3})$$

Using $n = 0.01$, $q = 0.00000667 \text{ ft}^2/\text{s}$, ($0.00223 \text{ m}^2/\text{hr}$) and $S = 0.005 \text{ ft/ft}$ (0.005 mm/mm) to obtain the highest $\partial y/\partial n$:

$$\frac{\partial y}{\partial n} = \frac{5.677 (0.006667)^{0.6}}{(0.01)^{0.4} (0.005)^{0.3}} = 8.685 \text{ in (220.6 mm)} \quad (\text{D-4})$$

Multiplying this value by the highest n ($= 0.05$) yields the highest change in $y = 0.434 \text{ in}$ (11.0 mm).

Using $n = 0.05$, $q = 0.0000694 \text{ ft}^2/\text{s}$, ($0.0232 \text{ in}^2/\text{hr}$) and $S = 0.03 \text{ ft/ft}$ (0.03 mm/mm) to obtain the lowest value of $\partial y/\partial n$:

$$\frac{\partial y}{\partial n} = \frac{5.677 (0.00006944)^{0.6}}{(0.05)^{0.4} (0.03)^{0.3}} = 0.1723 \text{ in (4.38 mm)} \quad (\text{D-5})$$

Multiplying this value by the lowest n ($= 0.01$) yields the lowest change in $y = 0.001723 \text{ in}$ (0.0438 mm).

SENSITIVITY OF THE MODEL TO VARIATIONS IN Q

The partial derivative of the kinematic wave equation with respect to q is:

$$\frac{\partial y}{\partial q} = \frac{5.677 n^{0.6}}{q^{0.4} S^{0.3}} \quad (\text{D-6})$$

Using $n = 0.05$, $q = 0.0000694 \text{ ft}^2/\text{s}$, ($0.0232 \text{ in}^2/\text{h}$) and $S = 0.005 \text{ ft/ft}$ (0.005 mm/mm) to obtain the highest $\partial y/\partial q$:

$$\frac{\partial y}{\partial q} = \frac{5.677 (0.05)^{0.6}}{(0.0000694)^{0.4} (0.005)^{0.3}} = 212 \text{ ft}^2/\text{s/in} \quad (\text{D-7})$$

Multiplying this value by the highest value of q, $0.00666 \text{ ft}^2/\text{s}$, ($0.00223 \text{ in}^2/\text{h}$) yields the highest change in y per unit flow.

Using $n = 0.01$, $q = 0.00000666 \text{ ft}^2/\text{s}$, and $S = 0.03 \text{ ft/ft}$ to obtain the lowest $\partial y/\partial n$:

$$\frac{\partial y}{\partial q} = \frac{5.677 (0.01)^{0.6}}{(0.006667)^{0.4} (0.03)^{0.3}} = 7.61 \text{ ft}^2/\text{s/in} \quad (\text{D-8})$$

Multiplying this value by the lowest q, $0.0000694 \text{ ft}^2/\text{s}$, ($0.0232 \text{ in}^2/\text{h}$) yields the lowest change in y per unit flow.

SENSITIVITY OF THE MODEL TO VARIATIONS IN S

The partial derivative of the kinematic wave equation with respect to S is:

$$\frac{\partial y}{\partial S} = \frac{-2.838 (n q)^{0.6}}{S^{1.3}} \quad (\text{D-9})$$

Using $n = 0.05$, $q = 0.00667 \text{ ft}^2/\text{s}$, and $S = 0.005 \text{ ft/ft}$ (0.005 mm/mm) to obtain the highest $\partial y/\partial S$:

$$\frac{\partial y}{\partial S} = \frac{-2.838 [(0.05) (0.006667)]^{0.6}}{(0.005)^{1.3}} = -22.808 \quad (\text{D-10})$$

Multiplying this value by the highest S, 0.03 ft/ft , yields the highest change in $|y| = 0.684 \text{ in}$ (17.4 mm).

Using $n = 0.01$, $q = 0.0000694 \text{ ft}^2/\text{s}$, ($0.0232 \text{ in}^2/\text{h}$) and $S = 0.03 \text{ ft/ft}$ (0.03 mm/mm) to obtain the lowest $\partial y/\partial n$:

$$\frac{\partial y}{\partial S} = \frac{-2.838 [(0.01) (0.00006944)]^{0.6}}{(0.03)^{1.3}} = -0.0546 \quad (\text{D-11})$$

Multiplying this value by the lowest S = 0.005 ft/ft (0.005 mm/mm) yields the lowest change in $|y| = 0.000273 \text{ in}$ (0.00694 mm).

ANALYSIS OF RESULTS

For the values of the highest change in the flow depth, y (see table D-3), the order of sensitivity is: $q > S > n$

Table D-3. Variables affecting changes in flow depth.

Variable	Changes in y , in (mm)	
	High	Low
Manning's n	0.434 (11.0)	0.00172 (0.0438)
Flow, q , (ft^2/s) (cm^3/s)	1.416 (36.0)	0.000528 (0.0134)
Slope, S (ft/ft) (mm/mm)	0.684 (17.4)	0.000273 (0.00694)

This shows that for high flows, the flow is the major factor that determines the flow depth. At high rainfall rates and long drainage path lengths, the quantity of the flow has the largest effect on the depth.

For the lowest values of the change in y , the order is: $n > q > S$

This shows that at low flows, the resistance of the pavement, which is characterized by the Manning roughness coefficient, is the most dominant factor affecting the depth of flow.